

Chapter – IV

Characterization, Thermoluminescence and Photoluminescence studies of BAM doped phosphors and Results and discussions

Chapter – IV

Characterization, Thermoluminescence and Photoluminescence studies of BAM doped phosphors and Results and discussions

Preparation of the phosphor:

The doping of BaMgAl₁₀O₁₇(BAM) with Eu²⁺ or Mn²⁺ yields highly efficient luminescent materials, which are widely employed as phosphors in plasma display panels (PDPs), Hg low pressure, and Xe low-pressure discharge lamps. Under photo excitation BAM:Eu shows a single emission band at 453 nm. Whereas BAM: Mn emits at 515nm. Since BAM. Eu has a deep blue color point, a short decay time (= 800 ns) and a high efficiency under vacuum ultraviolet (VUV) excitation, it is applied as the standard blue phosphor in PDPs by all PDP manufacturers

A considerable shortcoming of BAM Eu is its sensitivity towards elevated temperatures. The degree of thermal degradation is dependent on annealing conditions, i.e. temperature and atmosphere. However the detected reduction in light output is a sensitive function of the excitation wavelength. Moreover, the thermal stability of a given BAM:Eu powder is strongly determined by its synthesis conditions, viz. appropriate weigh-in of starting materials and annealing temperature. Additionally, BAM.Eu shows a severe degradation under VUV excitation, as it occurs in Xe discharge lamps and PDPs. Since its VUV degradation is much stronger than that of standard green- and red-emitting phosphors, i.e. (Y, Gd)BO₃:Eu and Zn₂SiO₄ Mn, used in these devices, the blue light intensity of lamps and displays is reduced over lifetime and the white color point becomes more yellowish. This can be recognized as color point shift of fluorescent lamps or as burn-in of plasma display panels. It was found that the photo degradation of BAM can be reduced by the optimization of its composition.

Although BAM-based phosphors are used in lamps and displays and degradation and afterglow are a matter of concern of all device manufacturers, the type and density of defects in BAM are less known. This is surprising since lattice defects, in particular oxygen vacancies, can act as electron traps and therefore force the photo oxidation of the unstable activators Eu²⁺ and Mn²⁺. It can be expected that the crystallinity or defect

concentration of BAM will strongly influence the stability of BAM and the luminescence properties.

By considering the advanced technology in phosphors materials the BAM is selected with various rare-earth activators for their commercial applications in view of their high spectral power of distribution of specific line with excellent efficiency. The rare-earths are costly but have provided stability to phosphors in the operating conditions of the devices. Because of the demand for rare-earth phosphors for television, X-ray excited materials and fluorescent lamps; the physical chemistry and availability of various fluxes for preparation and purification of these compounds has been improved greatly, providing consistent and reliable materials in purity levels required for efficient phosphor absorption and emission.

These powder specimens have been used for different experimental measurements. The general formula of present phosphor is



Where Y indicates the different activators like Eu, Ce, Nd, Pr and Mn.

All the 27 specimens prepared are studied for their TL, PL characteristics.

The main aim of this work is to gain insight in the influence of defects on the luminescence properties and to study the nature of the defects generated with gamma and beta radiation by performing thermoluminescence measurements and also study the photoluminescence properties of the prepared lamp phosphors. Finally, the influence of various dopant concentrations and the behavior of Eu^{2+} , Mn^{2+} , Ce^{2+} , Nd^{3+} , Pr^{3+} doped BAM are investigated.

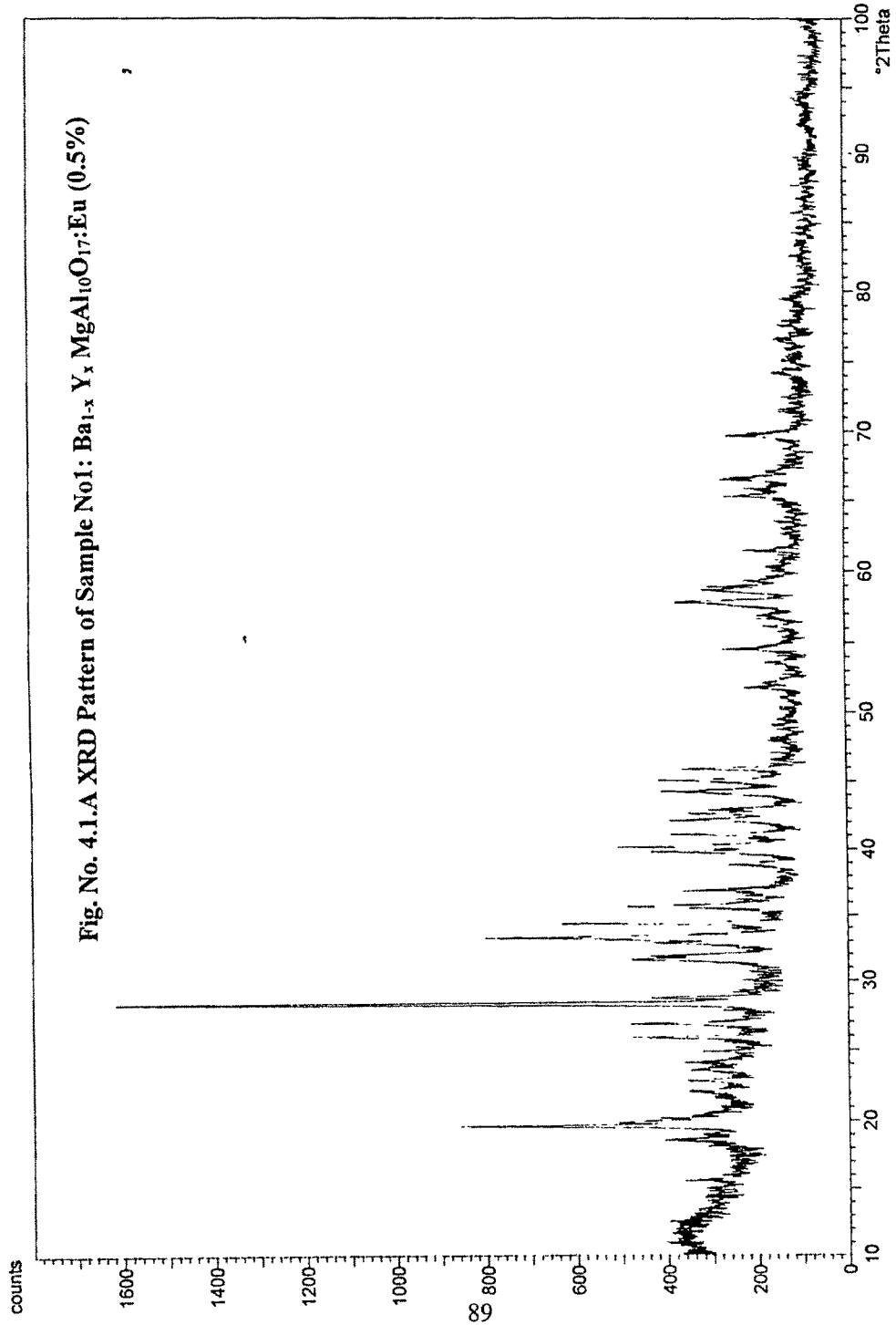
Characterization of the phosphor using X-ray diffraction:

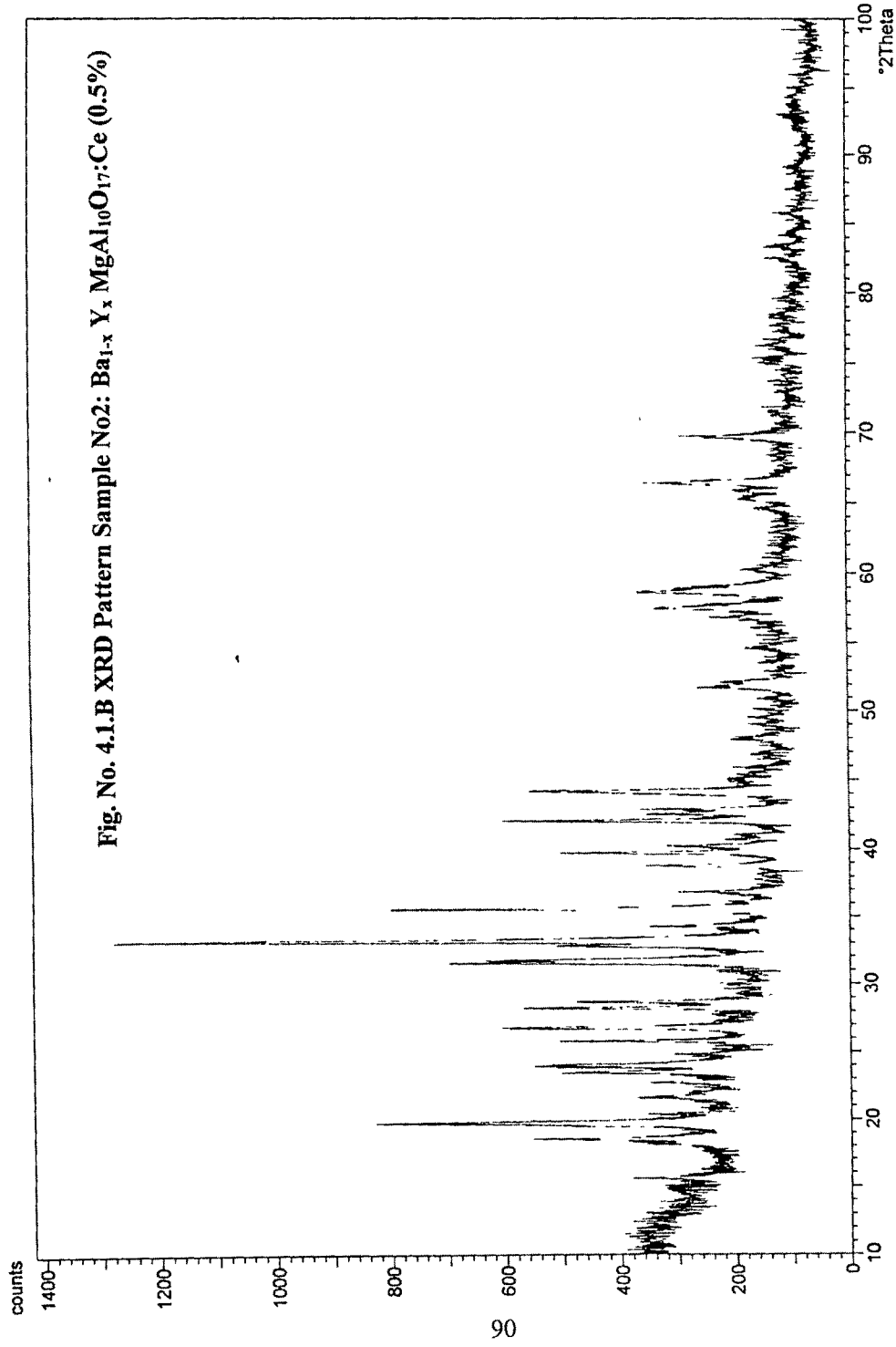
The $\text{Ba}_{1-x}\text{Y}_x\text{MgAl}_{10}\text{O}_{17}$, with various dopants like Eu, Mn, Ce, Nd and Pr studied for its structural properties using X-ray diffraction. The nine samples of lamp phosphors (BAM) were characterized using X-ray diffraction technique. The XRD-pattern was recorded on a PHILIPS XRD unit at RSIC, IIT, Mumbai, having a 2θ range from 10 to 100° . The wave length used is the copper K-Alpha1 line with wave length 1.5405600

A° The intensity range was selected automatically and printout can be taken as and when required. All samples were scanned for a 2θ range from 10° to 100°

All specimens had maxima around 33.2 corresponding to a d-value of around 2.69 followed by other less intense peak. Table 4.1 shows calculated and catalogue d-Values of sample $\text{BaMgAl}_{10}\text{O}_{17}$: (Ce,Mn,Nd,Eu,Pr) and XRD Patterns are presented in figure 4.1.A to 4.1.I (nine specimens) From the table-4.1, one can normally conclude that the sample formation is mostly single phase on comparison with the standard d values of BAMs

The crystal structure of Barium Magnesium Aluminates are well documented, it is a hexagonal structure. The color of the phosphor is white. The corresponding lattice constants $a=b=5.62$ and $c=22.64$. The spinal blocks separated by an intermediate layer containing one Barium and an oxygen ion. Due to the Barium ion in this structure results in excessive positive charge.





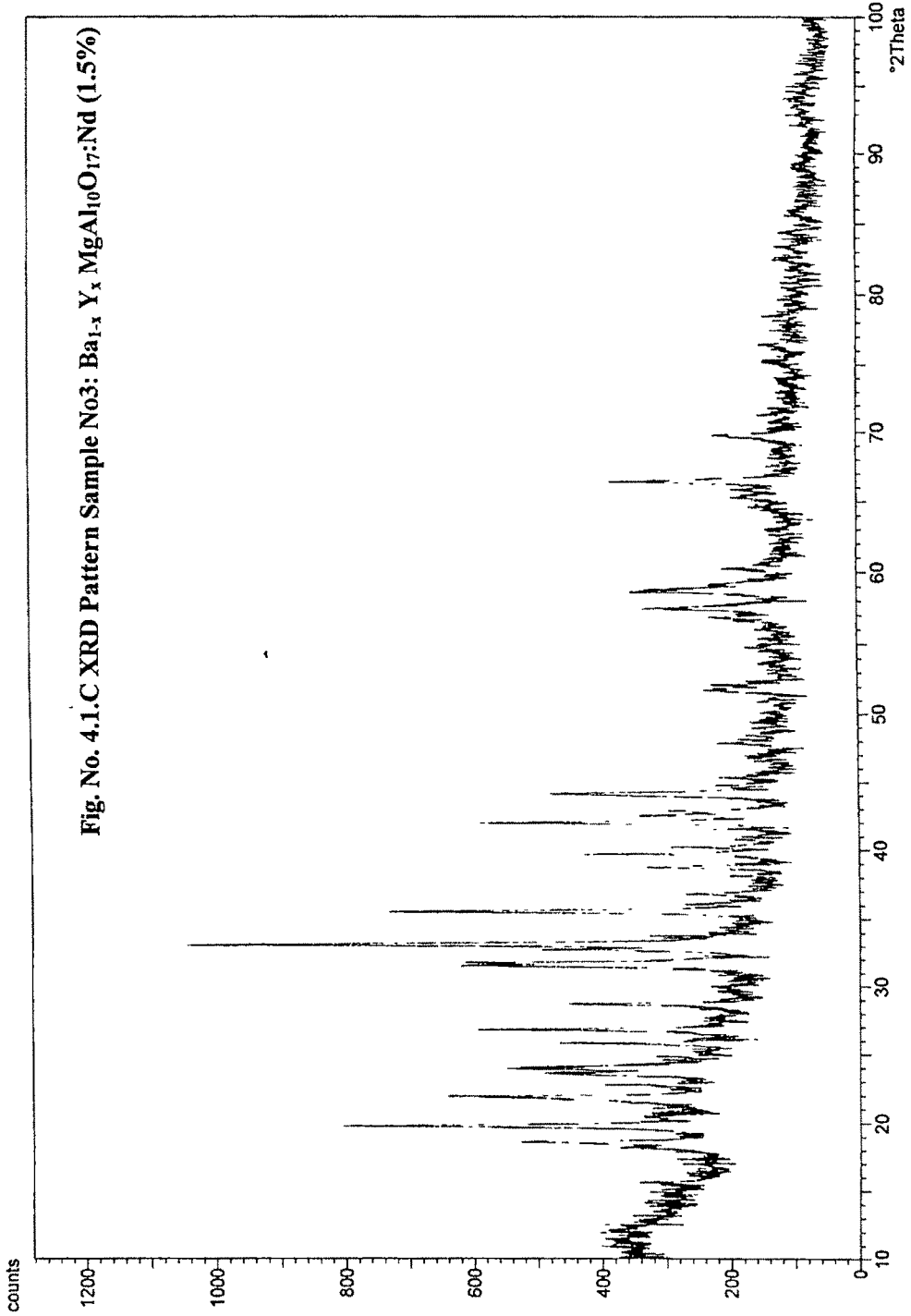
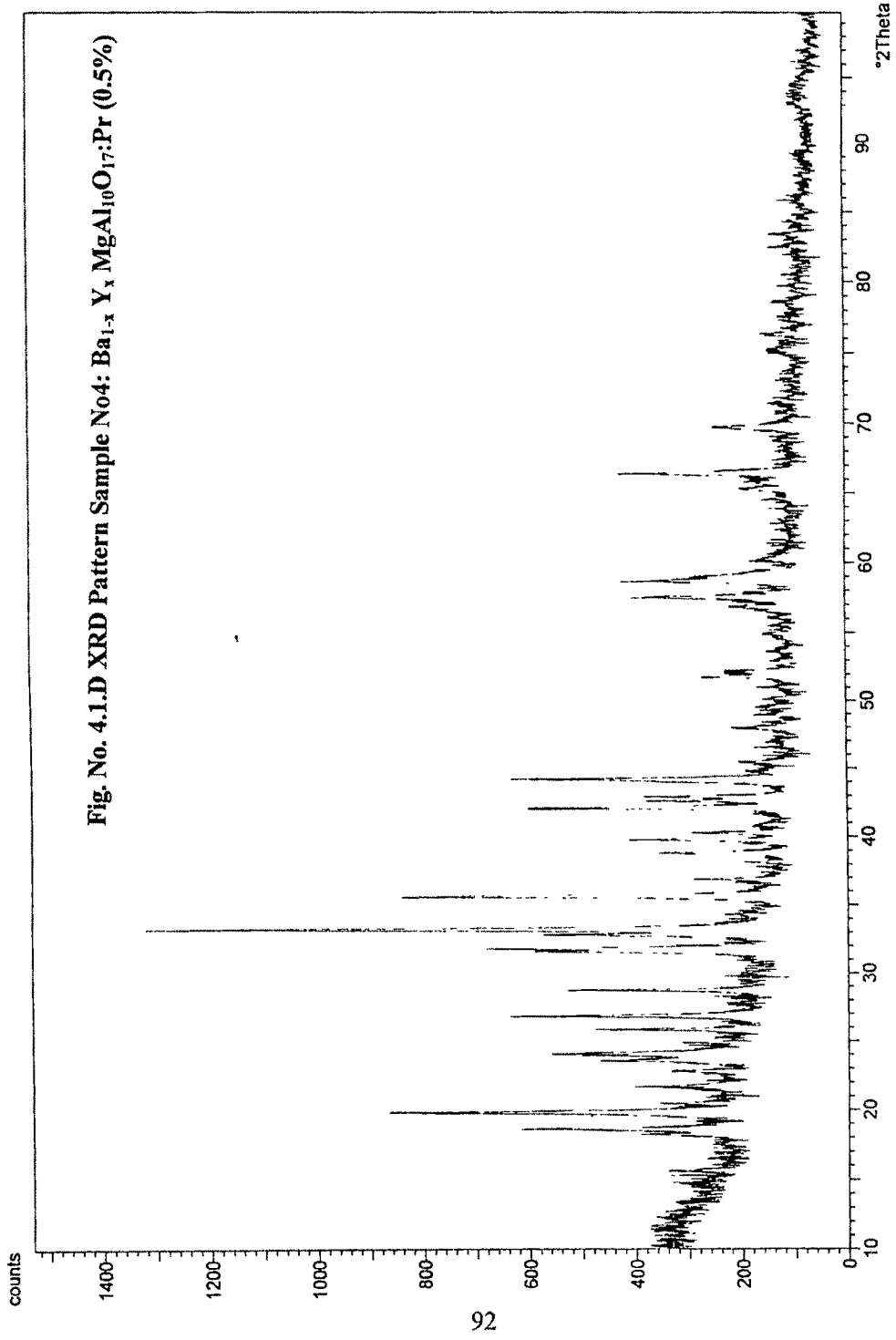
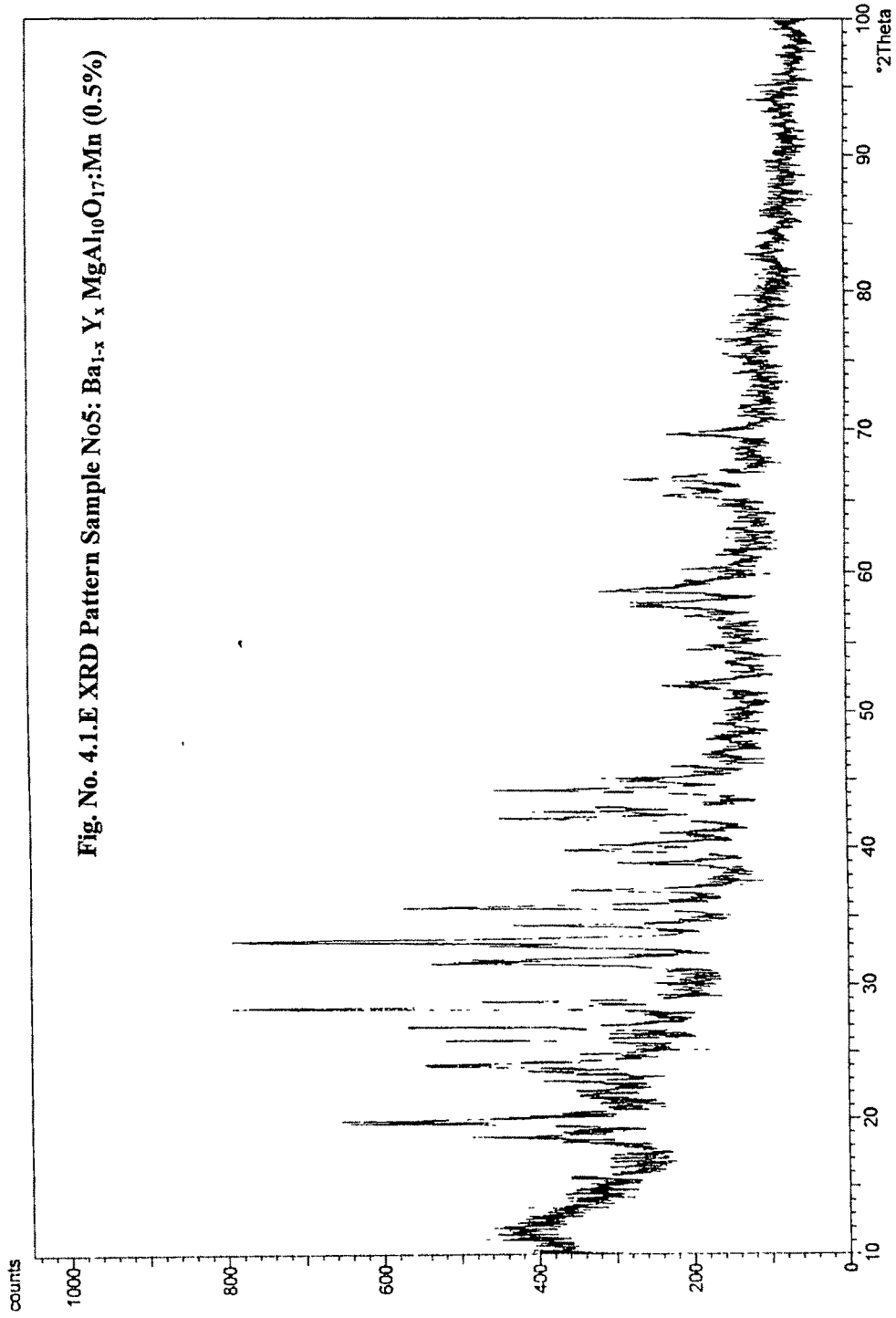
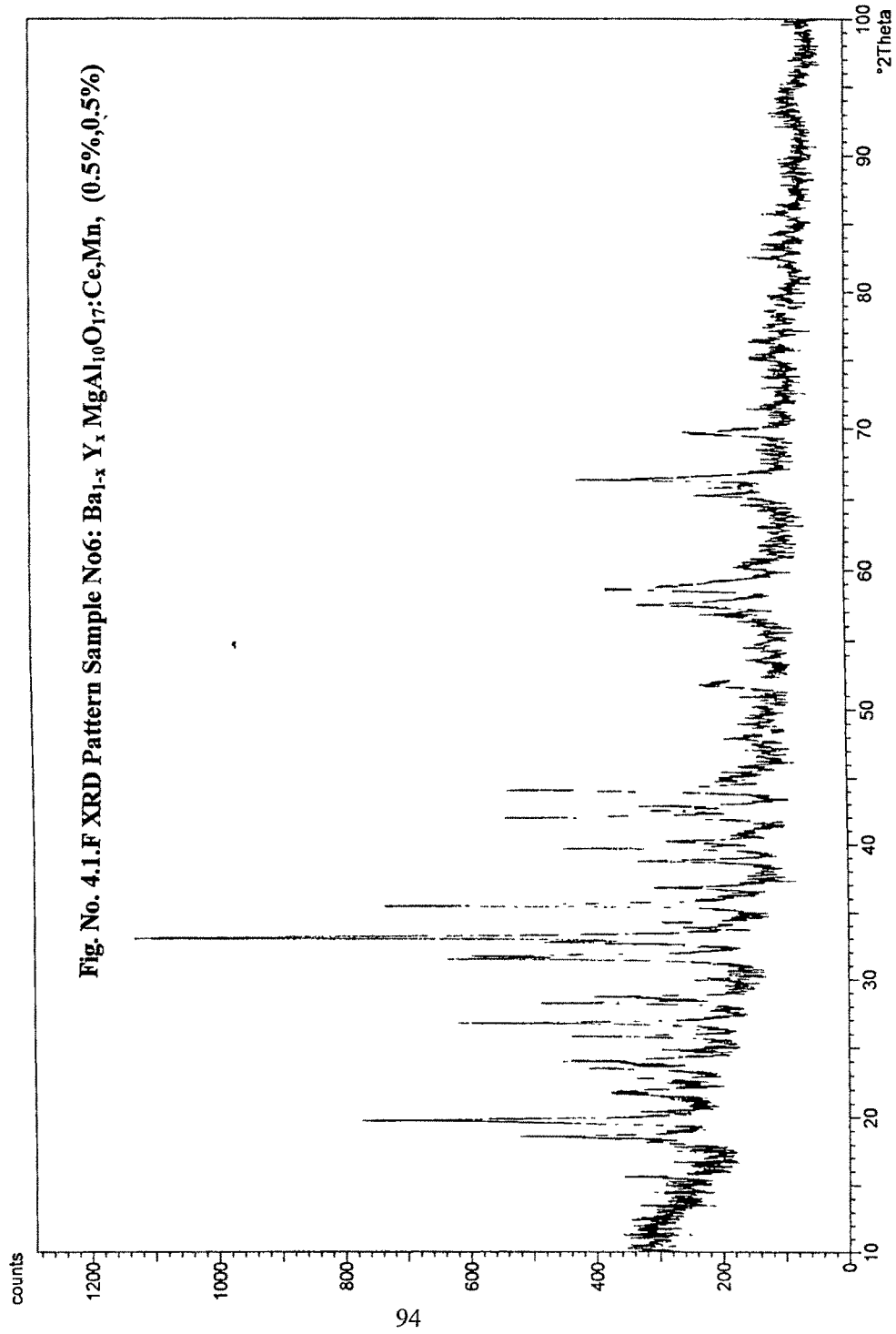
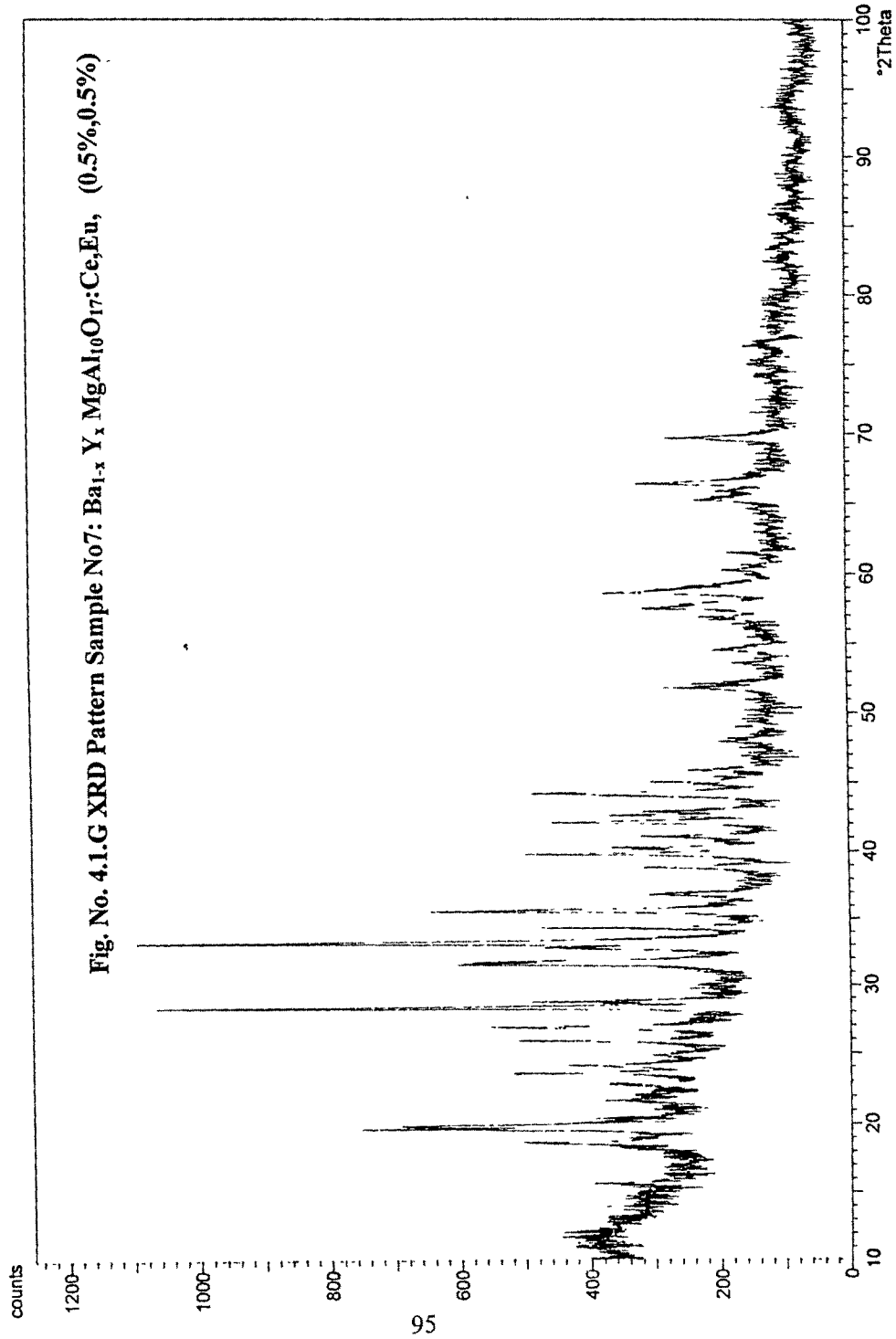


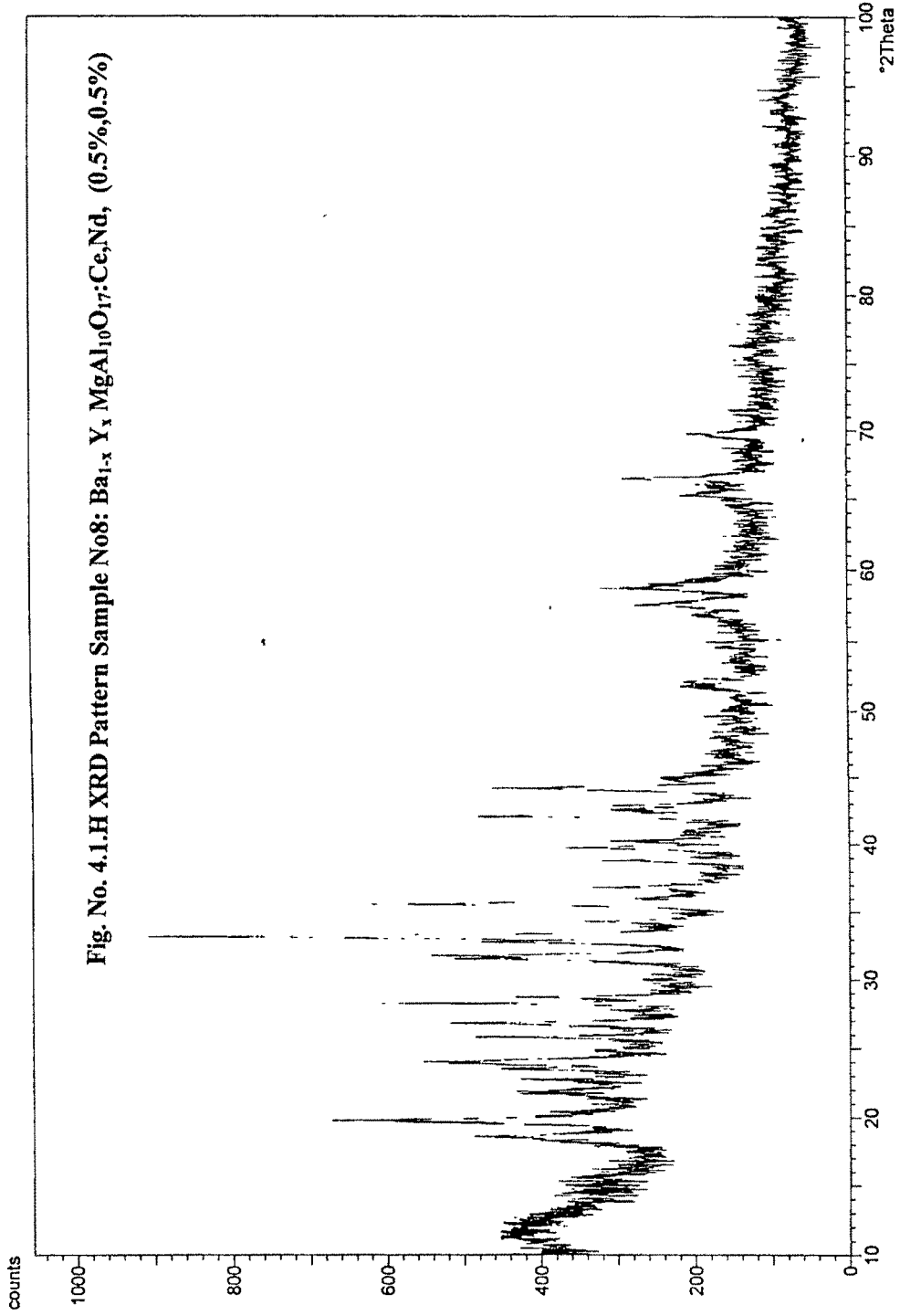
Fig. No. 4.1.C XRD Pattern Sample No3: Ba_{1-x}Y_xMgAl₁₀O₁₇:Nd (1.5%)











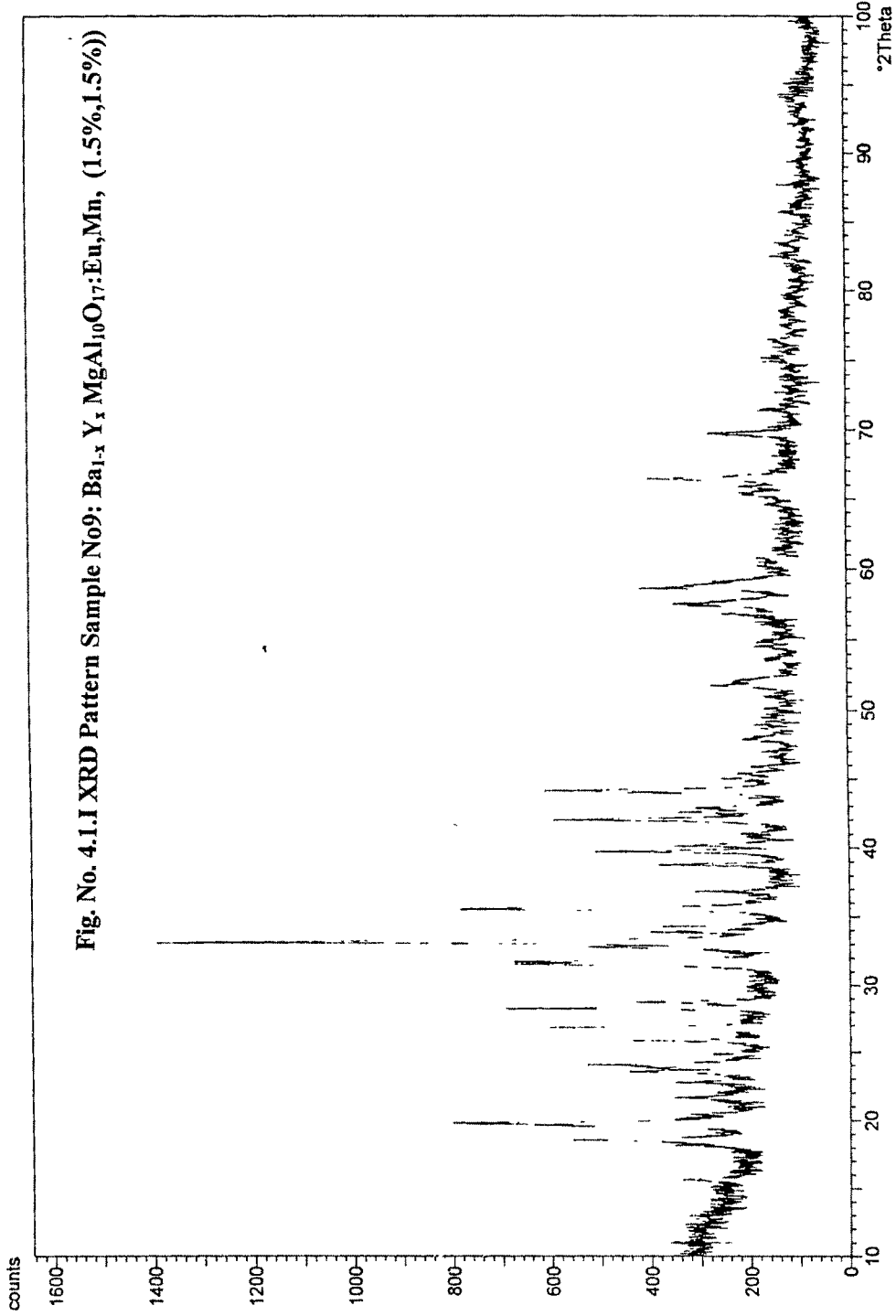


Table.4.1**Calculated “d” values of the various samples**Sample No1 Ba_{1-x} Y_x MgAl₁₀O₁₇ Eu (0.5%)Sample No2 Ba_{1-x} Y_x MgAl₁₀O₁₇:Ce (0.5%)Sample No3 Ba_{1-x} Y_x MgAl₁₀O₁₇ Nd (1.5%)Sample No4 Ba_{1-x} Y_x MgAl₁₀O₁₇ Pr (0.5%)Sample No5. Ba_{1-x} Y_x MgAl₁₀O₁₇ Mn (0.5%)Sample No6. Ba_{1-x} Y_x MgAl₁₀O₁₇:Ce,Mn, (0.5%,0.5%)Sample No7. Ba_{1-x} Y_x MgAl₁₀O₁₇:Ce,Eu, (0.5%,0.5%)Sample No8. Ba_{1-x} Y_x MgAl₁₀O₁₇:Ce,Nd, (0.5%,0.5%)Sample No9. Ba_{1-x} Y_x MgAl₁₀O₁₇ Eu,Mn, (1.5%,1.5%)

No.1	No.2	No.3	No.4	No.5	No.6	No.7	No.8	No.9	Standard d values
5.67	5.67	5.67	5.66	5.66	5.66	5.66	5.67	5.65	5.66
4.76	4.76	4.76	4.76	4.76	4.76	4.76	4.76	4.76	4.76
4.52	4.48	4.48	4.47	4.52	4.47	4.51	4.47	4.49	4.49
3.89	3.90	3.90	3.89	3.89	3.89	3.89	3.90	3.90	4.10
3.69	3.70	3.70	3.71	3.71	3.70	3.68	3.69	3.69	3.70
3.44	3.44	3.44	3.44	3.44	3.44	3.44	3.44	3.44	3.44
3.31	3.30	3.31	3.32	3.31	3.32	3.31	3.31	3.31	3.32
3.14	3.15	3.10	3.10	3.15	3.14	3.15	3.15	3.15	3.13
2.83	2.83	2.83	2.81	2.83	2.83	2.83	2.83	2.83	2.82
2.69	2.69	2.69	2.69	2.69	2.69	2.69	2.69	2.69	2.69
2.51	2.52	2.51	2.52	2.51	2.51	2.51	2.51	2.52	2.52
2.24	2.24	2.26	2.23	2.24	2.26	2.24	2.26	2.26	2.25
2.14	2.14	2.14	2.14	2.14	2.14	2.14	2.14	2.14	2.14

Thermoluminescence studies:

The thermoluminescence of prepared lamp phosphors is presented here. The TL glow curves of the various impurity doped BaMg aluminates have been recorded in the temperature range 25° to 400°C with uniform heating rate (6.6°C/sec) The phosphors have been given a test dose of 7Gy gamma and 7Gy beta doses. The TL of gamma irradiated sample exhibited by the phosphors are given as Fig.4.2 A to 4.2.I and also in the tabular form. Table –2 containing the TL of gamma irradiated samples immediately after irradiation and after 24 hours storage at room temperature. The main glow peaks exhibits by the phosphors are around 120, 210 and 340°C. After 24 hours of storage few peaks are missing and generation of other peak around 160°C is also observed.

Though all these are main peaks, in all cases they do not appear as isolated peaks on account of appearance and disappearance of few new peaks or shoulders or humps or siblings in the neighborhood of isolated main glow peak. It is known that the glow curve shape and peak temperatures of a given BaMg -aluminates are different depending on the impurities and quantity introduced in the host material. In this context, the assignment of the particular temperature to a TL glow peak may appear somewhat arbitrary. In spite of this the above mentioned peak temperatures are typical and these have been used to identify the glow peaks. The intensity of the glow peaks is given in arbitrary units. The characteristics glow curves obtained for the phosphors under investigations presented as follows.

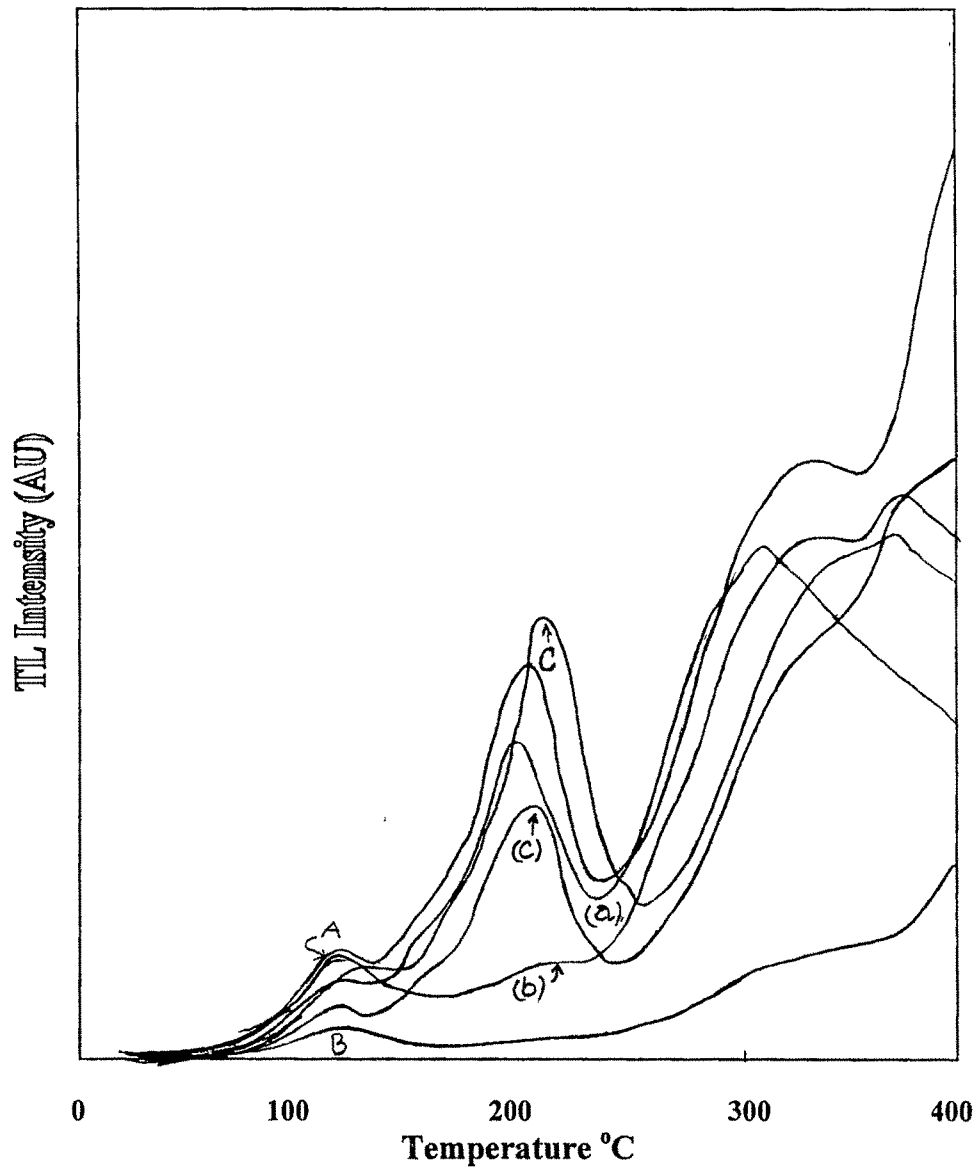


Fig.4.2.A

Thermoluminescence of gamma irradiated $\text{BaMgAl}_{10}\text{O}_{17} : \text{X}$

- Curve A: TL of $\text{BaMgAl}_{10}\text{O}_{17} : \text{Eu}$ (0.5%)
- Curve a: TL of $\text{BaMgAl}_{10}\text{O}_{17} : \text{Eu}$ (0.5%) after 24 hours of irradiation
- Curve B: TL of $\text{BaMgAl}_{10}\text{O}_{17} : \text{Eu}$ (1.0%)
- Curve b: TL of $\text{BaMgAl}_{10}\text{O}_{17} : \text{Eu}$ (1.0%) after 24 hours of irradiation
- Curve C: TL of $\text{BaMgAl}_{10}\text{O}_{17} : \text{Eu}$ (1.5%)
- Curve c: TL of $\text{BaMgAl}_{10}\text{O}_{17} : \text{Eu}$ (1.5%) after 24 hours of irradiation

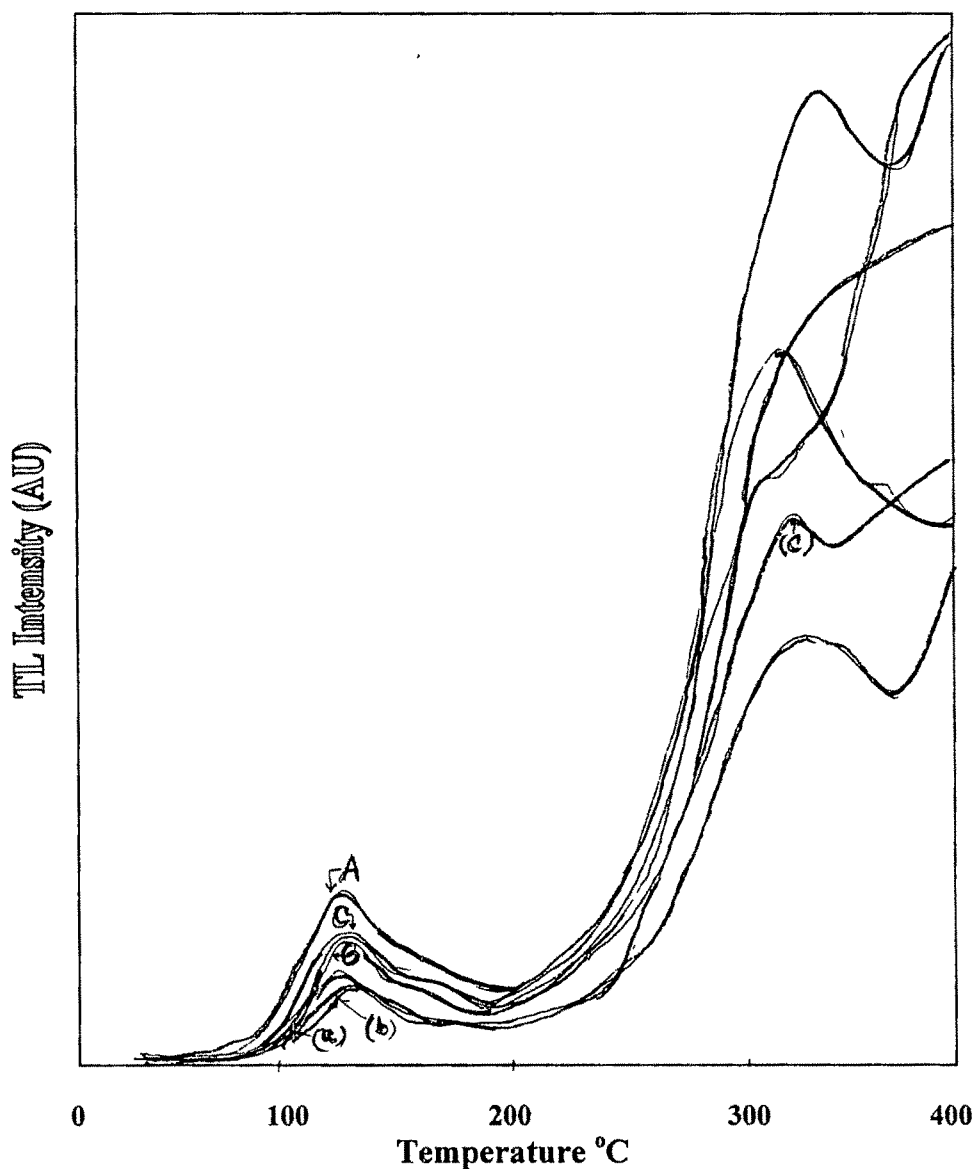


Fig.4.2.B

Thermoluminescence of gamma irradiated BaMgAl₁₀O₁₇ : X

- Curve A: TL of BaMgAl₁₀O₁₇ : Ce (0.5%)
- Curve a: TL of BaMgAl₁₀O₁₇ : Ce (0.5%) after 24 hours of irradiation
- Curve B: TL of BaMgAl₁₀O₁₇ : Ce (1.0%)
- Curve b: TL of BaMgAl₁₀O₁₇ : Ce (1.0%) after 24 hours of irradiation
- Curve C: TL of BaMgAl₁₀O₁₇ : Ce (1.5%)
- Curve c: TL of BaMgAl₁₀O₁₇ : Ce (1.5%) after 24 hours of irradiation

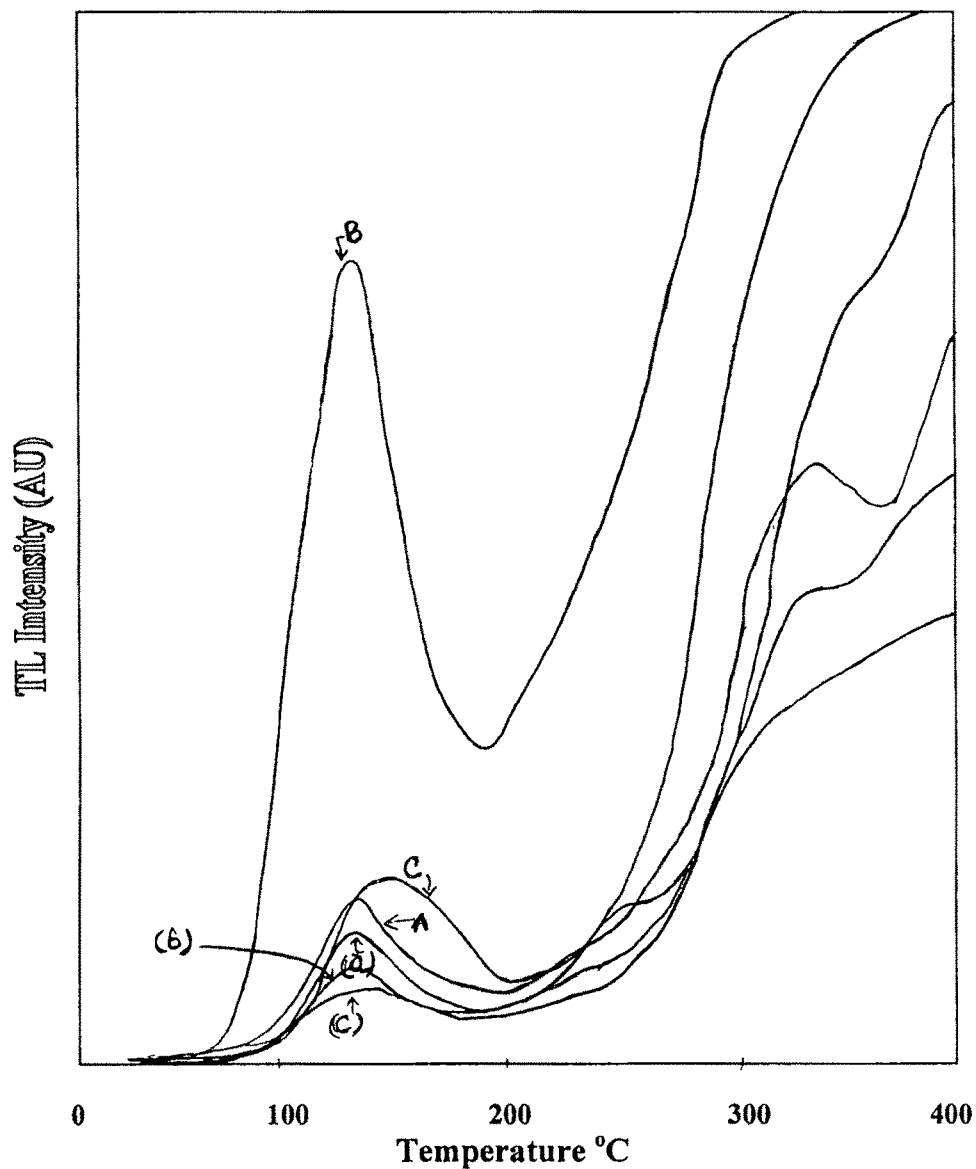


Fig.4.2.C

Thermoluminescence of gamma irradiated $\text{BaMgAl}_{10}\text{O}_{17} : \text{X}$

Curve A: TL of $\text{BaMgAl}_{10}\text{O}_{17} : \text{Nd}$ (0.5%)

Curve a: TL of $\text{BaMgAl}_{10}\text{O}_{17} : \text{Nd}$ (0.5%) after 24 hours of irradiation

Curve B: TL of $\text{BaMgAl}_{10}\text{O}_{17} : \text{Nd}$ (1.0%)

Curve b: TL of $\text{BaMgAl}_{10}\text{O}_{17} : \text{Nd}$ (1.0%) after 24 hours of irradiation

Curve C: TL of $\text{BaMgAl}_{10}\text{O}_{17} : \text{Nd}$ (1.5%)

Curve c: TL of $\text{BaMgAl}_{10}\text{O}_{17} : \text{Nd}$ (1.5%) after 24 hours of irradiation

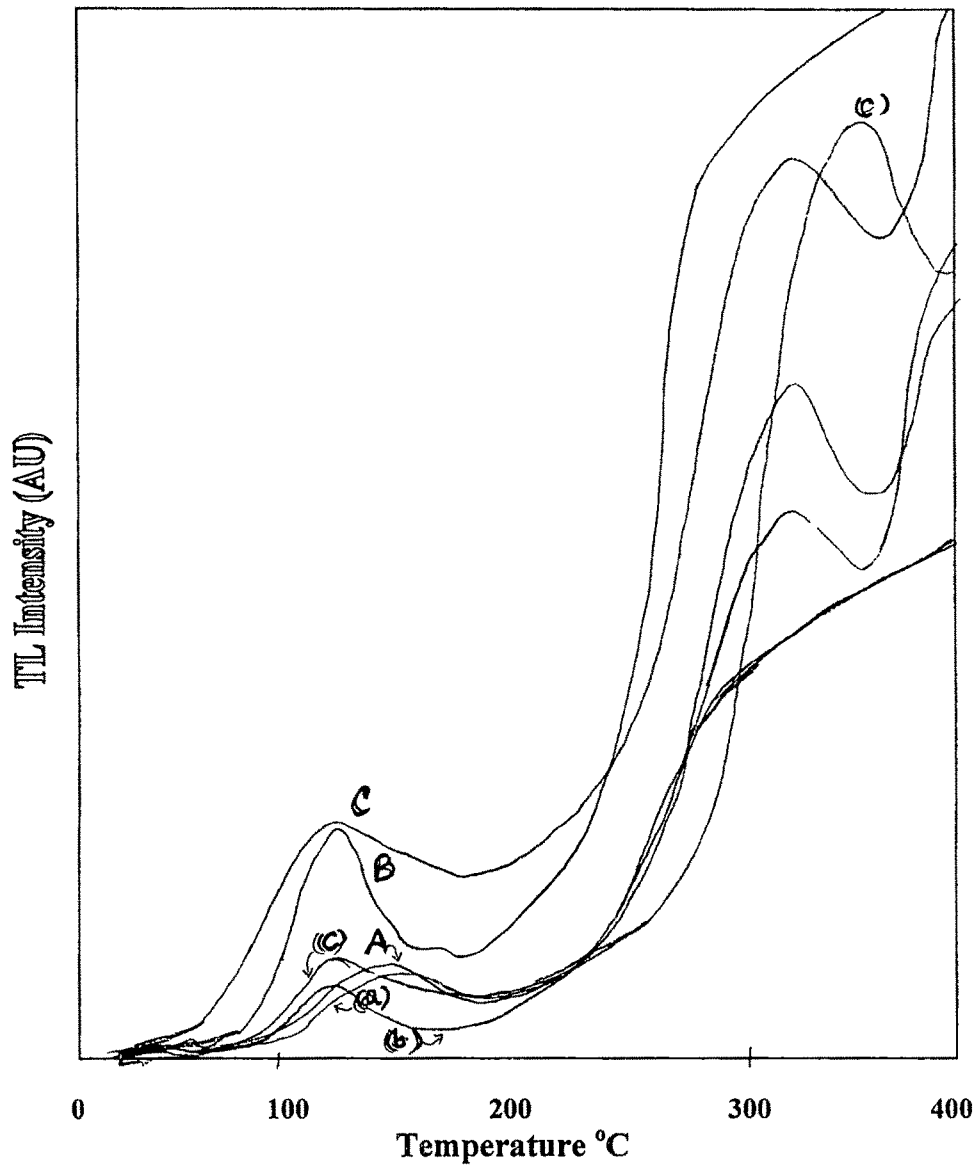


Fig.4.2.D

Thermoluminescence of gamma irradiated BaMgAl₁₀O₁₇ : X

Curve A: TL of BaMgAl₁₀O₁₇ : Pr (0.5%)

Curve a: TL of BaMgAl₁₀O₁₇ : Pr (0.5%) after 24 hours of irradiation

Curve B: TL of BaMgAl₁₀O₁₇ : Pr (1.0%)

Curve b: TL of BaMgAl₁₀O₁₇ : Pr (1.0%) after 24 hours of irradiation

Curve C: TL of BaMgAl₁₀O₁₇ : Pr (1.5%)

Curve c: TL of BaMgAl₁₀O₁₇ : Pr (1.5%) after 24 hours of irradiation

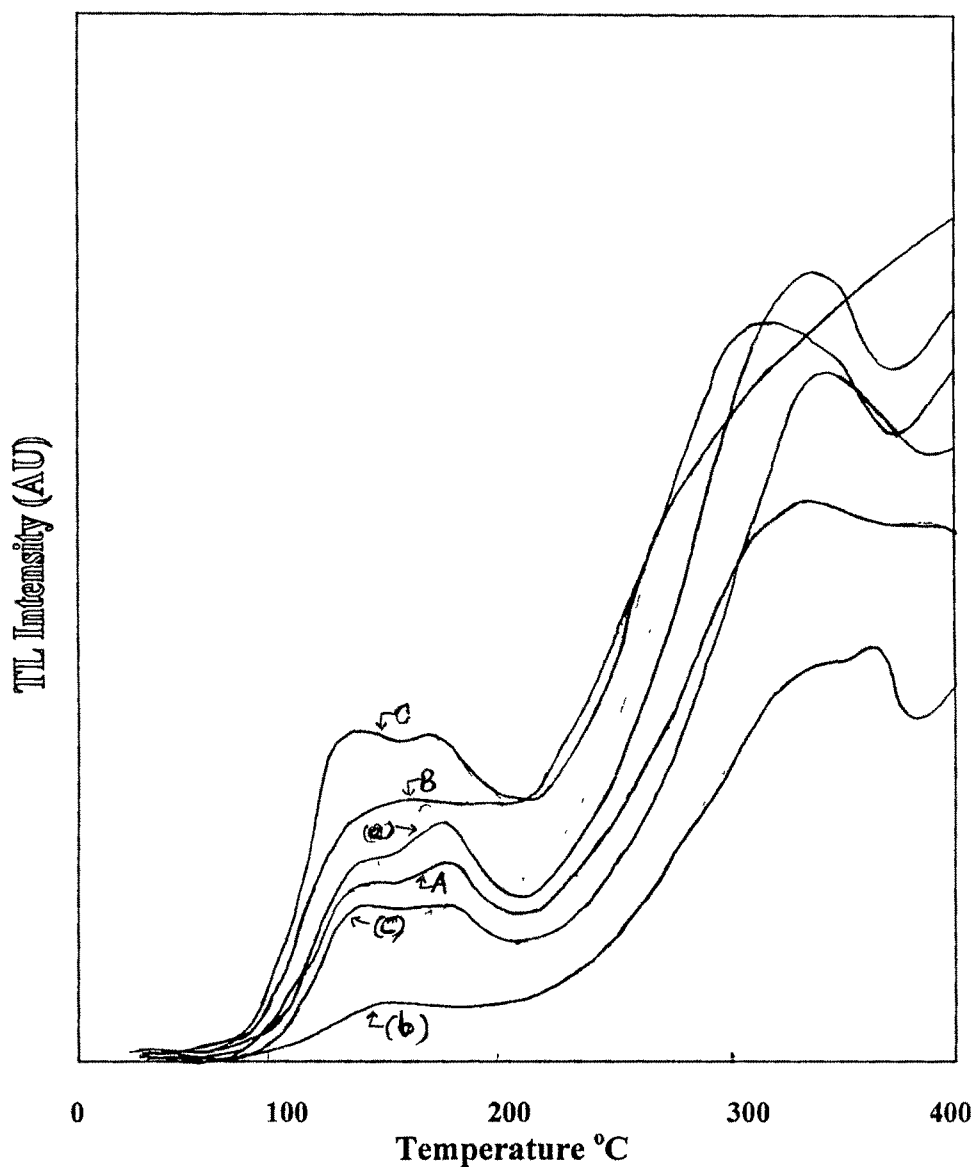


Fig.4.2.E

Thermoluminescence of gamma irradiated BaMgAl₁₀O₁₇ : X

Curve A: TL of BaMgAl₁₀O₁₇ : Mn (0.5%)

Curve a: TL of BaMgAl₁₀O₁₇ : Mn (0.5%) after 24 hours of irradiation

Curve B: TL of BaMgAl₁₀O₁₇ : Mn (1.0%)

Curve b: TL of BaMgAl₁₀O₁₇ : Mn (1.0%) after 24 hours of irradiation

Curve C: TL of BaMgAl₁₀O₁₇ : Mn (1.5%)

Curve c: TL of BaMgAl₁₀O₁₇ : Mn (1.5%) after 24 hours of irradiation

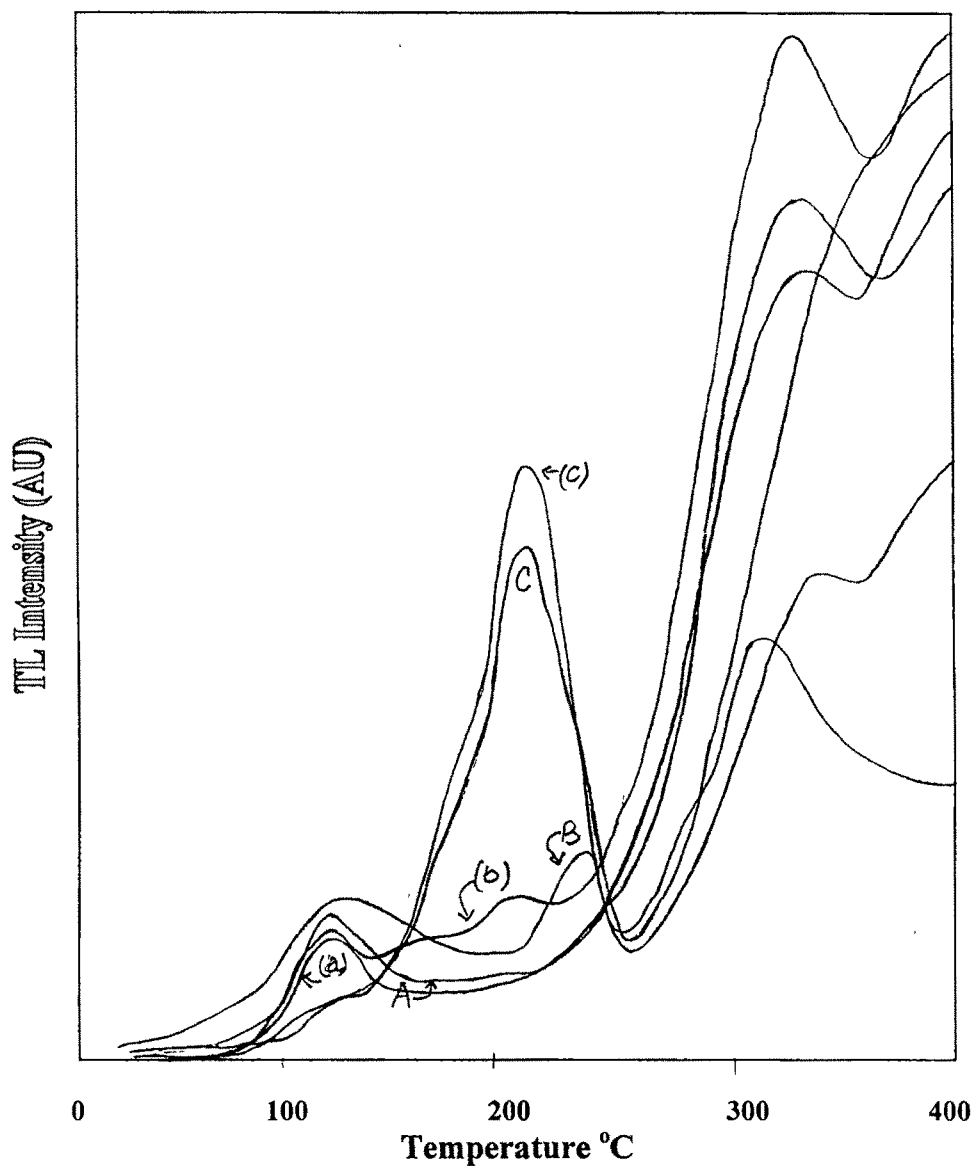


Fig.4.2.F

Thermoluminescence of gamma irradiated BaMgAl₁₀O₁₇ : X

Curve A: TL of BaMgAl₁₀O₁₇ : Ce:Mn (0.5:0.5%)

Curve a: TL of BaMgAl₁₀O₁₇ : Ce:Mn (0.5:0.5%) after 24 hours of irradiation

Curve B: TL of BaMgAl₁₀O₁₇ : Ce:Mn (1.0:1.0%)

Curve b: TL of BaMgAl₁₀O₁₇ : Ce:Mn (1.0:1.0%) after 24 hours of irradiation

Curve C: TL of BaMgAl₁₀O₁₇ : Ce:Mn (1.5:1.5%)

Curve c: TL of BaMgAl₁₀O₁₇ : Ce:Mn (1.5:1.5%) after 24 hours of irradiation

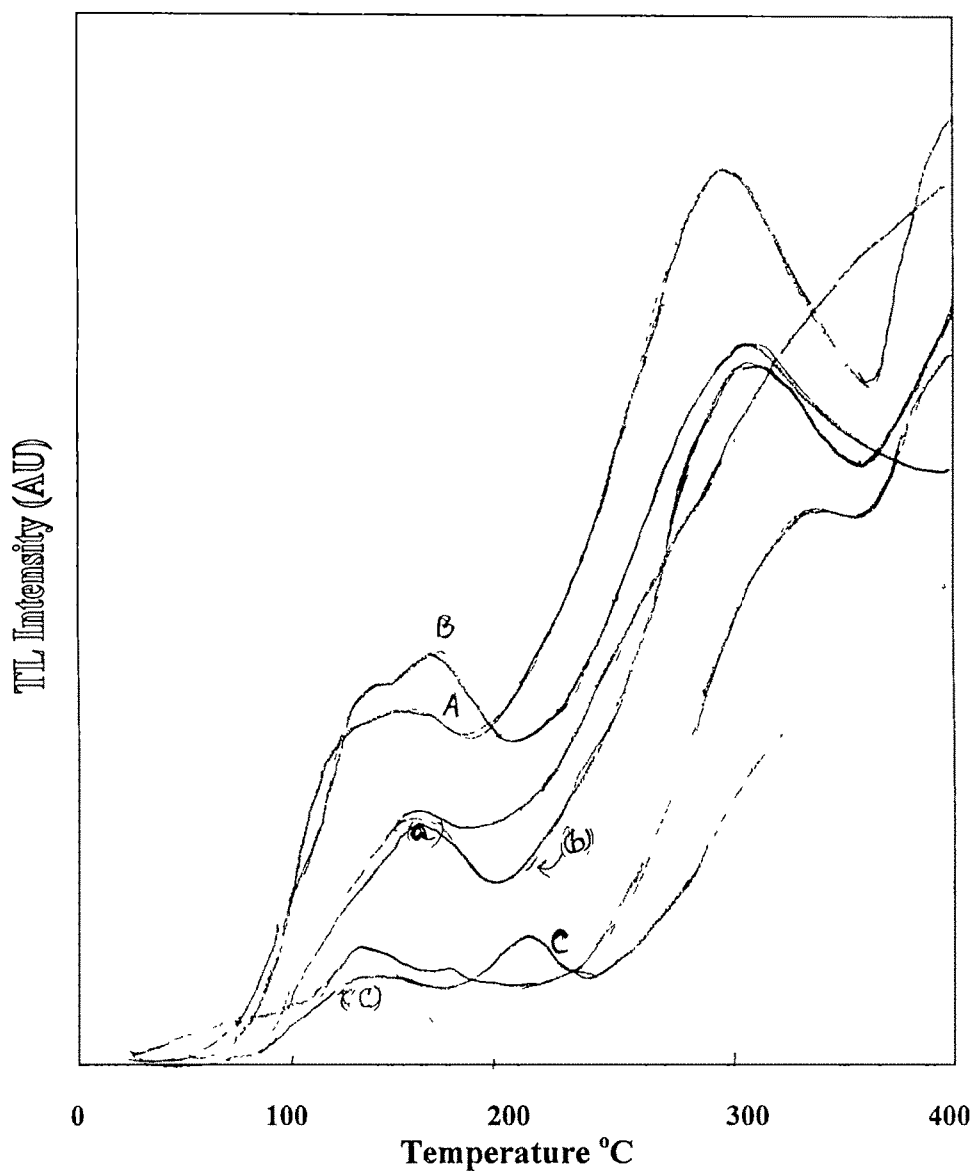


Fig.4.2.G

Thermoluminescence of gamma irradiated $\text{BaMgAl}_{10}\text{O}_{17} : \text{X}$

- Curve A: TL of $\text{BaMgAl}_{10}\text{O}_{17} : \text{Ce:Eu}$ (0.5:0.5%)
- Curve a: TL of $\text{BaMgAl}_{10}\text{O}_{17} : \text{Ce:Eu}$ (0.5:0.5%) after 24 hours of irradiation
- Curve B: TL of $\text{BaMgAl}_{10}\text{O}_{17} : \text{Ce:Eu}$ (1.0:1.0%)
- Curve b: TL of $\text{BaMgAl}_{10}\text{O}_{17} : \text{Ce:Eu}$ (1.0:1.0%) after 24 hours of irradiation
- Curve C: TL of $\text{BaMgAl}_{10}\text{O}_{17} : \text{Ce:Eu}$ (1.5:1.5%)
- Curve c: TL of $\text{BaMgAl}_{10}\text{O}_{17} : \text{Ce:Eu}$ (1.5:1.5%) after 24 hours of irradiation

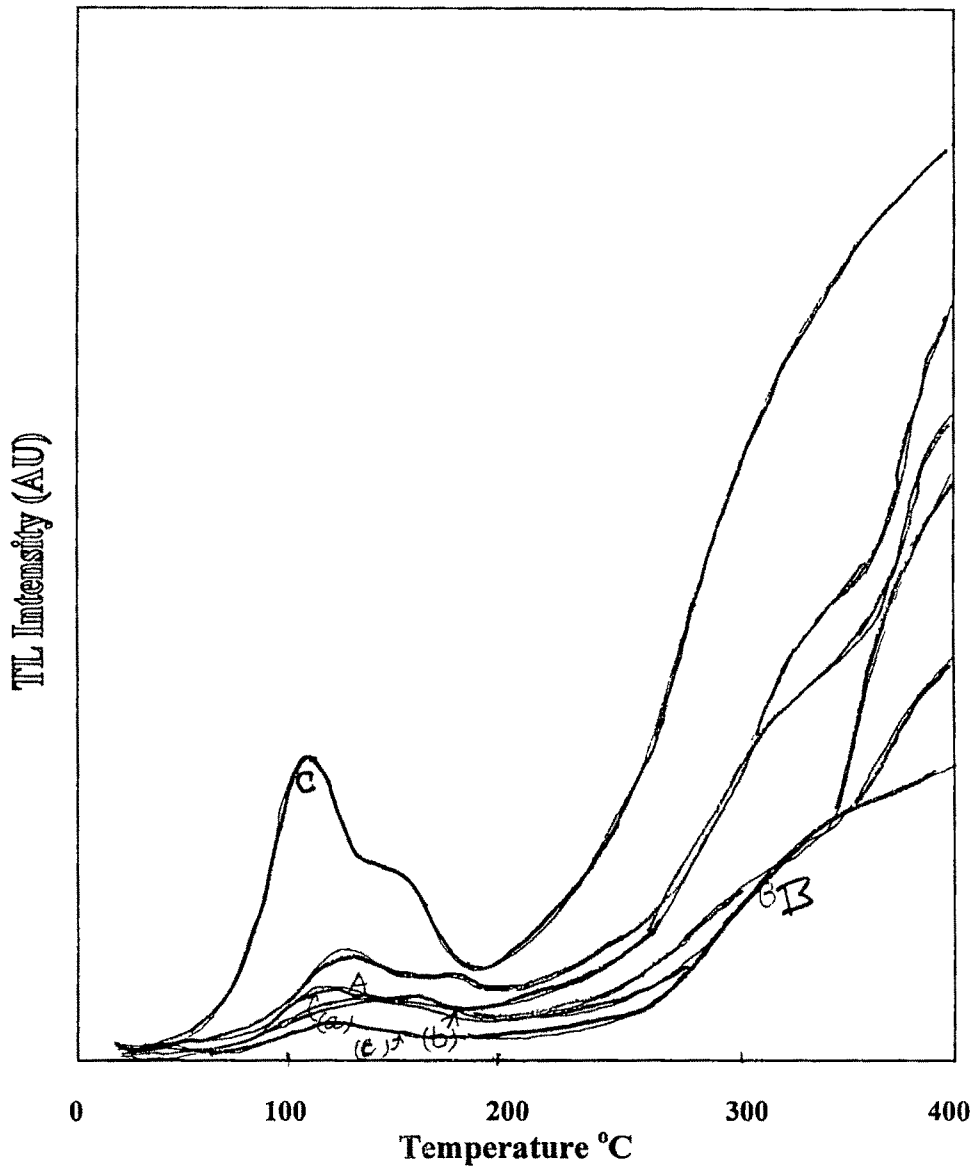


Fig.4.2.H

Thermoluminescence of gamma irradiated BaMgAl₁₀O₁₇ : X

- Curve A: TL of BaMgAl₁₀O₁₇ : Ce:Nd (0.5:0.5%)
- Curve a: TL of BaMgAl₁₀O₁₇ : Ce: Nd (0.5: 0.5%) after 24 hours of irradiation
- Curve B: TL of BaMgAl₁₀O₁₇ : Ce: Nd (1.0:1.0%)
- Curve b: TL of BaMgAl₁₀O₁₇ : Ce: Nd (1.0:1.0%) after 24 hours of irradiation
- Curve C: TL of BaMgAl₁₀O₁₇ : Ce: Nd (1.5:1.5%)
- Curve c: TL of BaMgAl₁₀O₁₇ : Ce: Nd (1.5:1.5%) after 24 hours of irradiation

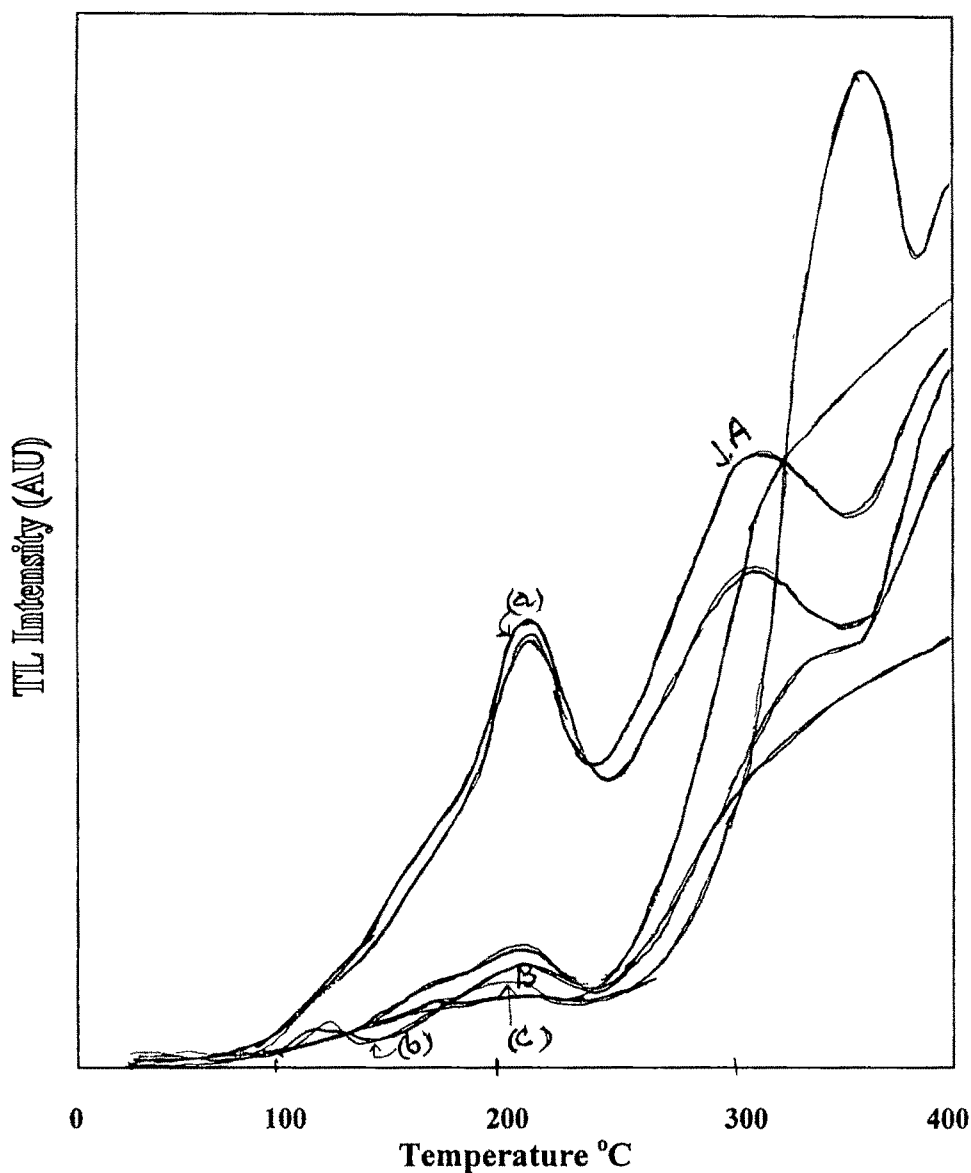


Fig.4.2.I

Thermoluminescence of gamma irradiated $\text{BaMgAl}_{10}\text{O}_{17} : \text{X}$

- Curve A: TL of $\text{BaMgAl}_{10}\text{O}_{17} : \text{Eu:Mn (0.5:0.5\%)}$
- Curve a: TL of $\text{BaMgAl}_{10}\text{O}_{17} : \text{Eu:Mn (0.5:0.5\%)}$ after 24 hours of irradiation
- Curve B: TL of $\text{BaMgAl}_{10}\text{O}_{17} : \text{Eu:Mn (1.0:1.0\%)}$
- Curve b: TL of $\text{BaMgAl}_{10}\text{O}_{17} : \text{Eu:Mn (1.0:1.0\%)}$ after 24 hours of irradiation
- Curve C: TL of $\text{BaMgAl}_{10}\text{O}_{17} : \text{Eu:Mn (1.5:1.5\%)}$
- Curve c: TL of $\text{BaMgAl}_{10}\text{O}_{17} : \text{Eu:Mn (1.5:1.5\%)}$ after 24 hours of irradiation

Table.4.2 TL of Gamma Irradiation

Sr No	Sample Name	Peak temp °C	Peak intensity	After 24 hrs peak temp °C	After 24 hrs peak intensity
1	BaMgAl ₁₀ O ₁₇ -Eu (0.5%)	121	4.86	121	4.847
		209, 340	25, 20	204	19.396
2	BaMgAl ₁₀ O ₁₇ -Eu (1%)	121, 340	5.0, 10	121, 204	4.35, 4.46
3	BaMgAl ₁₀ O ₁₇ -Eu (1.5%)	121	4.2	121	2.70
		209, 340	22.25, 26	209, 340	15.85, 26
4	BaMgAl ₁₀ O ₁₇ -Ce (0.5%)	121	8	121	6.60
		340	47.5	340	35
5	BaMgAl ₁₀ O ₁₇ -Ce (1%)	121	6.6	121	6.0
		340	40.43	340	30
6	BaMgAl ₁₀ O ₁₇ -Ce (1.5%)	121	6.5	121	5.6
		340	35	340	24
7	BaMgAl ₁₀ O ₁₇ -Nd (0.5%)	121	6.90	121	6.35
		340	25.53	340	15
8	BaMgAl ₁₀ O ₁₇ -Nd (1%)	121, 211	11.0, 19	121, 340	5.6, 15
9	BaMgAl ₁₀ O ₁₇ -Nd (1.5%)	121	8	121	3.565
		340	32.48	340	24
10	BaMgAl ₁₀ O ₁₇ -Pr (0.5%)	121, 340	3.65, 32	170, 340	3.03, 28
11	BaMgAl ₁₀ O ₁₇ -Pr (1%)	121	4.9	121, 340	4.5, 12
12	BaMgAl ₁₀ O ₁₇ -Pr (1.5%)	121, 340	4.93, 52	121, 340	4.42, 45
13	BaMgAl ₁₀ O ₁₇ -Mn (0.5%)	121	8.865	121	8.0
		168, 340	10.4, 34	187, 373	9.37, 32
14	BaMgAl ₁₀ O ₁₇ -Mn (1%)	157, 313	10.75, 33	121, 340	7.05, 53
15	BaMgAl ₁₀ O ₁₇ -Mn (1.5%)	121	14.75	121	6.62
		164	15.12	150, 340	6.82, 31
16	BaMgAl ₁₀ O ₁₇ -Ce, Mn (0.5%, 0.5%)	121	6.3	121	5.1
		340	38	340	37.5
17	BaMgAl ₁₀ O ₁₇ -Ce, Mn (1%, 1%)	121	6	121	4.68
		240	8	206, 340	4.14, 41
18	BaMgAl ₁₀ O ₁₇ -Ce, Mn (1.5%, 1.5%)	121	4.1	121	2.74
		209, 340	26.5, 23	209, 340	25.5, 22
19	BaMgAl ₁₀ O ₁₇ -Ce, Eu (0.5%, 0.5%)	121	16.9	160	10.35
		340	43.34	340	15
20	BaMgAl ₁₀ O ₁₇ -Ce, Eu (1%, 1%)	121, 164	20	160	12
		340	38.25	340	33

21	BaMgAl ₁₀ O ₁₇ -Ce,Eu (1.5%,1.5%)	121	7.95	160	4.09
		209	8.03	340	26.8
22	BaMgAl ₁₀ O ₁₇ -Ce,Nd (0.5%,0.5%)	121	4.468	121	3.63
		340	20.21	340	20
23	BaMgAl ₁₀ O ₁₇ - Ce,Nd(1%,1%)	121	2.235	121	2.39
		340	8	340	12.5
24	BaMgAl ₁₀ O ₁₇ -Ce,Nd (1.5%,1.5%)	121	5.04	121	2.05
		153	3		
25	BaMgAl ₁₀ O ₁₇ -Eu,Mn (0.5%,0.5%)	209	28	209	25
		340	39	340	36
26	BaMgAl ₁₀ O ₁₇ -Eu,Mn (1%,1%)	161	3.5	121	1.17
		204, 350	19.5, 5.15	206	3.92
27	BaMgAl ₁₀ O ₁₇ -Eu,Mn (1.5%,1.5%)	211	5.08	209	4.76
		340	47.6		

Figures 4.2 .A Curves A,a B,b C,c

BaMgAl₁₀O₁₇: Eu (with Eu concentration 0.5, 1.0, 1.5 molar percentages) phosphors have been studied for their TL characteristics with a standard gamma doses of 7Gy. The observed glow curves are presented in figures 4.2 A curves A,a B,b C,c respectively.

Curve A,a are the TL of BaMgAl₁₀O₁₇: Eu with 0.5% . Curve A indicates TL of the phosphor immediately after gamma irradiation and curve 'a' denotes TL of the phosphor after 24 hours of gamma irradiation. The main TL peaks in the phosphor are 121,209 and 340°C. However after 24hours of irradiation the TL pattern did not change much except the disappearance of 340°C peak. From the table 4.2 the important point to be noted of these TL curves are the fading effect of the 121 and 209°C peaks are very less i.e the intensity of these peaks are not effected much however the 121 °C peak intensity remains nearly same The fading of 209°C peak is nearly 20%.

Curve B,b are the TL of BaMgAl₁₀O₁₇: Eu with 1.0% Curve B indicates TL of the phosphor immediately after gamma irradiation and curve 'b' denotes TL of the phosphor after 24 hours of gamma irradiation. The main TL peaks in the phosphor are 121 and 340°C. However after 24 hours of irradiation the TL pattern changed much i.e the emergence of 204°C peak and the disappearance of 340°C peak. From the table 4.2 the important points to be noted of these TL cures are the fading effect of the 121°C

peaks is very less. However the 121°C peak intensity remains nearly same with a reduction of intensity 10% after 24 hours of storage. The important point to be noted is the disappearance of 340°C peak and generation of 204°C peak.

Curves C,c are the TL of BaMgAl₁₀O₁₇: Eu with 1.5%. Curve C indicates TL of the phosphor immediately after gamma irradiation and curve 'c' denotes TL of the phosphor after 24 hours of gamma irradiation. The main TL peaks in the phosphor are 121, 209 and 340°C. However after 24 hours of irradiation the TL pattern did not change much except the reduction of TL intensities of 121 and 209°C peaks. From the table 4.2 the important point to be noted of these TL curves are the fading effect of the 121 and 209°C peaks are very high i.e the intensity of these peaks are reduced by 40%. The 340°C peak intensity remains nearly same.

The TL of BaMgAl₁₀O₁₇: Eu. When compared to all the Eu concentrations studied one main point to be noted is that the 121°C peak appears to be a strong. However it is not well resolved but the 209°C is a very well resolved one. It is very interesting to note that the doublet disappears and well defined dominant peak at 209°C appears. Besides this, the peak at 340°C appears, but with a higher intensity not resolved properly in all above cases. It seems that the isolated strong peak at 209°C develops at the cost of doublet and 340°C high temperature peak. It is believed that 209°C peak may be associated with the Eu impurity. One another point to be noted is irrespective of Eu concentration in the host matrix the 209°C peak remains as a well resolved one with high intensity in 4 cases of the above TL study.

Figures 4.2 .B Curves A,a B,b C,c

BaMgAl₁₀O₁₇: Ce (with Ce concentration 0.5, 1.0, 1.5 molar percentages) phosphors have been studied for their TL characteristics with a standard gamma doses of 7Gy. The observed glow curves are presented in figures 4.2 B curves A,a B,b C,c respectively.

Curve A,a are the TL of BaMgAl₁₀O₁₇: Ce with 0.5%. Curve A indicates TL of the phosphor immediately after gamma irradiation and curve 'a' denotes TL of the phosphor after 24 hours of gamma irradiation. The main TL peaks in the phosphor are 121 and 340°C. However after 24 hours of irradiation the TL pattern did not change much except the fall in TL intensities of 121 and 340°C peak about 15 to 20%. From

the table 4.2 the important point to be noted of these TL curves the fading effect of the 121 and 340°C peaks are very less i.e the intensity of these peaks are not effected much.

Curve B,b are the TL of BaMgAl₁₀O₁₇: Ce with 1.0% . Curve B indicates TL of the phosphor immediately after gamma irradiation and curve 'b' denotes TL of the phosphor after 24 hours of gamma irradiation. The main TL peaks in the phosphor are 121 and 340°C. However after 24 hours of irradiation the TL pattern did not change much expect the fall in TL intensities of 121 and 340°C peak about 10 to 20%. From the table 4.2 the important point to be noted of these TL curves, the fading effect of the 121 and 340°C peaks are very less i.e the intensity of these peaks are not effected much. However the 340°C peak is not well resolved it appears as a hump in most of the cases The peak at 121°C is a stable and well resolved one.

Curve C,c are the TL of BaMgAl₁₀O₁₇:Ce with 1.5% . Curve C indicates TL of the phosphor immediately after gamma irradiation and curve 'c' denotes TL of the phosphor after 24 hours of gamma irradiation. The main TL peaks in the phosphor are 121 and 340°C However after 24 hours of irradiation the TL pattern did not change much expect the fall in TL intensities of 121 and 340°C peak about 15 to 20%. From the table 4.2 the important point to be noted of these TL cure intensities are follows a regular pattern i.e the fading effect of the 121 and 340°C peaks are very less. However the 340°C peak is not well resolved it appears as a hump in most of the cases. The peak at 121°C is a stable and well-resolved one.

The TL (all curves) of BaMgAl₁₀O₁₇: Ce when compared to all the Ce concentrations studied one main point to be noted is that the 121°C peak appears to be a strong and a very well resolved one It is very interesting to note that the doublet peak at 340°C not resolved, but with a higher intensity in all above cases. It seems that the isolated strong peak at 121°C believed that it may be associated with the basic BaMgAl₁₀O₁₇ (BAM). The impurity Ce effect is not much seen in the present set of samples. One another point to be noted is irrespective of Ce concentration variation in the host matrix the 121°C peak remains as a well resolved one with good intensity in all 6 cases of the above TL study. Only the intensity of 121°C peak decreases by 15% with increase in Ce concentration.

Figures 4.2 .C Curves A,a B,b C,c

BaMgAl₁₀O₁₇: Nd (with Nd concentration 0.5, 1.0, 1.5 molar percentages) phosphors have been studied for their TL characteristics with a standard gamma doses of 7Gy. The observed glow curves are presented in figures 4 2.C curves A,a B,b C,c respectively.

Curve A,a are the TL of BaMgAl₁₀O₁₇: Nd with 0.5% . Curve A indicates TL of the phosphor immediately after gamma irradiation and curve 'a' denotes TL of the phosphor after 24 hours of gamma irradiation. The main TL peak in the phosphor is at 121°C and an unresolved peak around 340°C. However after 24hours of irradiation the TL pattern did not change much except the fall in TL intensities of 121°C peak about 5 %.

Curve B,b are the TL of BaMgAl₁₀O₁₇: Nd with 1.0% . Curve B indicates TL of the phosphor immediately after gamma irradiation and curve 'b' denotes TL of the phosphor after 24 hours of gamma irradiation. The main TL peak in the phosphor is at 121°C and an unresolved peak around 340°C. However after 24 hours of irradiation the TL pattern did not change much except the fall in TL intensities of 121°C peak about 50 % . However the TL intensity of 121°C peak is very high (around 100%) when compared to all Nd doped phosphors. However the 340°C peak is not well resolved it appears as a hump in most of the cases. The peak at 121°C is a stable and well-resolved one

Curve C,c are the TL of BaMgAl₁₀O₁₇.Nd with 1.5% . Curve C indicates TL of the phosphor immediately after gamma irradiation and curve 'c' describes the TL of the phosphor after 24 hours of gamma irradiation The main TL peaks in the phosphor are 121and 340°C. However after 24hours of irradiation the TL pattern did not change much except the fall in TL intensities of 121 and 340°C peak about 100 to 30% . However the 340°C peak is not well resolved it appears as a hump in most of the cases. The peak at 121°C is a stable and well-resolved one.

The TL (all curves) of BaMgAl₁₀O₁₇. Nd when compared to all the Nd concentrations studied one main point to be noted is that the 121°C peak appears to be a strong and a very well resolved one It is very interesting to note that the doublet peak at 340°C not

resolved, but with a higher intensity in all above cases. It seems that the isolated strong peak at 121°C believed that may be associated with the basic BaMgAl₁₀O₁₇ (BAM). The impurity Nd effect is seen only the increase and decrease in intensities in the present set of samples. One another point to be noted is irrespective of Nd concentration variation in the host matrix the 121°C peak remains as a well resolved one with good intensity in all 6 cases of the above TL study.

It is interesting to note that the lower temperature peak occurs at 121°C and it develops as well defined intense peak. This variation in intensity may be the property of Nd³⁺ impurity.

Figures 4.2 .D Curves A,a B,b C,c:

BaMgAl₁₀O₁₇: Pr (with Pr concentration 0.5, 1.0, 1.5 molar percentages) phosphors have been studied for their TL characteristics with a standard gamma doses of 7Gy. The observed glow curves are presented in figures 4.2 D curves A,a B,b C,c respectively

Curve A,a are the TL of BaMgAl₁₀O₁₇: Pr with 0.5% . Curve A indicates TL of the phosphor immediately after gamma irradiation and curve 'a' denotes TL of the phosphor after 24 hours of gamma irradiation. The main TL peak in the phosphor is at 121°C and an unresolved peak around 340°C. However after 24 hours of irradiation the TL pattern did not change much except the fall in TL intensities of 121°C peak about 12 %.

Curve B,b are the TL of BaMgAl₁₀O₁₇: Pr with 1.0% . Curve B indicates TL of the phosphor immediately after gamma irradiation and curve 'b' denotes TL of the phosphor after 24 hours of gamma irradiation. The main TL peak in the phosphor is at 121°C and an unresolved peak around 340°C. However after 24 hours of irradiation the TL pattern did not change much except the fall in TL intensities of 121°C peak about 50 %. However the TL intensity of 121°C peak increased (around 10%) when compared to Pr 0.5% doped phosphor One important point to be noted here is a hump at 170°C is observed the same disappeared after 24 hours of storage. However the 340°C peak is not well resolved it appears as a hump in most of the cases. The peak at 121°C is a stable and well-resolved one.

Curve C,c are the TL of BaMgAl₁₀O₁₇:Pr with 1.5% . Curve C indicates TL of the phosphor immediately after gamma irradiation and curve 'c' describes the TL of the phosphor after 24 hours of gamma irradiation. The main TL peaks in the phosphor are 121 and 340°C. However after 24 hours of irradiation the TL pattern did not change much except the fall in TL intensities of 121 and 340°C peak about 20%. Mostly the TL pattern follows as curve A,a and B,b.

The TL (all curves) of BaMgAl₁₀O₁₇: Pr when compared to all the Pr concentrations studied one main point to be noted is that the 121°C peak appears to be a strong and a very well resolved one. It is very interesting to note that the doublet peak at 340°C not

resolved, but with a higher intensity in all above cases. It seems that the isolated strong peak at 121°C believed that might be associated with the basic BaMgAl₁₀O₁₇ (BAM) The impurity Pr effect is not seen only the increase and decrease in intensities in the present set of samples

Figures 4.2 .E Curves A,a B,b C,c

BaMgAl₁₀O₁₇: Mn (with Mn concentration 0.5, 1.0, 1.5 molar percentages) phosphors have been studied for their TL characteristics with a standard gamma doses of 7Gy The observed glow curves are presented in figures 4.2 E curves **A,a B,b C,c** respectively.

From fig.4.2E and table Sr. No 14,15 and 16 it is evident that the TL of BaMgAl₁₀O₁₇: Mn with various Mn concentrations does not show any well resolved peaks but a doublet at 121 and 170°C followed by 340°C unresolved peak. However after 24 hours of irradiation the TL pattern did not change much except the fall in TL intensities of 121°C peak about 40 % It seems that the mixed peaks in the BaMgAl₁₀O₁₇ (BAM) Mn believed that might be associated with the basic impurity Mn effect. The above TL pattern is not seen in the other set of samples studied.

TL of double doped Phosphors

Figures 4.2 .F Curves A,a B,b C,c;

BaMgAl₁₀O₁₇: Ce,Mn (with Ce,Mn concentrations 0.5, 1.0, 1.5 molar percentages) phosphors have been studied for their TL characteristics with a standard gamma doses of 7Gy. The observed glow curves are presented in figures 4.2 F curves **A,a B,b C,c** respectively.

Curve A,a are the TL of BaMgAl₁₀O₁₇: Ce,Mn with 0.5% . Curve A indicates TL of the phosphor immediately after gamma irradiation and curve 'a' denotes TL of the phosphor after 24 hours of gamma irradiation. The main TL peak in the phosphor is at 121°C and an unresolved peak around 340°C. However after 24hours of irradiation the TL pattern did not change much except the fall in TL intensities of 121°C peak about 15 % and 340°C peak by 3%. Curve B,b are the TL of BaMgAl₁₀O₁₇ Ce,Mn with 1.0% . Curve B indicates TL of the phosphor immediately after gamma irradiation and curve

'b' denotes TL of the phosphor after 24 hours of gamma irradiation. The main TL peak in the phosphor is at 121°C and an unresolved peak around 340°C. However after 24 hours of irradiation the TL pattern did not change much except the fall in TL intensities of 121°C peak about 20 %. However the TL intensity of 121°C peak remains same (around 5% less) when compared to Ce,Mn 0.5% doped phosphor. One important point to be noted here is a hump at 165°C is observed after 24 hours of storage. However the 340°C peak is not well resolved it appears as a hump in most of the cases. The peak at 121°C is a stable and well-resolved one.

Curve C,c are the TL of BaMgAl₁₀O₁₇: Ce,Mn with 1.5% . Curve C indicates TL of the phosphor immediately after gamma irradiation and curve 'c' describes the TL of the phosphor after 24 hours of gamma irradiation. The main TL peak is around 209°C in the phosphor and 121 and 340°C peaks look like humps or siblings. However after 24 hours of irradiation the TL pattern did not change much except the fall in TL intensities of 209°C peak about 5%.

The TL (all curves) of BaMgAl₁₀O₁₇: Ce,Mn when compared to all the Ce,Mn concentrations studied one main point to be noted is that the 121°C peak appears to be a strong and a very well resolved one in the single dopants but in the present case it appears as a hump in Ce,Mn 1.5% concentrations and a main peak at 209°. It seems that the isolated strong peak at 209°C believed that might be associated with the BaMgAl₁₀O₁₇: Ce,Mn (1.5%). It is clearly observed that, the TL pattern displays two humps around 121°C and 340°C. The main peak at 209°C develops and appears as a strong peak. It is interesting to note that, peak at 209°C may be the combined effect of Ce,Mn

Figures 4.2 .G Curves A,a B,b C,c

BaMgAl₁₀O₁₇: Ce,Eu (with Ce,Eu concentration 0.5, 1.0, 1.5 molar percentages) phosphors have been studied for their TL characteristics with a standard gamma dose of 7Gy. The observed glow curves are presented in figures 4.2 G curves A,a B,b C,c respectively.

From fig.4 2G and table Sr. No 19,20 and 21 it is evident that the TL of $\text{BaMgAl}_{10}\text{O}_{17}:\text{Ce,Eu}$ with various Ce, Eu concentrations does not show any well resolved peaks but a doublet at 121 and 170°C followed by 340°C unresolved peak. However after 24 hours of irradiation the TL pattern did not change much except the fall in TL intensities of 121°C peak about 40 %. It appears the effect of double doping of BAM leads the over all TL pattern change many peaks formed and merged after 24hours storage.

It seems that the mixed peaks in the $\text{BaMgAl}_{10}\text{O}_{17}(\text{BAM})\cdot\text{Ce,Eu}$ believed that might be associated with the basic impurity Ce, Eu effect. The above TL pattern is not seen in the other set of samples studied.

Figures 4.2 .H Curves A,a B,b C,c

$\text{BaMgAl}_{10}\text{O}_{17}:\text{Ce,Nd}$ (with Ce,Nd concentration 0.5, 1.0, 1.5 molar percentages) phosphors have been studied for their TL characteristics with a standard gamma doses of 7Gy. The observed glow curves are presented in figures 4.2 H curves A,a B,b C,c respectively.

From fig.4.2H and table Sr. No 22,23 and 24 it is evident that the TL of $\text{BaMgAl}_{10}\text{O}_{17}:\text{Ce,nd}$ with various Ce, Nd concentrations does not show any well resolved peaks but a doublet at 121 and 170°C followed by 340°C unresolved peak. However after 24 hours of irradiation the TL pattern did not change much except the fall in TL intensities of 121°C peak about 40 %. It appears the effect of double doping of BAM leads the over all TL pattern change many peaks formed and merged after 24hours storage It is one interesting point to be noted is in BAM doped with Ce,Nd 1.5% the peak at 121°C appears well resolved followed by 154°C peak.

It seems that the mixed peaks in the $\text{BaMgAl}_{10}\text{O}_{17}(\text{BAM})\cdot\text{Ce,Nd}$ believed that might be associated with the basic impurity Ce, Nd effect. The above TL pattern is seen in the other set of samples studied i.e BAM Ce,Eu.

Figures 4.2 .I Curves A,a B,b C,c

BaMgAl₁₀O₁₇: Eu, Mn (with Eu, Mn concentration 0.5, 1.0, 1.5 molar percentages) phosphors have been studied for their TL characteristics with a standard gamma doses of 7Gy. The observed glow curves are presented in figures 4.2 I curves A,a B,b C,c respectively.

From fig 4 2I and table Sr No 25,26 and 27 it is evident that the TL of BaMgAl₁₀O₁₇. Eu, Mn with various Eu, Mn concentrations does not show any well resolved peaks but a doublet at 200°C followed by above 300°C unresolved peak. However after 24 hours of irradiation the TL pattern did not change much except the fall in TL intensities of 200°C peak about 40 %. It appears the effect of double doping of BAM leads the over all TL pattern change many unresolved peaks formed and merged after 24 hours storage. It is one interesting point to be noted is in BAM doped with Eu, Mn 0 5% the peak at 209°C appears well resolved followed.

It seems that the mixed peaks in the BaMgAl₁₀O₁₇ (BAM): Eu, Mn believed that might be associated with the basic impurity Eu, Mn effect. The above TL pattern is seen in the other set of samples studied expect BAM Ce, Eu.

The TL behavior of the prominent peaks exhibited by RE, NRE, RE·RE and RE.NRE impurities doped BaMg aluminates is mixed behavior The main peaks at 121 and 340°C are not well resolved in double dopants.

Thermoluminescence (TL) Emission Studies:

The TL emission spectra of three samples consisting the well resolved peaks are studied (BaMgAl₁₀O₁₇: Eu 1%, BaMgAl₁₀O₁₇: Mn 1% and BaMgAl₁₀O₁₇: Eu.Mn 1 5%). The same are presented in Fig. 4.3.A and 4.3.B The dimmer stat was used to maintained constant temperature. The scanning speed, duration and range chosen for recording emission spectrum were 12.2 second, 2 to 4 nm and 350 nm to 700nm wavelengths, respectively. The standard gamma dose subjected to specimen prior to the record of TL-emission spectrum was 7Gy. The range of temperature 100 to 400°C was selected for the record of TL emission spectrum.

- i) The phosphor $\text{BaMgAl}_{10}\text{O}_{17}:\text{Eu}$ shows a broad emission peaking around 400nm followed by 500nm and 600nm. Between them larger wavelength peak, emission (400nm) is observed with higher intensity than the smaller one (500 nm), figure 4.3.A
- ii) The emission spectrum displayed in fig. 4.3.B (A5b) gives TL emission at temperature of main peak observed in $\text{BaMgAl}_{10}\text{O}_{17}:\text{Mn}$. It shows a good peak around 516 nm.
- iii) TL-emission spectra exhibited by Eu and Mn impurities doped $\text{BaMgAl}_{10}\text{O}_{17}$ specimens are presented in figures Fig 4.3B (A 9 C). It is significant to note that well defined emission peaks around 516nm in Eu, Mn activated $\text{BaMgAl}_{10}\text{O}_{17}$.

From the TL emission studies (figure 4.3 A) it is evident that the $\text{BaMgAl}_{10}\text{O}_{17}$ activated with Eu^{2+} gives emission in the entire visible range the same is observed

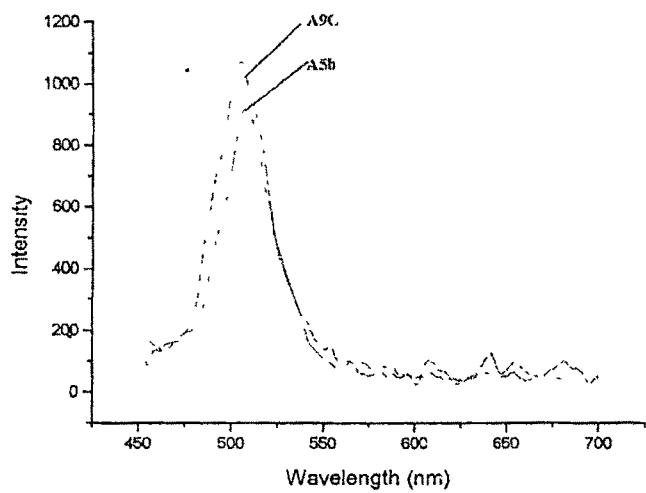
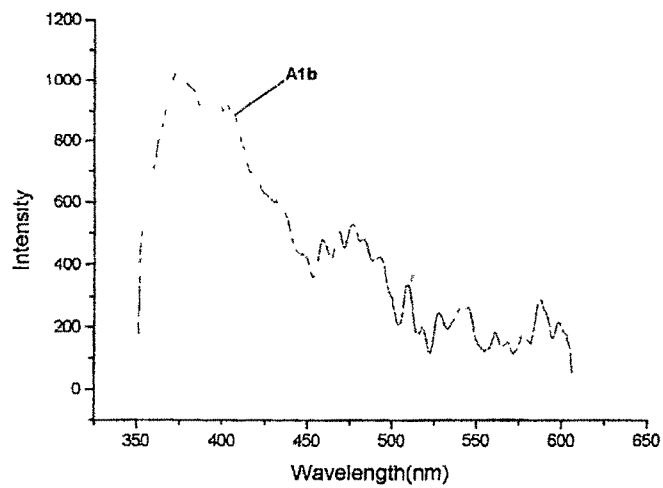


Fig.4.3 A. A1bTL Emission Spectrum of $\text{BaMgAl}_{10}\text{O}_{17}:\text{Eu}$ (1.0%)

**Fig.4.3.B A5b. TL Emission Spectrum of $\text{BaMgAl}_{10}\text{O}_{17}:\text{Mn}$ (1.0%)
A9c.TL Emission Spectrum of $\text{BaMgAl}_{10}\text{O}_{17}:\text{Eu, Mn}$ (1.0%)**

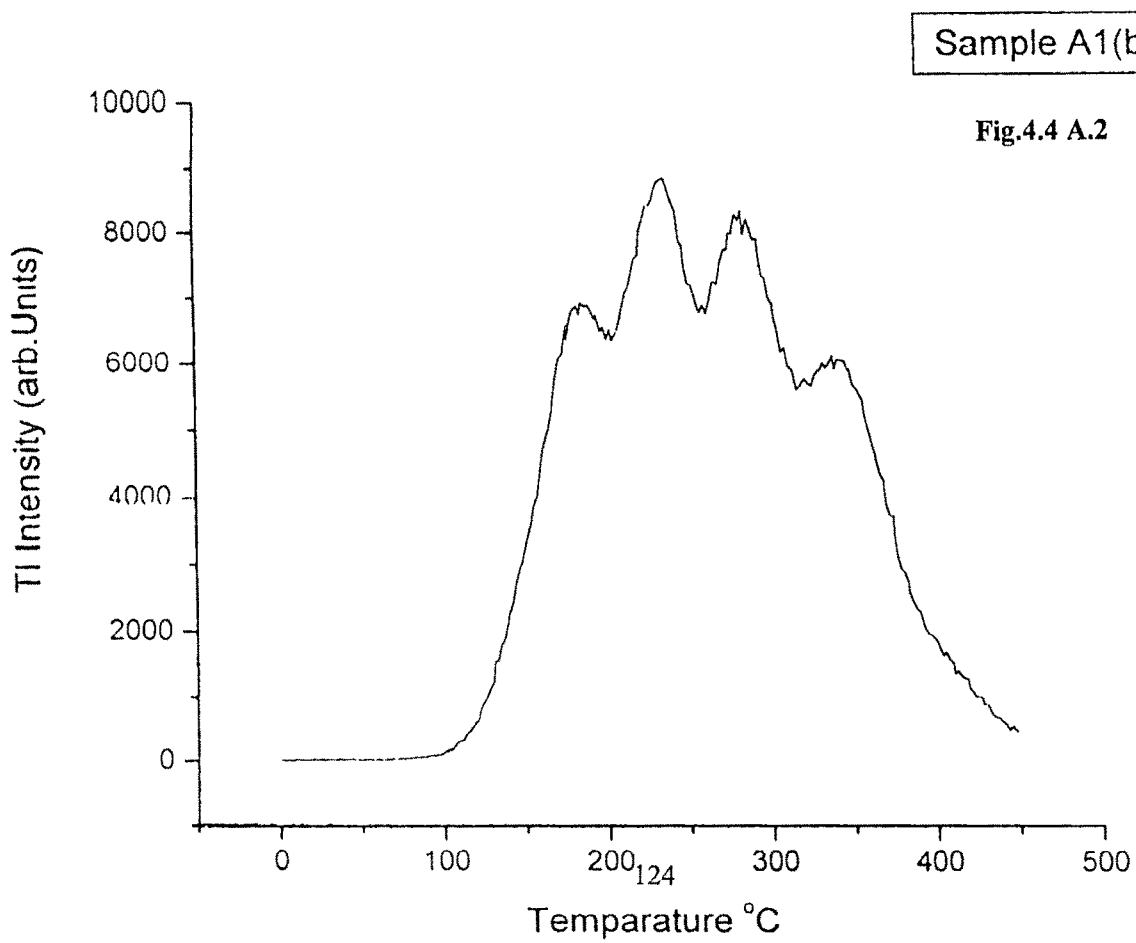
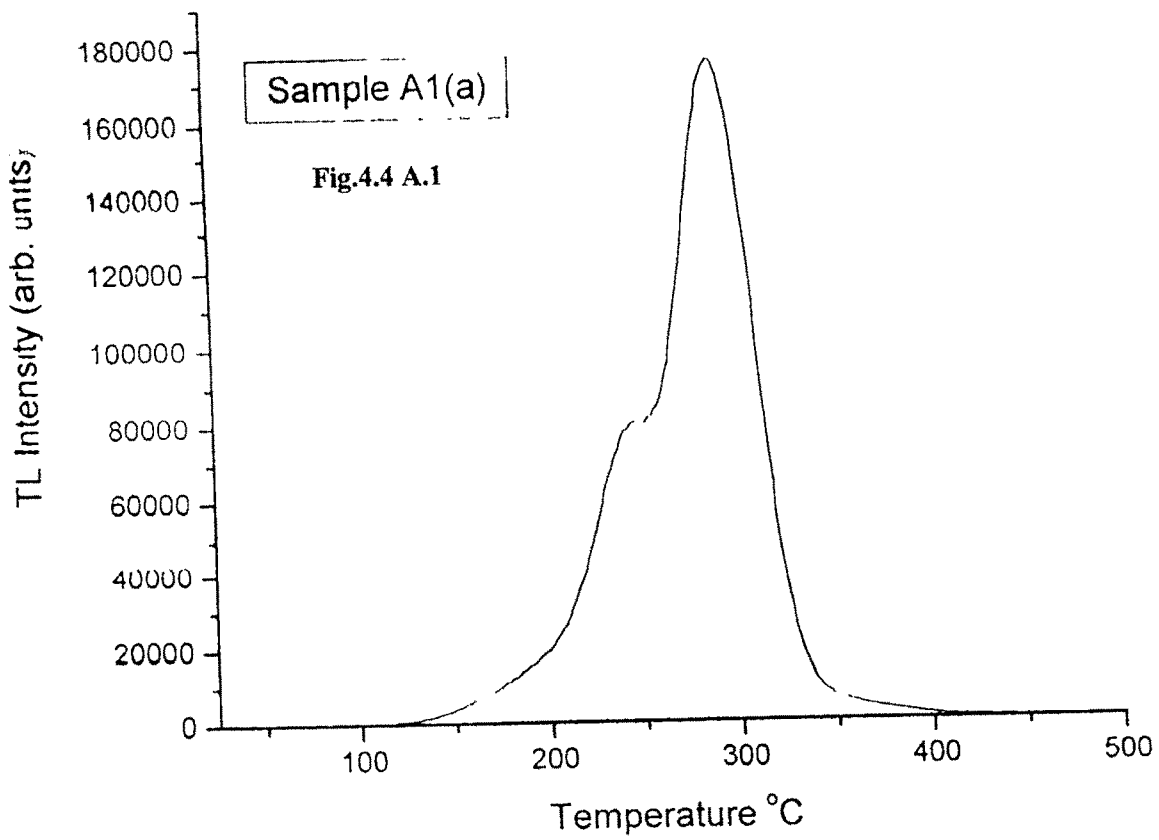
From the TL emission studies (4.3.B Curve A5b) it is evident that the $\text{BaMgAl}_{10}\text{O}_{17}$ activated with Mn^{2+} gives emission in the blue green region the same is observed. From the TL emission studies it is evident that the $\text{BaMgAl}_{10}\text{O}_{17}$ activated with Eu^{2+} , Mn^{2+} gives emission at 516nm (4.3.B Curve A9c) with higher intensity followed by 610 and 640nm emissions. It is evident from the figures of TL emission that the 516nm emission is more for Eu, Mn specimen followed by few red lines. Since the effect of Temperature on Eu emission is studied by Iwama and Takawa. The same result is observed in case of Eu, Mn doped BAM.

Thermoluminescence studies of β irradiated Specimens:

The thermoluminescence of beta irradiated prepared lamp phosphors is presented here. The TL glow curves of the various impurity doped BaMg aluminates have been recorded in the temperature range 25° to 450°C with uniform heating rate (6.6°C/sec). The phosphors have been given a test dose 7Gy beta doses. The TL of beta irradiated sample exhibited by the phosphors are given as Fig 4.4 A to 4.2.I and also in the tabular form. Table –3 containing the TL of β - irradiated samples immediately after irradiation. The TL studies of β - irradiated samples are recorded using the RISO TL/OSL system described by Mohan Chougankar et al.,

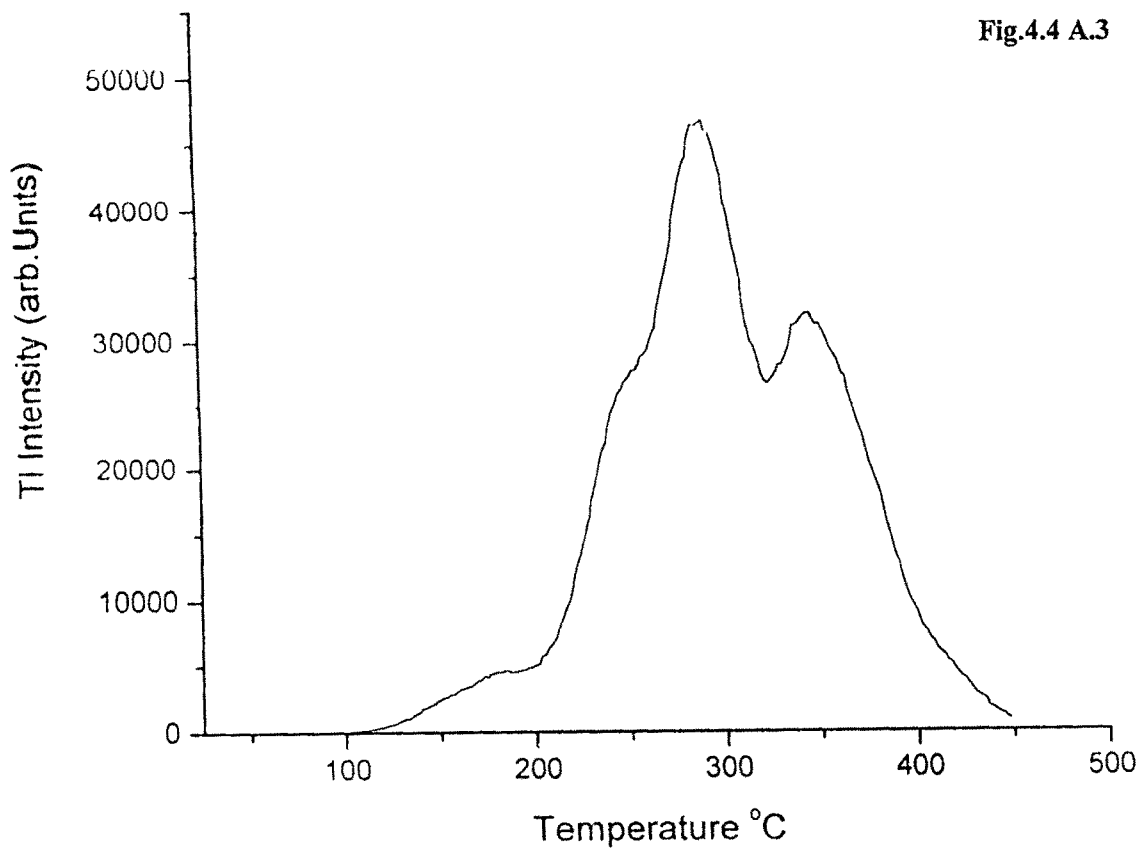
Though all these are main peaks, in all cases they do not appear as isolated peaks on account of appearance and disappearance of few new peaks or shoulders or humps or siblings in the neighborhood of isolated main glow peak. It is known that the glow curve shape and peak temperatures of a given BaMg -aluminates are different depending on the impurities and quantity introduced in the host material. In this context, the assignment of the particular temperature to a TL glow peak may appear somewhat arbitrary. In spite of this the above mentioned peak temperatures are typical and these have been used to identify the glow peaks. The intensity of the glow peaks is given in counts. The characteristics glow curves obtained for the phosphors under investigations presented as follows

Figures 4.4 .A 1,2,3:BaMgAl₁₀O₁₇: Eu (with Eu concentration 0.5, 1.0, 1.5 molar percentages) phosphors have been studied for their TL characteristics with a standard beta doses of 7Gy from a strontium-90 source. The observed glow curves are presented in figures 4.4 A 1,2,3 respectively.



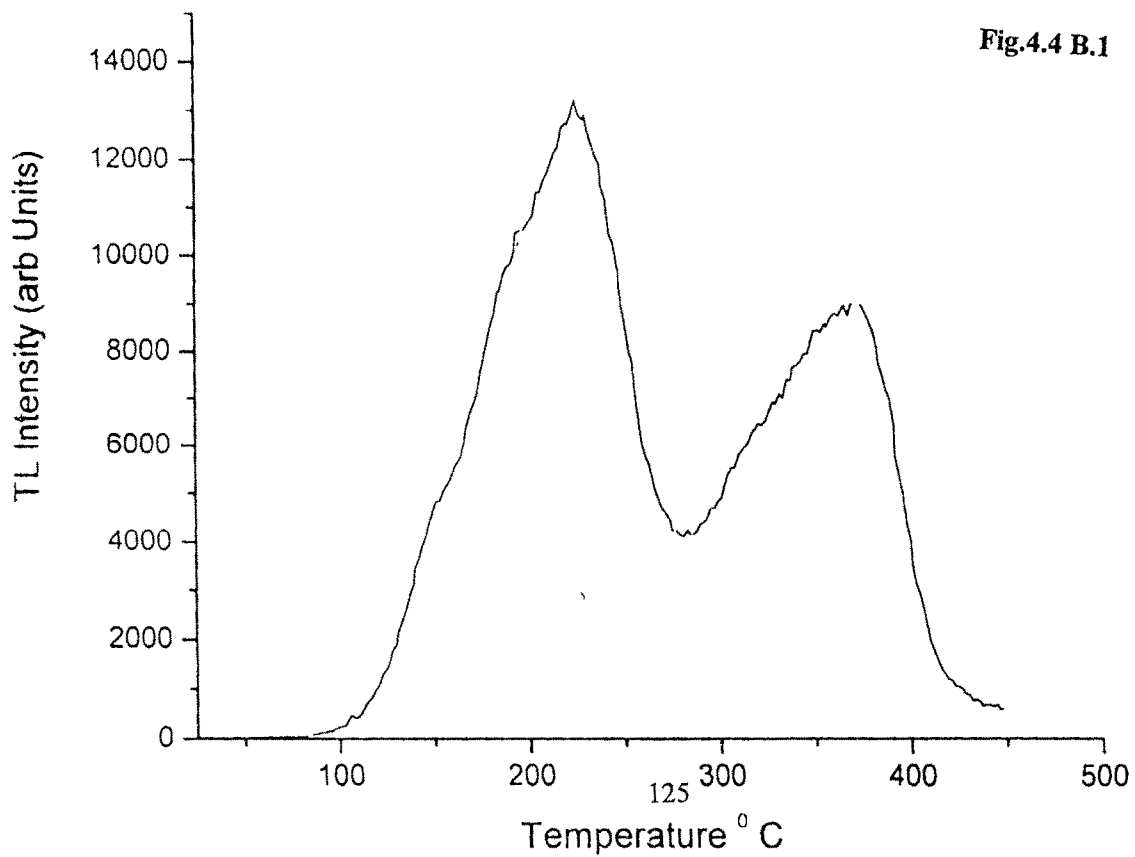
Sample A1(c)

Fig.4.4 A.3



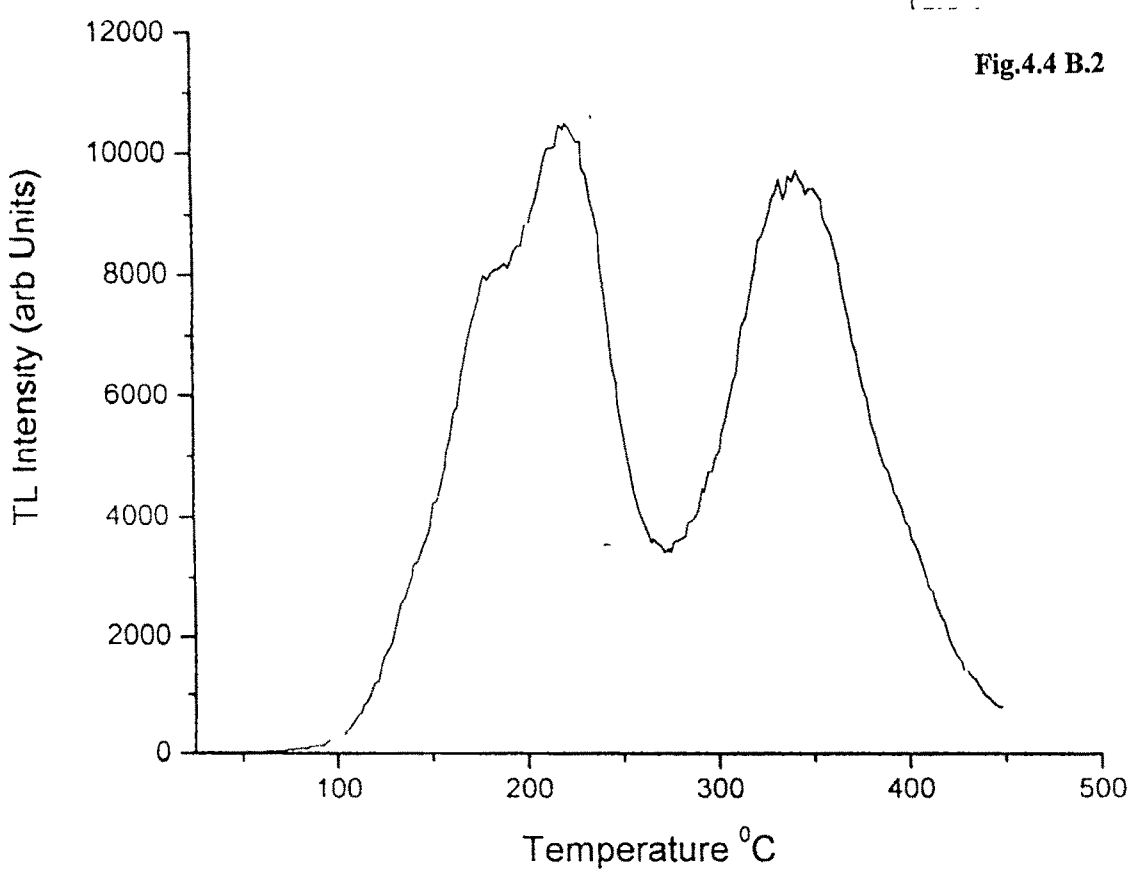
Sample A2(a)

Fig.4.4 B.1



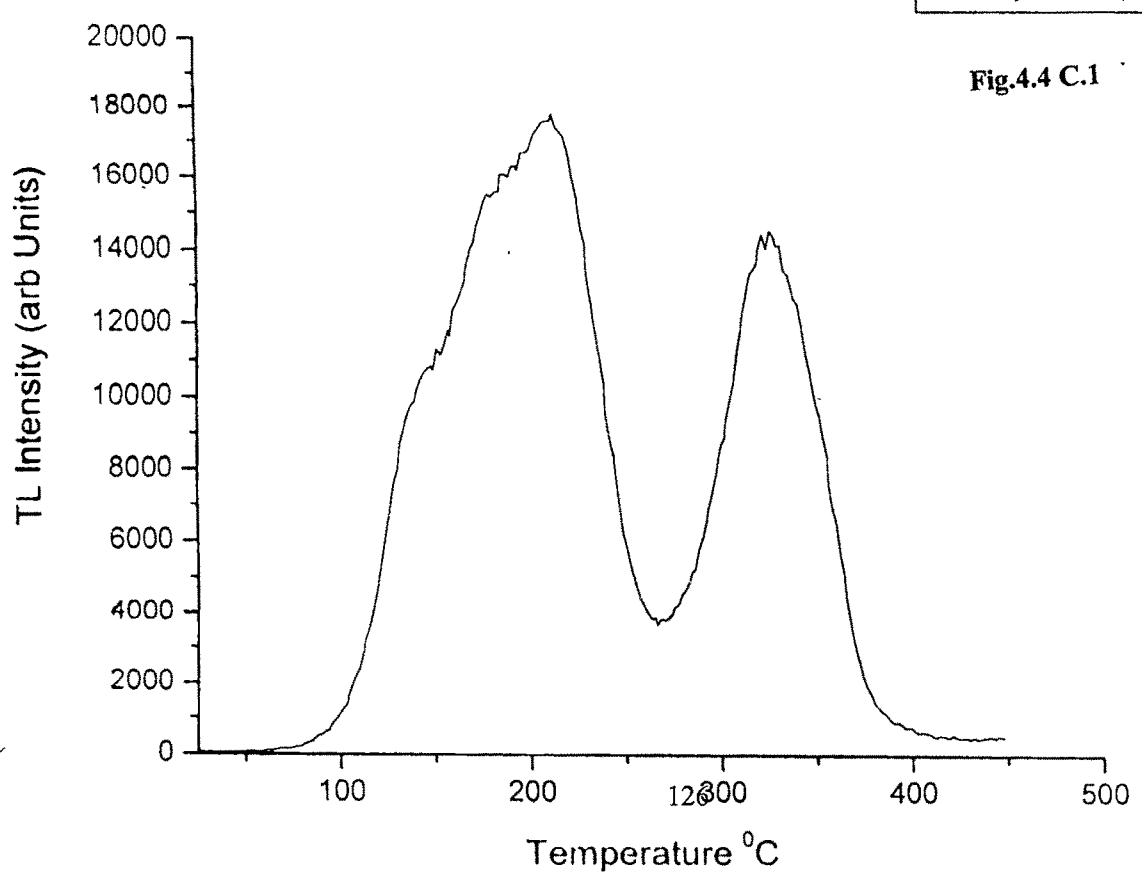
Sample A2(b)

Fig.4.4 B.2

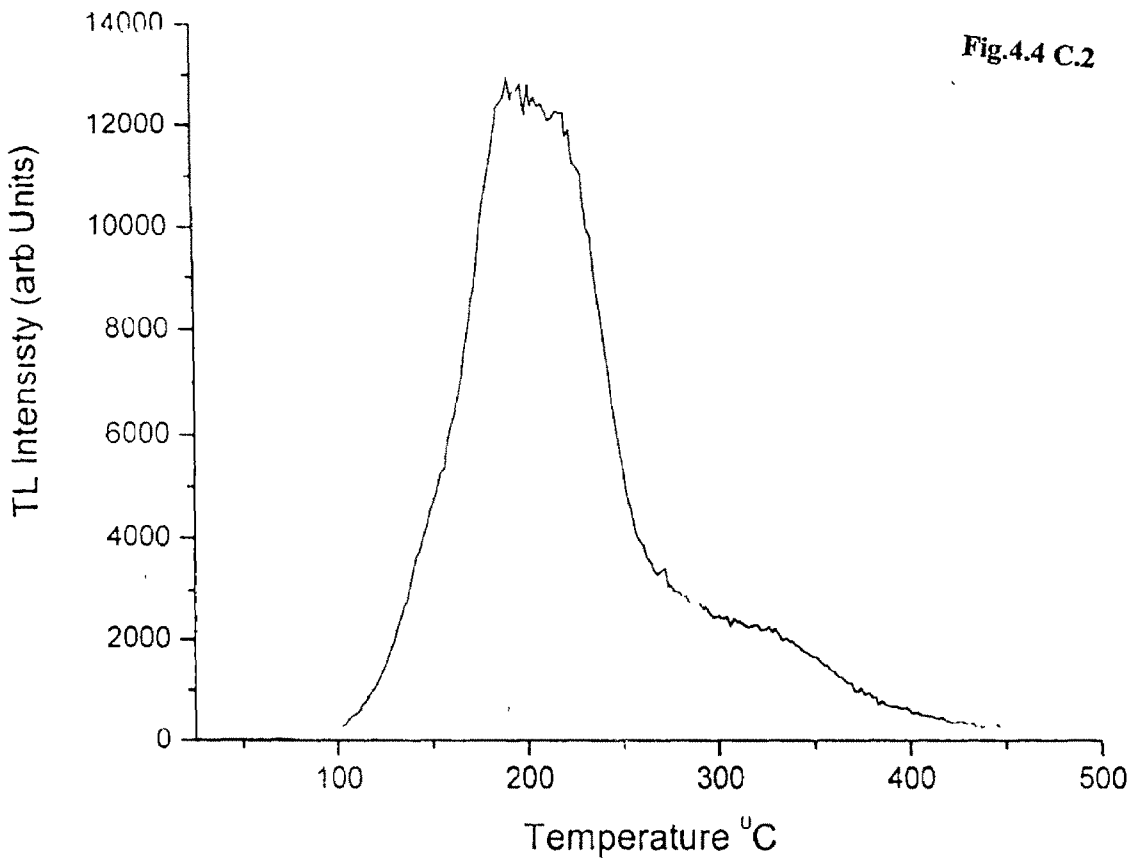


Sample A3(a)

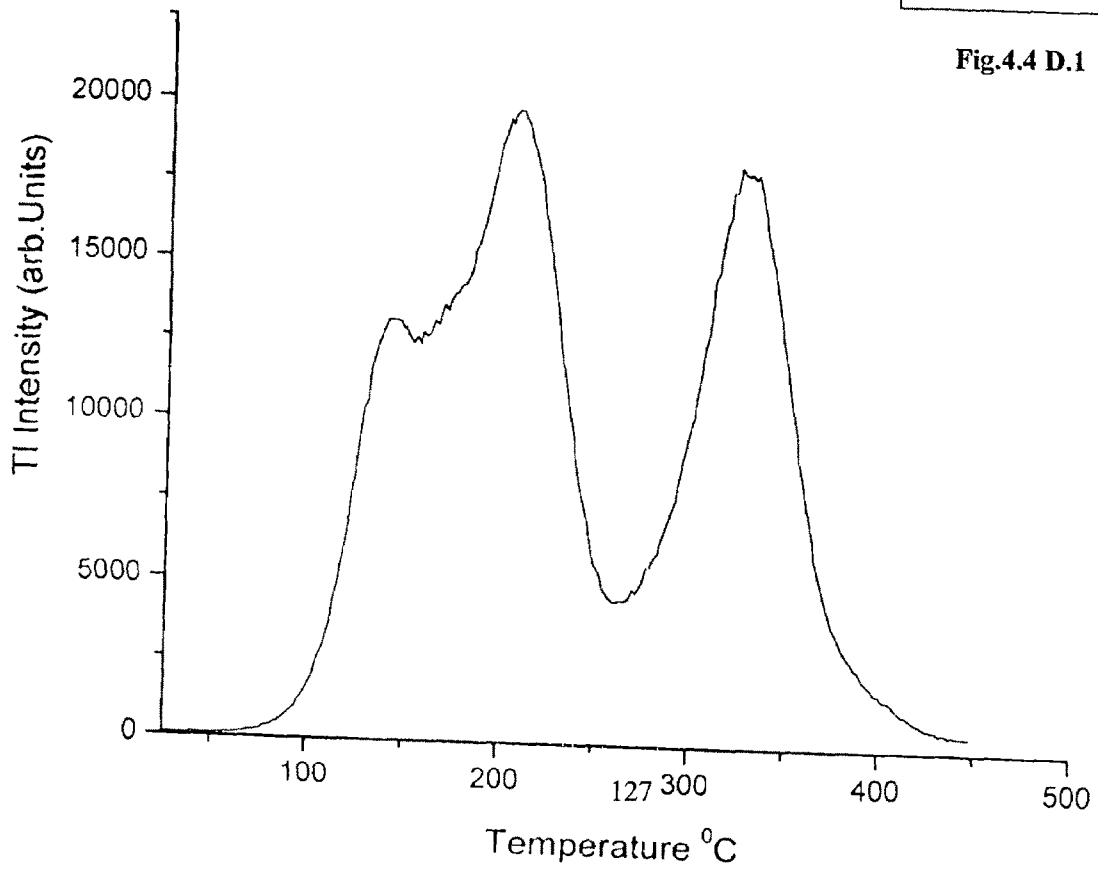
Fig.4.4 C.1



Sample A3(b)

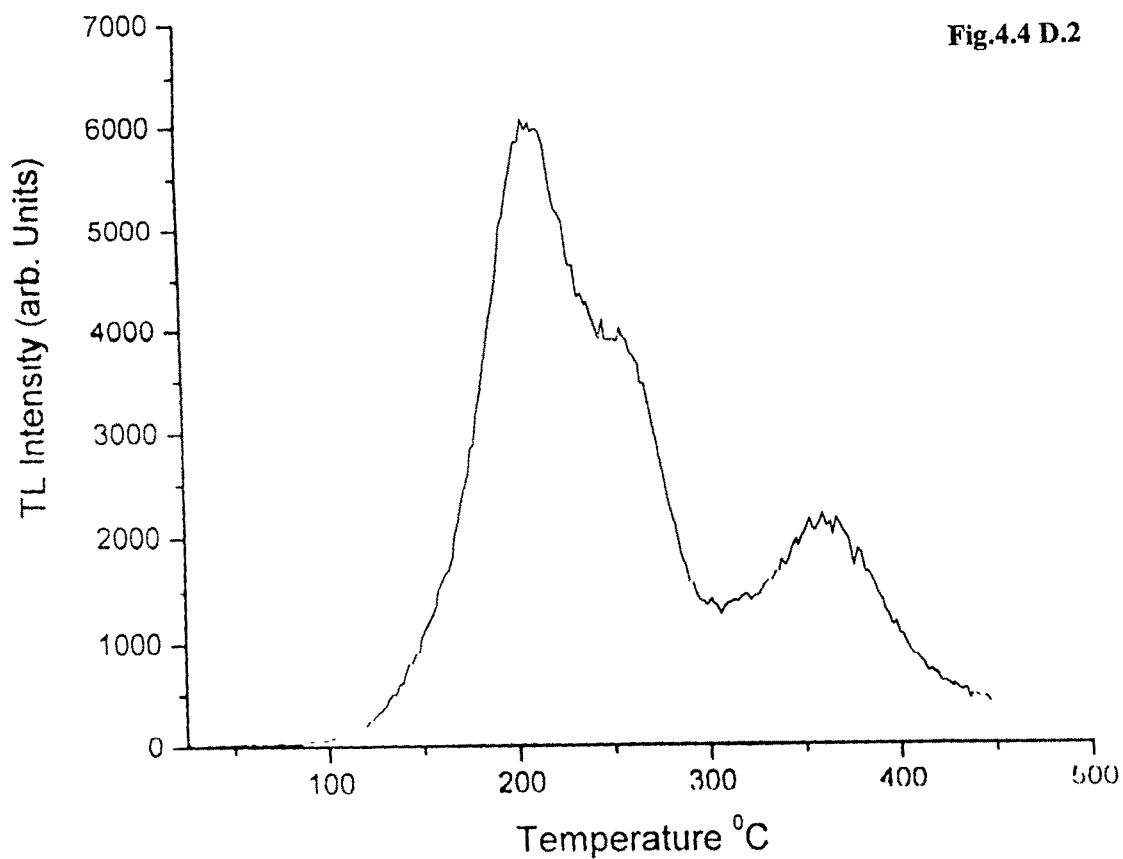


Sample A4(a)



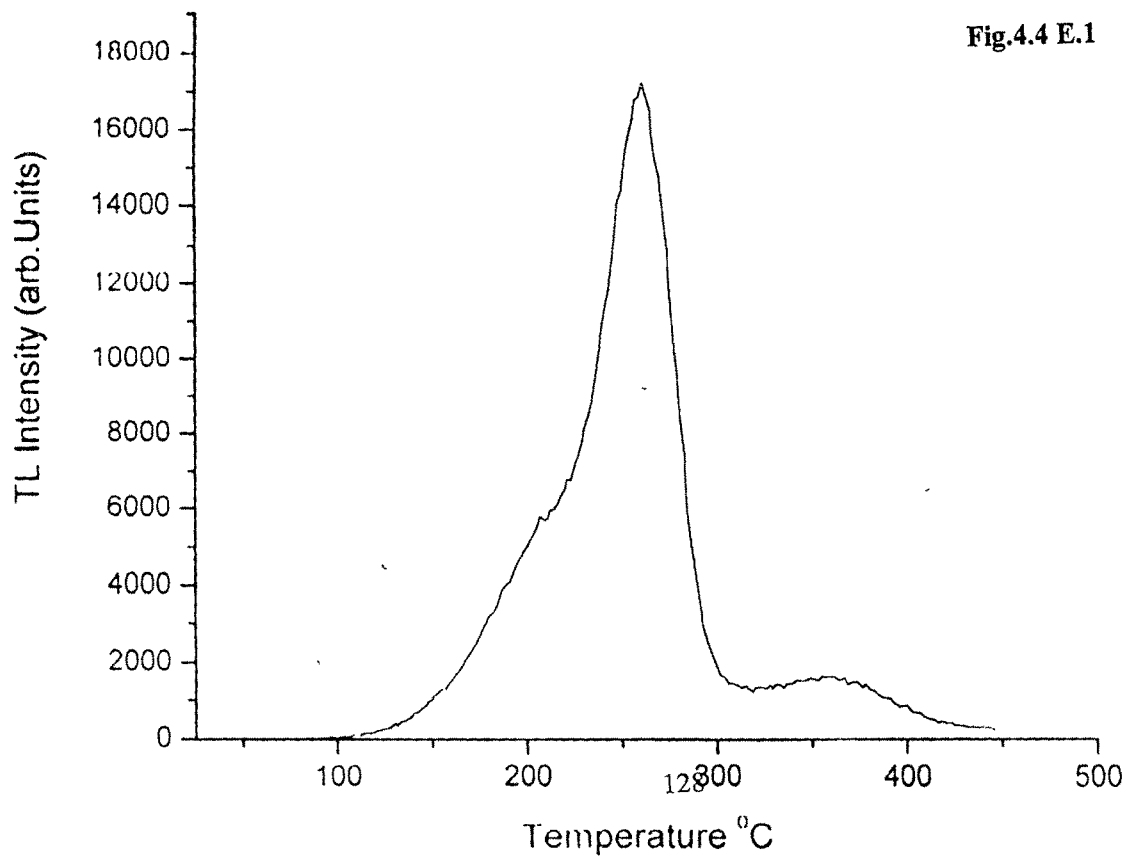
Sample A4(b)

Fig.4.4 D.2



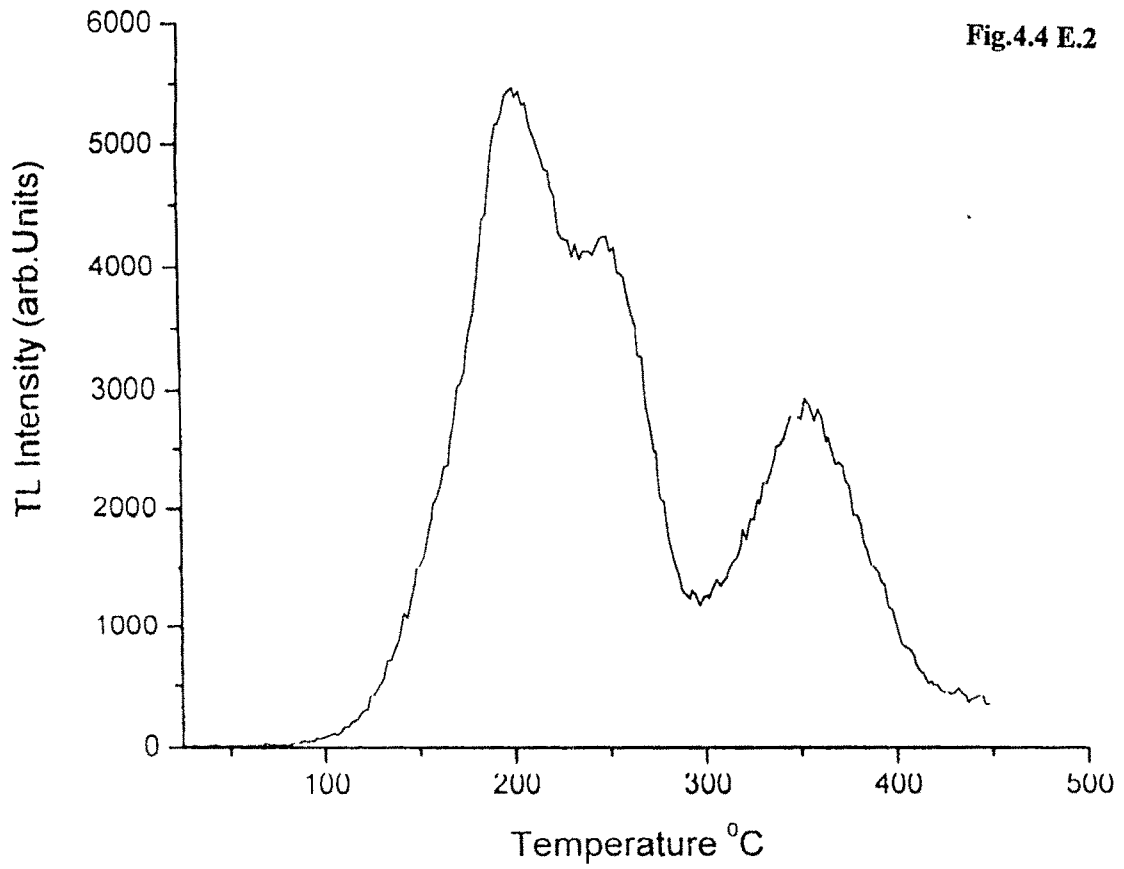
Sample A5(a)

Fig.4.4 E.1



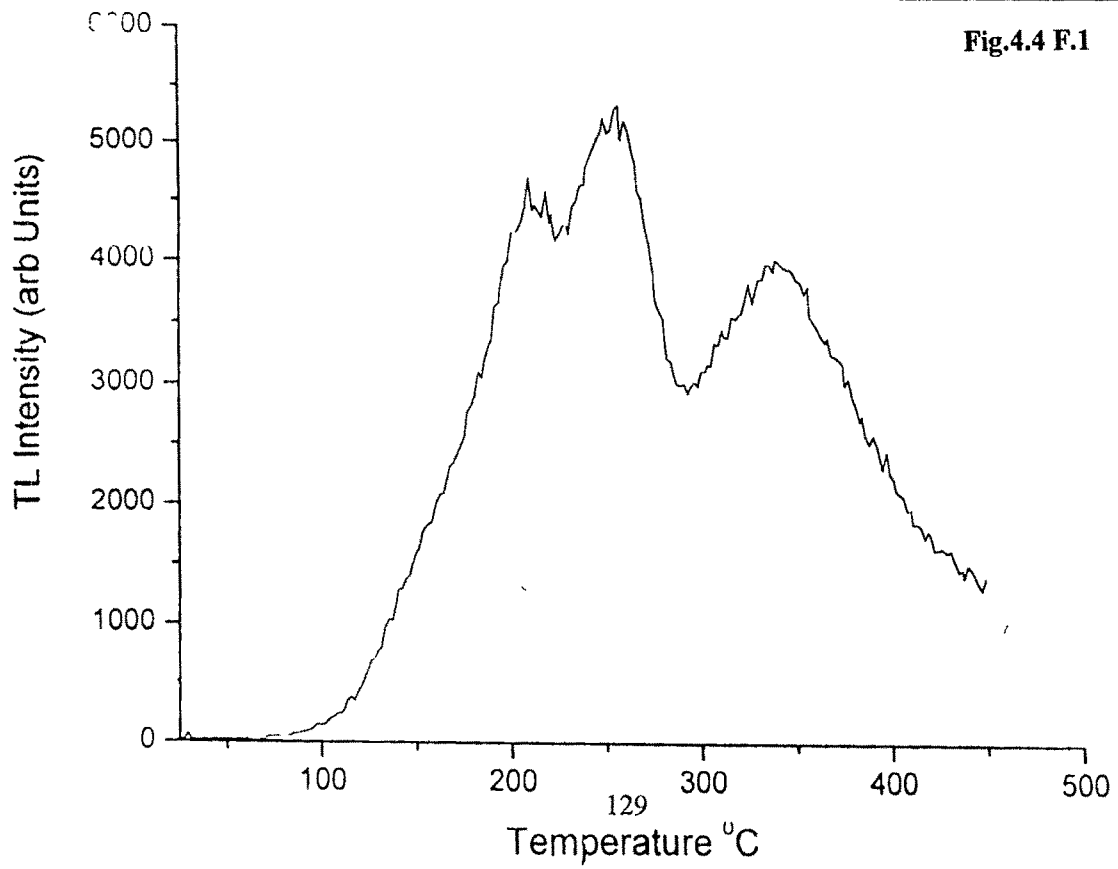
Sample A5(b)

Fig.4.4 E.2



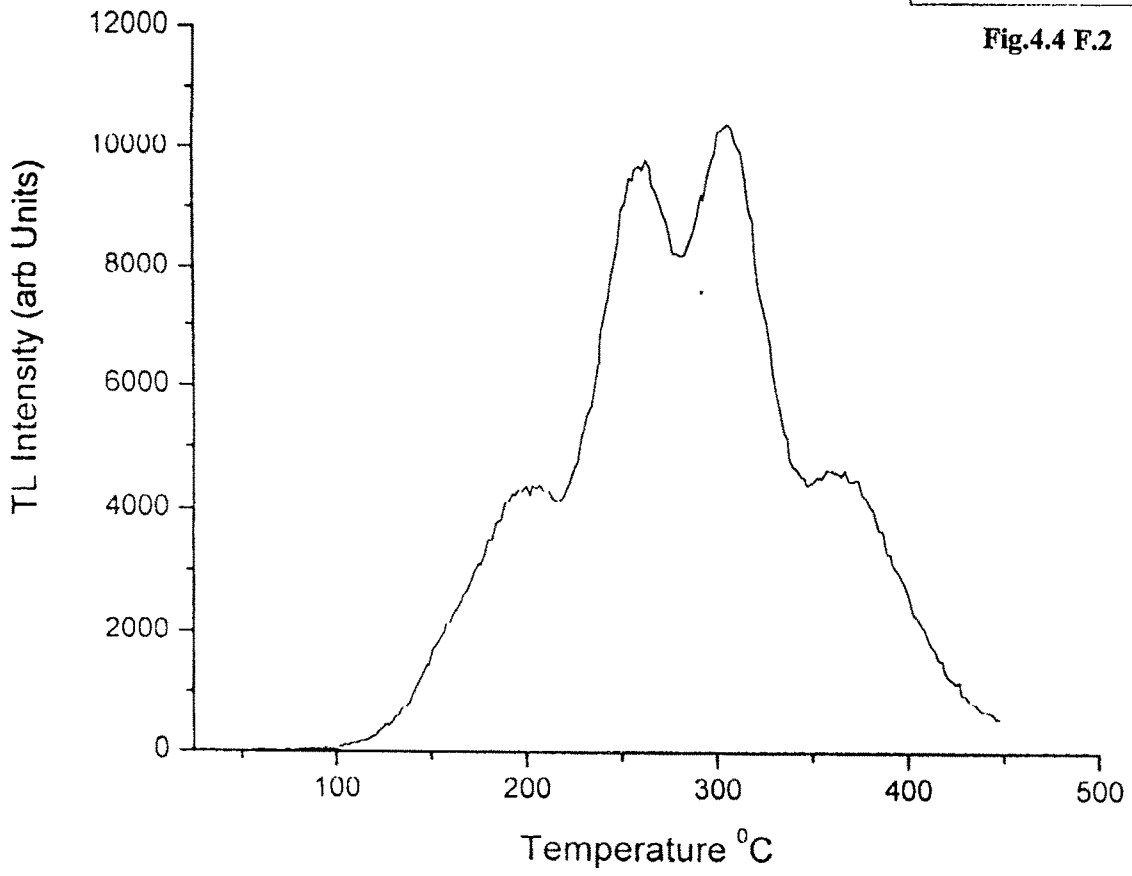
Sample A 6(a)

Fig.4.4 F.1



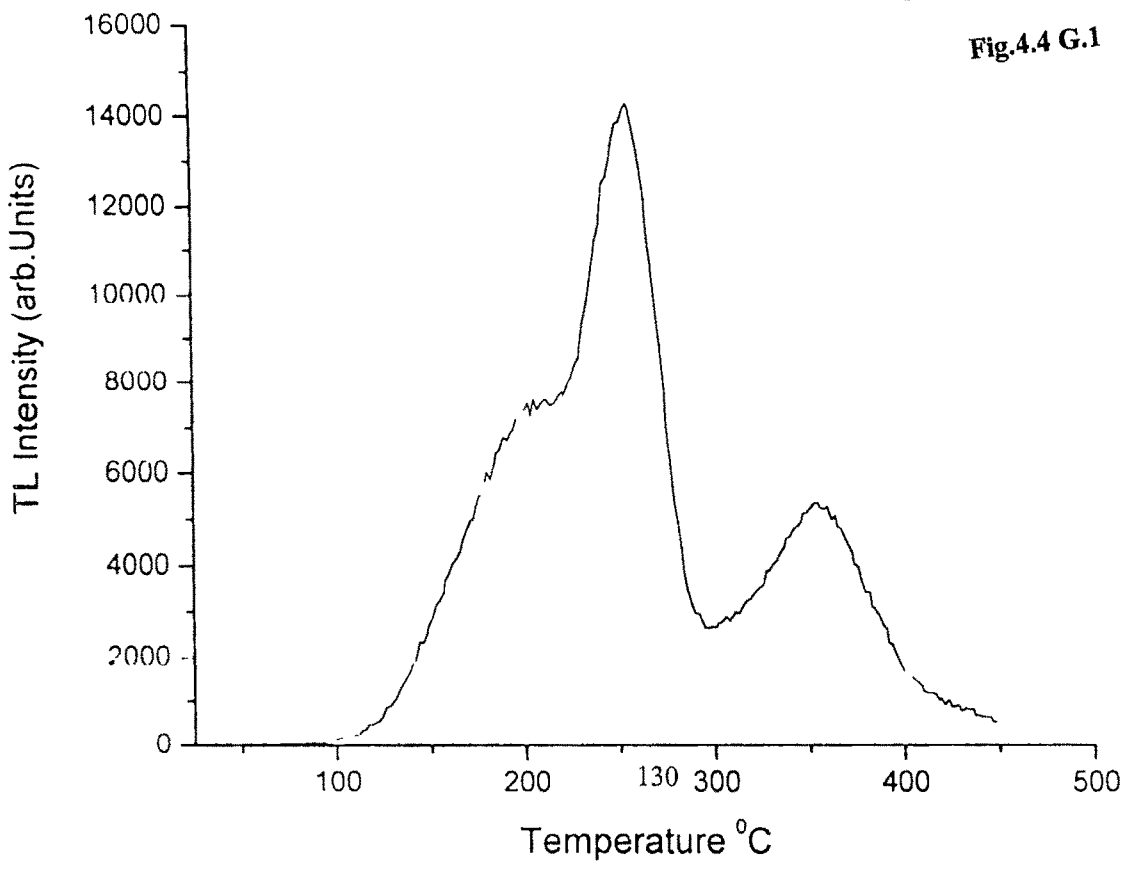
Sample A6(b)

Fig.4.4 F.2



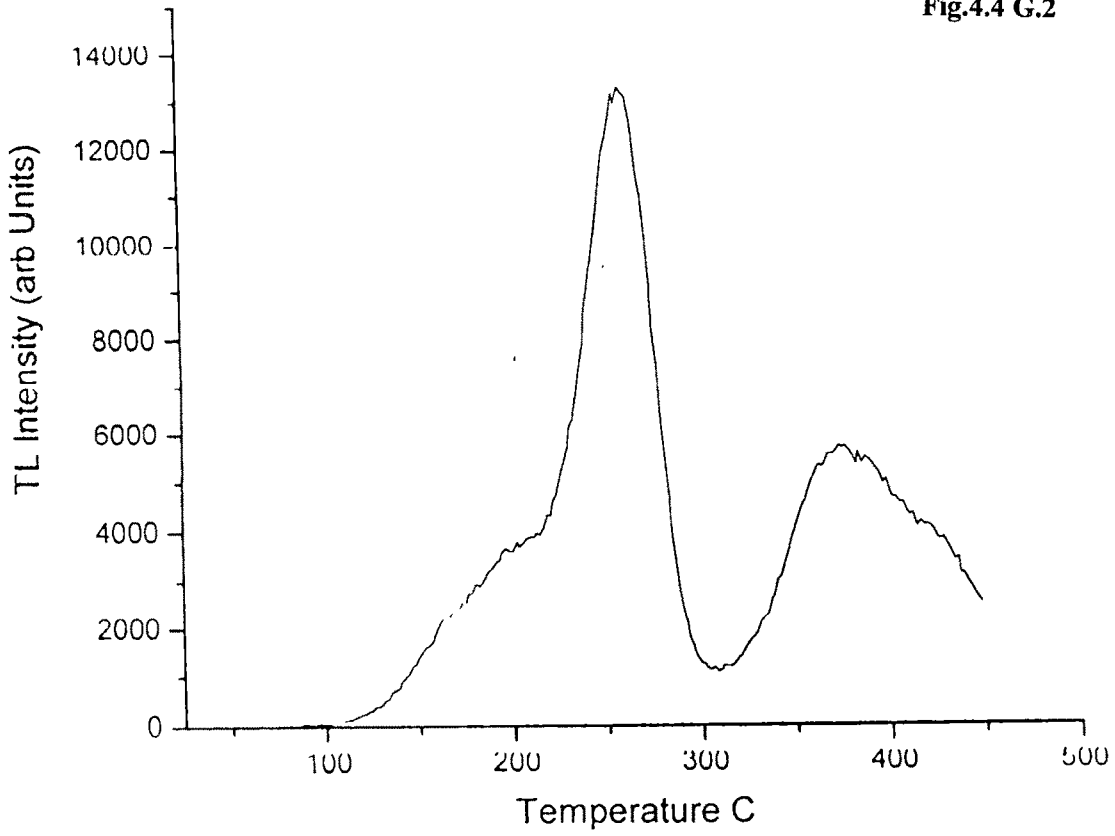
Sample A7(a)

Fig.4.4 G.1



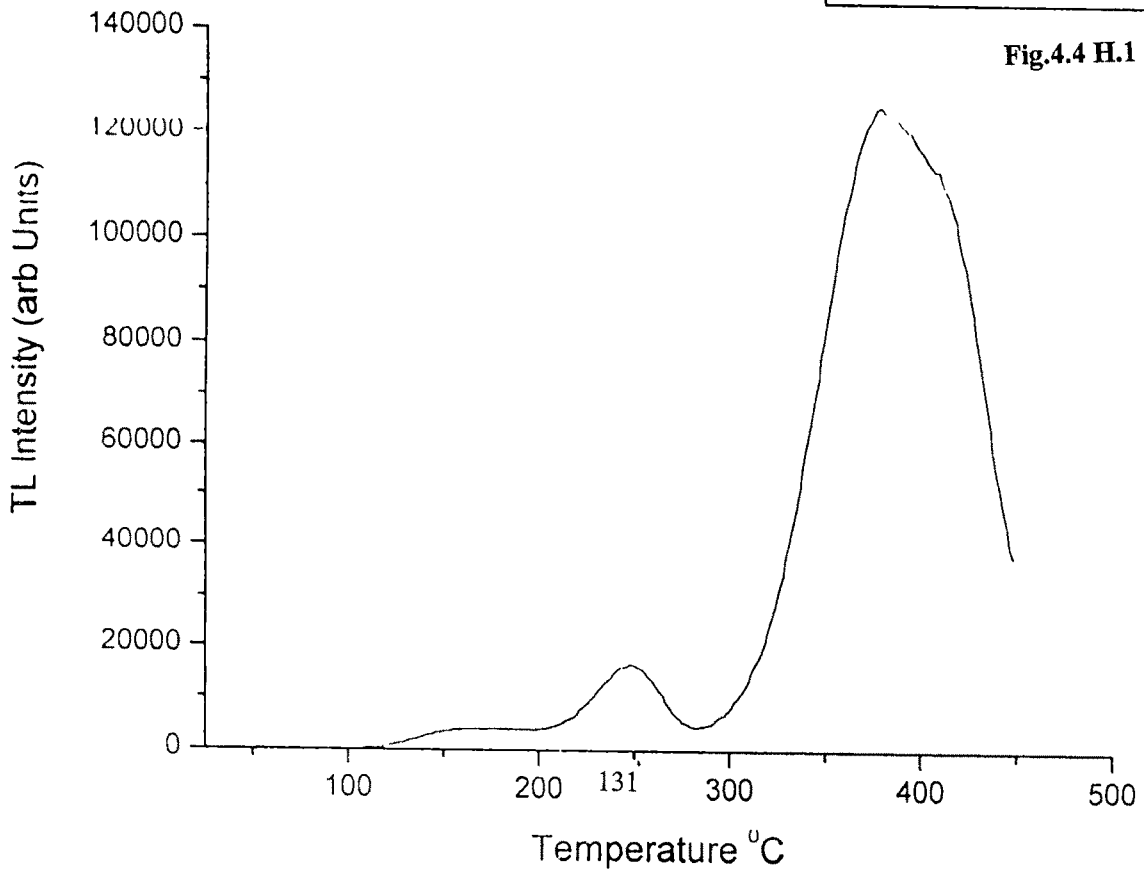
Sample A7(b)/7/8/2003

Fig.4.4 G.2



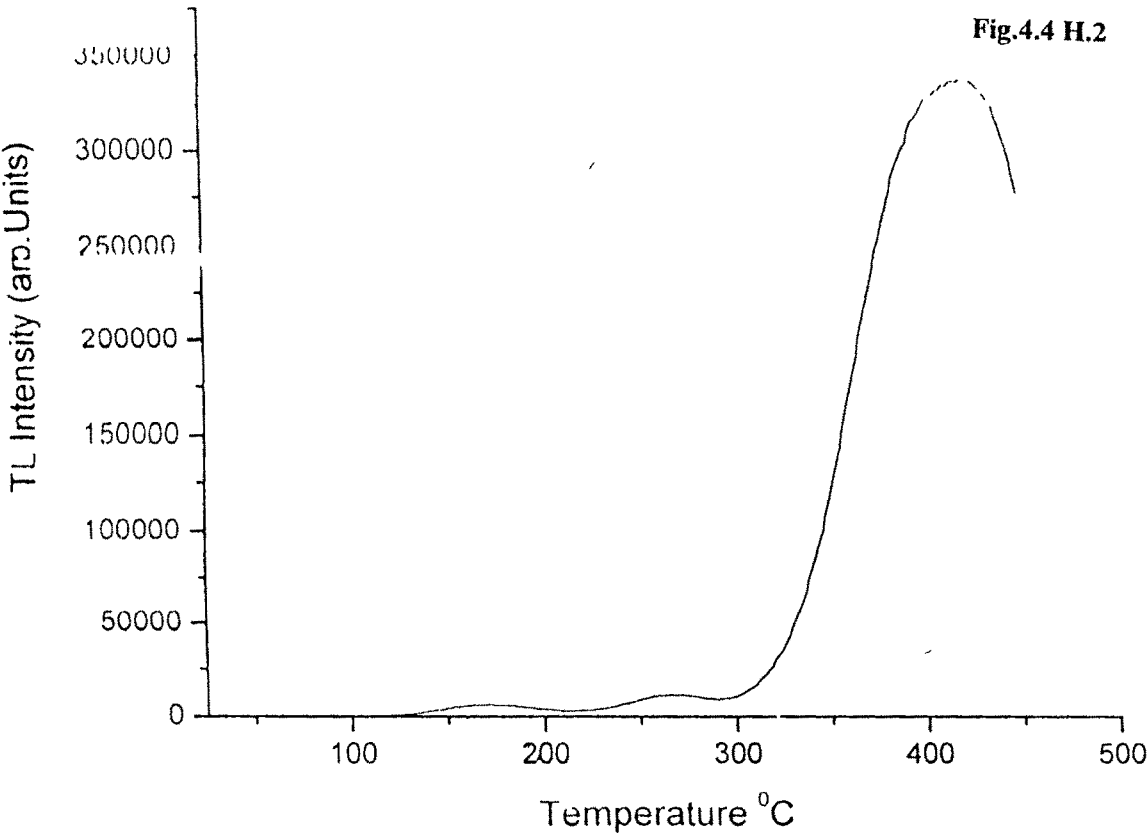
Sample A8(a)/7/8/2003

Fig.4.4 H.1

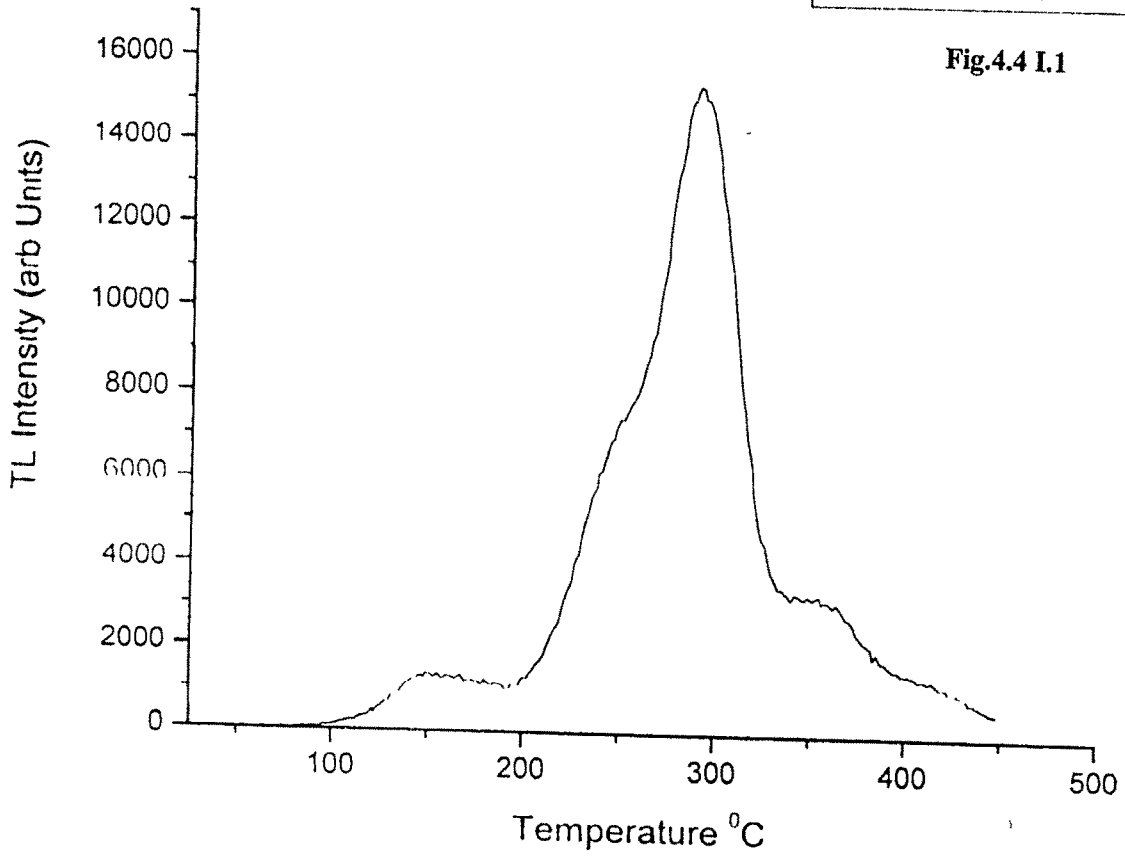


Sample A8(b)/7/8/2003

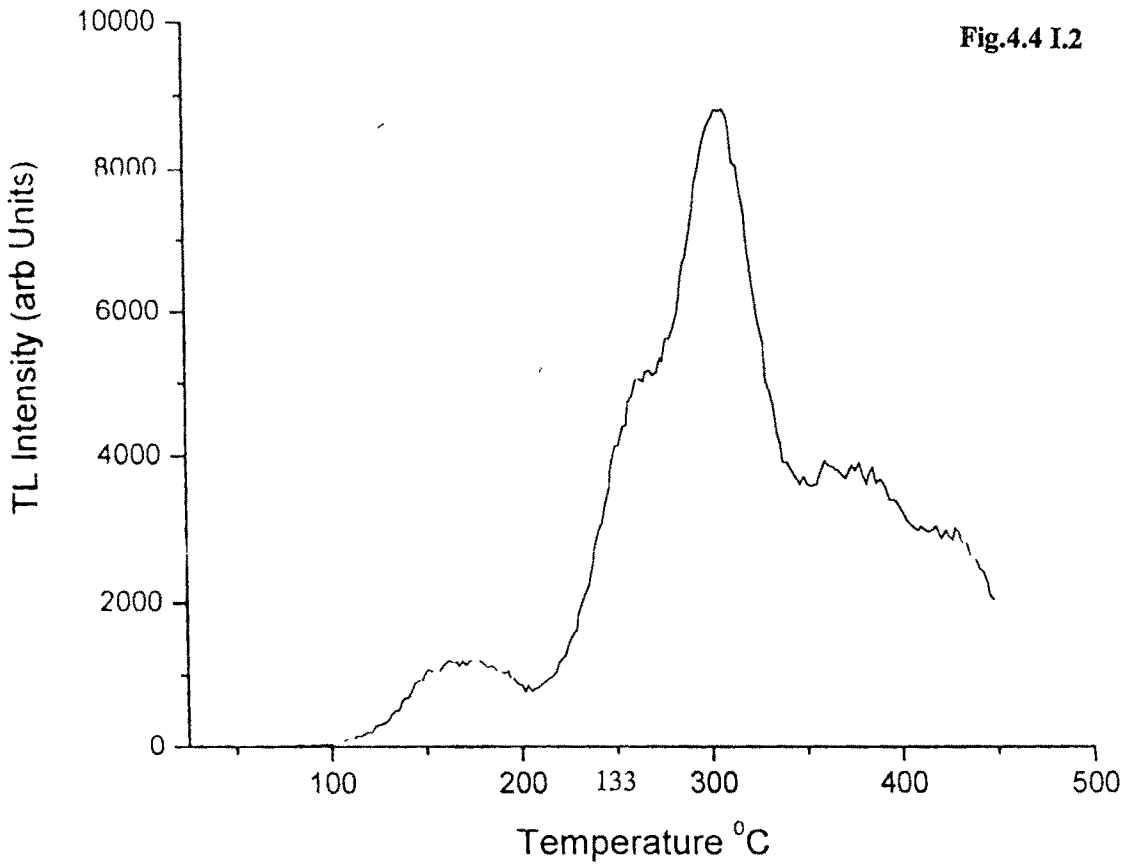
Fig.4.4 H.2



Sample A9B)/7/8/2003



Sample A9(c)/7/8/2003



Figures 4.4 .A.1

Fig.4.4.A.1 is the TL of $\text{BaMgAl}_{10}\text{O}_{17}:\text{Eu}$ with 0.5% . The TL of the phosphor is recorded immediately after beta irradiation. The main TL peak in the phosphor is at 280°C with high intensity and also a hump present at 240°C . From the table 4.3 the important point to be noted of these TL curve is the very high intensity at 280°C peak.

Figures 4.4 .A.2

Fig 4.4 A.2 is the TL of $\text{BaMgAl}_{10}\text{O}_{17}:\text{Eu}$ with 1.0% . The TL of the phosphor is recorded immediately after beta irradiation. Many TL peaks are observed in the phosphor however the peak around 280°C with high intensity and also two humps present on ascending and descending 170 and 325°C . From the table 4.3 the important point to be noted of these TL curve is the intensity 280°C peak reduced by $1/100$ times when compared to Eu concentration 0.5% in the host matrix.

Figures 4.4 .A.3

Fig.4.4.A.3 the TL of $\text{BaMgAl}_{10}\text{O}_{17}:\text{Eu}$ with 1.5% . The TL of the phosphor immediately after beta irradiation. Many TL peaks are observed in the phosphor however the peak around 280°C with high intensity and also two humps present on ascending and descending 240 and 340°C . From the table 4.3 the important point to be noted of these TL curve is the intensity 280°C peak reduced by $1/4$ times when compared to Eu concentration 0.5% in the host matrix and increased by five times when compared to Eu concentration 1.0%. However a small unresolved peak at 240°C is observed.

Table No. 4.3 TL of Beta Irradiated BAM doped Lamp Phosphors

Serial No.	Sample Name	Sample Number	TL peak Temperature in °C	TL peak intensity Counts
1.	BaMgAl ₁₀ O ₁₇ -Eu (0.5%)	A-1 (a)	240	80000
			280	177000
2.	BaMgAl ₁₀ O ₁₇ -Eu (1%)	A-1 (b)	170	6500
			220, 280	9000, 8000
			325	5800
3.	BaMgAl ₁₀ O ₁₇ -Eu (1.5%)	A-1 (c)	280	47000
			340	32500
4.	BaMgAl ₁₀ O ₁₇ -Ce (0.5%)	A-2 (a)	225	13000
			370	9000
5.	BaMgAl ₁₀ O ₁₇ -Ce (1%)	A-2 (b)	210	10400
			340	9000
6.	BaMgAl ₁₀ O ₁₇ -Nd (0.5%)	A-3 (a)	210	17500
			320	14000
7.	BaMgAl ₁₀ O ₁₇ -Nd (1%)	A-3 (b)	200	13100
8.	BaMgAl ₁₀ O ₁₇ -Pr (0.5%)	A-4 (a)	140	13000
			210	19500
			330	18000
9.	BaMgAl ₁₀ O ₁₇ -Pr (1%)	A-4 (b)	210	6000
			360	2400
10.	BaMgAl ₁₀ O ₁₇ -Mn (0.5%)	A-5 (a)	275	1700
			360	1500
11.	BaMgAl ₁₀ O ₁₇ -Mn (1%)	A-5 (b)	200	5500
			360	2600
12.	BaMgAl ₁₀ O ₁₇ -Ce, Mn (0.5%, 0.5%)	A-6 (a)	200	4700
			250, 350	5350, 4100
13.	BaMgAl ₁₀ O ₁₇ -Ce, Mn (1%, 1%)	A-6 (b)	200	4300
			255	9600
			320, 355	10400, 4700
14.	BaMgAl ₁₀ O ₁₇ -Ce, Eu (0.5%, 0.5%)	A-7 (a)	200	7800
			250, 350	14400, 5800
15.	BaMgAl ₁₀ O ₁₇ -Ce, Eu (1%, 1%)	A-7 (b)	250	13200
			370	5500
16.	BaMgAl ₁₀ O ₁₇ -Ce, Nd (0.5%, 0.5%)	A-8 (a)	250	18000
			375	127000
17.	BaMgAl ₁₀ O ₁₇ -Ce, Nd (1%, 1%)	A-8 (b)	410	325000
18.	BaMgAl ₁₀ O ₁₇ -Eu, Mn (0.5%, 0.5%)	A-9 (b)	150	1200
			300, 350	15400, 3000
19.	BaMgAl ₁₀ O ₁₇ -Eu, Mn (1.0%, 1.0%)	A-9 (c)	165, 255	1300, 5200
			300, 360	9800, 3800

The TL of $\text{BaMgAl}_{10}\text{O}_{17}:\text{Eu}$ when compared to all the Eu concentrations studied one main point to be noted is that the peak at 280°C appears to be a strong and interesting in nature. It is believed that 280°C peak may be associated with the Eu impurity. One another point to be noted is concentration of Eu in the host matrix changes the TL pattern.

Figures 4.4 .B 1,2

$\text{BaMgAl}_{10}\text{O}_{17}:\text{Ce}$ (with Ce concentration 0.5, 1.0 molar percentages) phosphors have been studied for their TL characteristics with a standard beta doses of 7Gy from a Strontium-90 source. The observed glow curves are presented in figures 4.4 B 1,2 respectively.

Fig.4.4.B.1 is the TL of $\text{BaMgAl}_{10}\text{O}_{17}:\text{Ce}$ with 0.5% . The TL of the phosphor is recorded immediately after beta irradiation. The main TL peak in the phosphor is at 225°C followed by another well-resolved peak at 370°C . It is to be noted of these TL curve is the very high intensity at 225°C peak.

Fig.4.4 B.2 is the TL of $\text{BaMgAl}_{10}\text{O}_{17}:\text{Ce}$ with 1.0% . The TL of the phosphor is recorded immediately after beta irradiation. The main TL peak in the phosphor is at 210°C followed by another well resolved peak at 370°C . It is interesting to note the TL curve is the very high equal intensity of 210 and 370°C peaks. However a hump is present at the ascending side of the 210°C peak.

The important point to be noted here is the TL intensity of 225°C peak reduced when the Ce concentration increased from 0.5 to 1.0%. The TL intensity of 370°C peak remains same in both the samples

Figures 4.4 .C 1,2

BaMgAl₁₀O₁₇: Nd (with Nd concentration 0.5, 1.0 molar percentages) phosphors have been studied for their TL characteristics with a standard beta doses of 7Gy from a Strontium-90 source. The observed glow curves are presented in figures 4.4 C 1,2 respectively.

Fig.4.4.C.1 is the TL of BaMgAl₁₀O₁₇: Nd with 0.5% . The TL of the phosphor is recorded immediately after beta irradiation. The main TL peak in the phosphor is at 210°C followed by another well-resolved peak at 320°C. It is to be noted of these TL curve is the very high intensity at 210°C peak. A small hump is observed at 150°C.

Fig 4.4 C.2 is the TL of BaMgAl₁₀O₁₇: Nd with 1.0% . The TL of the phosphor is recorded immediately after beta irradiation. The main TL peak in the phosphor is around 200°C followed by a hump at 320°C. It is interesting to note the TL intensity of 200°C peak is maximum and the peak appears as a mixed one.

It is to be noted here is the peak around 200°C is the same one as in the case of Nd 0.5% concentration only point is the well-resolved peak at 320°C reduced as an hump in Nd 1.0% concentration.

Figures 4.4 .D 1,2

BaMgAl₁₀O₁₇: Pr (with Pr concentration 0.5, 1.0 molar percentages) phosphors have been studied for their TL characteristics with a standard beta doses of 7Gy from a Strontium-90 source. The observed glow curves are presented in figures 4.4 D 1,2 respectively.

Fig 4.4 D.1 is the TL of BaMgAl₁₀O₁₇: Pr with 0.5% . The TL of the phosphor is recorded immediately after beta irradiation. The main TL peak in the phosphor is at 210°C followed by another well-resolved peak at 320°C. It is to be noted of these TL peaks are very high intensity and nearly same intensity. A small hump is observed at 150°C.

Fig.4.4 D.2 is the TL of BaMgAl₁₀O₁₇: Pr with 1.0% . The TL of the phosphor is recorded immediately after beta irradiation. The main TL peak in the phosphor at 210°C

followed by a resolved low intensity peak at 360°C. It is interesting to note the TL intensity of 210°C peak is maximum and the peak appears as a mixed one since there is a hump at descending side at 260°C

It is to be noted here is the peak around 210°C is the same one as in the case of Pr 0.5% concentration only point is the well-resolved peak at 360°C reduced as an less intensity peak in Pr 1.0% concentration. An other point to be noted is the TL intensity of both the peaks reduced by 1/3 in case of 210°C and 1/6th in case of 360°C peak when compared to 0.5% Pr

Figures 4.4 .E 1,2

BaMgAl₁₀O₁₇ Mn (with Mn concentration 0.5, 1.0 molar percentages) phosphors have been studied for their TL characteristics with a standard beta doses of 7Gy from a Strontium-90 source. The observed glow curves are presented in figures 4.4 E 1,2 respectively.

Fig.4.4.E 1 is the TL of BaMgAl₁₀O₁₇.Mn with 0.5% . The TL of the phosphor is recorded immediately after beta irradiation . The main peak is well resolved high intensity TL peak in the phosphor is at 275°C followed by another small peak at 360°C. A small hump is observed around 160°C.

Fig.4.4.E.2 is the TL of BaMgAl₁₀O₁₇.Mn with 1.0 % . The TL of the phosphor is recorded immediately after beta irradiation. The main well resolved high intensity TL peak in the phosphor is at 200°C followed by another well resolved small peak at 360°C. A small hump is observed around 240°C. The small hump is observed around 160°C in earlier concentration is missing.

It is to be noted here is the peak around 200°C is the same one as in the case of Mn 0.5% concentration only point is the well-resolved peak at 360°C emerged as a high intensity peak in Mn 1.0% concentration. An other point to be noted is the TL intensity of the 200°C peak reduced by 1/3 when compared to 275°C peak in 0.5% Mn concentration

TL of β - irradiated Double doped Phosphors:

Figures 4.4 .F 1,2

BaMgAl₁₀O₁₇ Ce,Mn (with Ce,Mn concentration 0.5, 1.0 molar percentages) phosphors have been studied for their TL characteristics with a standard beta doses of 7Gy from a strontium-90 source. The observed glow curves are presented in figures 4 4 F 1,2 respectively.

Fig.4 4.F 1 is the TL of BaMgAl₁₀O₁₇:Ce,Mn with 0.5% . The TL of the phosphor is recorded immediately after beta irradiation. The main TL peak in the phosphor is at 250°C followed by another peak at 350°C. A small hump is observed around 200°C

Fig.4.4.F.2 is the TL of BaMgAl₁₀O₁₇ Ce,Mn with 1 0 % . The TL of the phosphor is recorded immediately after beta irradiation. The main TL peaks in the phosphor are at 250 and 300°C followed two humps around 200 and 350°C. The main peak shape is like fork type. It is to be noted here is the peak around 300°C emerged as a high intensity one when compared to 0 5% Ce,Mn concentration.

Figures 4.4 .G 1,2

BaMgAl₁₀O₁₇: Ce,Eu (with Ce,Eu concentration 0.5, 1.0 molar percentages) phosphors have been studied for their TL characteristics with a standard beta doses of 7Gy from a strontium-90 source The observed glow curves are presented in figures 4.4 G 1,2 respectively.

Fig.4.4.G.1 is the TL of BaMgAl₁₀O₁₇:Ce,Eu with 0.5% . The TL of the phosphor is recorded immediately after beta irradiation. The main TL peak in the phosphor is at 250°C followed by another peak at 350°C. A small hump is observed around 200°C

Fig 4 4.G.2 is the TL of BaMgAl₁₀O₁₇:Ce,Eu with 1.0 % . The TL of the phosphor is recorded immediately after beta irradiation. The main TL peaks in the phosphor are at 250 and 370°C followed hump around 200°C. The main point to be noted is that the intensities are same in both cases except the change in TL pattern. Only point to be noted the intensity of hump at 200°C is reduced by 50%.

Figures 4.4 .H 1,2

BaMgAl₁₀O₁₇: Ce,Nd (with Ce,Nd concentration 0.5, 1.0 molar percentages) phosphors have been studied for their TL characteristics with a standard beta doses of 7Gy from a Strontium-90 source. The observed glow curves are presented in figures 4 4 H 1,2 respectively.

Fig.4.4.H.1 is the TL of BaMgAl₁₀O₁₇ Ce,Nd with 0.5% . The TL of the phosphor is recorded immediately after beta irradiation. The main TL peak in the phosphor is at very high temperature and a well resolved one at 375°C A small hump is observed around 250°C

Fig.4.4.H 2 is the TL of BaMgAl₁₀O₁₇:Ce,Nd with 1.0 % . The TL of the phosphor is recorded immediately after beta irradiation. The main TL peaks in the phosphor are at 410°C with very very high intensity Two small peaks are also observed at low intensity around 170 and 270°C. The main point to be noted is that the intensity of 410°C peak very high when compared to 0.5 Ce,Nd concentration.

Figures 4.4 .I 1,2

BaMgAl₁₀O₁₇: Eu, Mn (with Eu, Mn concentration 0.5, 1.0 molar percentages) phosphors have been studied for their TL characteristics with a standard beta doses of 7Gy from a Strontium-90 source The observed glow curves are presented in figures 4 4 I 1,2 respectively.

Fig.4.4.I 1 is the TL of BaMgAl₁₀O₁₇: Eu, Mn with 0.5% . The TL of the phosphor is recorded immediately after beta irradiation. The main TL peak in the phosphor a well resolved one at 300°C. A few small humps observed around 150 and 350°C. The TL peak in the phosphor around 300°C is sharp one with high intensity.

Fig.4.4.I.2 is the TL of BaMgAl₁₀O₁₇: Eu, Mn with 1 0 % . The TL of the phosphor is recorded immediately after beta irradiation The main TL peak in the phosphor a well resolved one at 300°C. A few small humps observed around 170 and 350°C. The TL peak in the phosphor around 300°C is a sharp one with 2/3 intensity when compared to Eu,Mn 0.5% specimen. The hump at 260°C really spoils the shape of the curve

Effect of grain size on the Thermoluminescence output of BaMgAl₁₀O₁₇:Eu (1.5%) Phosphor

By considering the application of these phosphors in lamps where even particle size plays a major role, the following experiment is carried. The present section reports the thermoluminescence (TL) studies of β -irradiated (7Gy) BaMgAl₁₀O₁₇:Eu (1.5%), phosphors prepared in the laboratory. The prepared phosphor cake is ground to a fine powder using mortar & pestle. Then the powder is sieved using standard sieves. The TL glow peaks of the above phosphors are well resolved and interesting in nature. An attempt is made to examine the effect of TL- behavior on the grain size of the present prepared phosphor.

Then the received phosphor cake was ground to a fine powder using mortar and pestle. The received powder was then sieved using a standard sieve sizes ASTM 50, 60, 80, 120, 140, 230, 320 to get the grain of 180, 125, 106, 63 and 45 microns. Thermally stimulated luminescence was recorded by using the experimental set-up described in chapter-3. A uniform heating rate of 6.66 °C/sec was used in the present work for all the samples throughout the range of 25-400°C/s. Equal aliquots (5mg) of these samples were then subjected to irradiation with Strontium – 90, β radiation source of 50 mCi strength. Every time a test dose of 7Gy was given and the TSL curves for these irradiated samples were recorded immediately after irradiation.

Result and Discussions:

The effect of the phosphor particle grain size on the TL glow curve pattern of BaMgAl₁₀O₁₇ doped with europium (1.5%) was studied and presented here. For the various particle sizes the TL glow curve were recorded and their respective peak temperature and peak intensities is presented in Table-4.4. In fig.4.5 the TL of β -irradiated 45-micron size BaMgAl₁₀O₁₇ doped with europium (1.5%) is presented. The TL pattern is almost same in all the particle sizes studied except the generation and disappearance of humps and kinks on both sides. From the table –4.4; it is observed that for the grain size above 80 microns, two small peaks were observed with intensities of 79 and 165 at 245 °C and 285 °C. The well resolved peak is also observed in the higher temperature of 337 °C having intensity of 303.

For the grain size of 180-125 microns the TL glow curve shows four peaks having very low intensity in the higher temperature region. In the TL glow curve for the grain size of 125-106 microns, two hump peaks are observed. First peak was obtained at the peak temperature of 297 ° C having intensity 117, whereas for the well-resolved peak temperature of 362 °C the peak intensity is 304. Whereas for the grain size of 106-63 microns a hump is observed at 338 °C & a peak at 362 °C. It is also observed that the peaks are shifting towards the higher temperature region. For the peak temperature of 338 °C the peak intensity observed are 51 and for the 362 °C peak the intensity observed is 59.

However, for the grain size of 63-45 microns the peak hump is observed at 297°C showing an increase in the intensity of the peak up to 84. Another peak is also observed at 359 °C having a well-defined and dominant peak of intensity 184. In the grain size of below 45 microns the TL glow curve shows the well resolved peak of higher intensity. For the peak temperature of 284 °C the peak intensity is 105 and for the peak temperature of 362 ° C the peak intensity is 282

Table-4.4.1

Serial Number	Sample Name	Peak Temperature °C	Peak Intensity
1	BaMgAl ₁₀ O ₁₇ Eu, Above 180 microns	245 285,337	79 165,303
2	BaMgAl ₁₀ O ₁₇ Eu = 180 - 125 microns	230,258 302,333	13,39 61,77
3	BaMgAl ₁₀ O ₁₇ Eu = 125-106 microns	297 362	117 304
4	BaMgAl ₁₀ O ₁₇ Eu = 106 – 63 microns	338 362	51 59
5	BaMgAl ₁₀ O ₁₇ Eu = 63- 45 microns	297 362	84 184
6	BaMgAl ₁₀ O ₁₇ Eu Below 45 microns	284 362	105 282

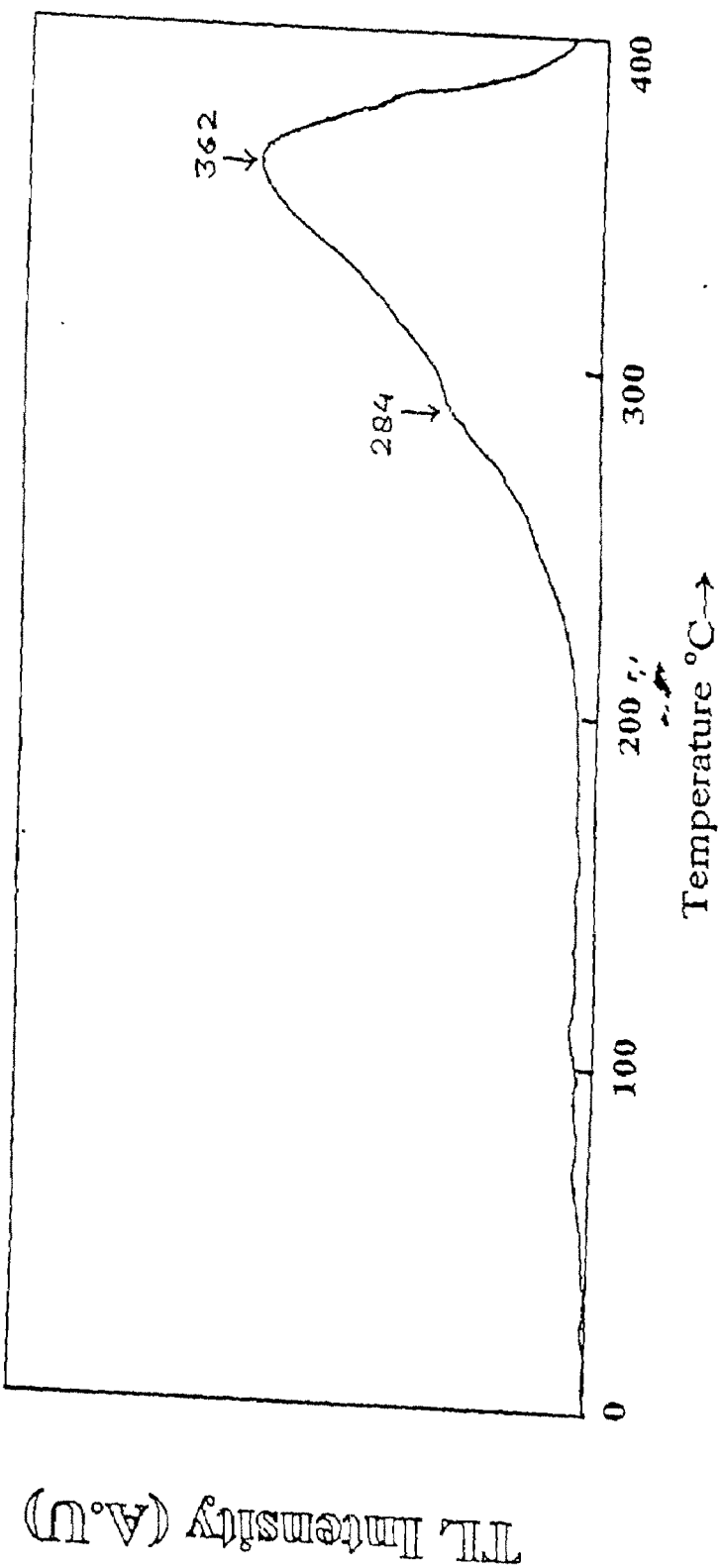


Fig. 4.5 : TL of β -irradiated $BaMgAl_{10}O_{17}$: Eu phosphor particle size less than 45 microns

Fluorescence (Photoluminescence) studies:

The fluorescence study of phosphors brings out lot of information which throws light on the use of the materials as a phosphor in the lamps. In present thesis, the emission and excitation spectra of synthesized phosphors have been recorded at room temperature. The emission spectra have been examined for the materials prepared and the influence of various dopant concentrations (0.5, 1.0, 1.5 molar concentrations) and the behavior of Eu^{2+} , Mn^{2+} , Ce^{2+} , Nd^{3+} , Pr^{3+} doped BAM are investigated. The above dopant activated BaMg- aluminates and the characteristic spectra are presented here for discussion. In all cases, the emission band is specified by the wavelength at which its peak appears. Some times, changes in the relative intensities of the component within a composite band would give rise to apparent shift in the position of its maximum. In that cases, the standard emission /excitation positions have been mentioned. The intensities of the emission as well as excitation bands are given in real units in table 4.4. Mostly all the 27 phosphor specimens are excited with 254nm which is the low pressure discharge of mercury.

The following are the instrument parameters used in the present investigation.

Instrument : RF 5301
Spectrum Type Emission
Scan range . 350- 650nm
Excitation wave length: 254nm
Sample pitch : 1.0
Slit width : Ex: 1.5nm, Em: 1.5nm
Scan Speed . Super
Sensitivity : High
Response Time Auto
Shutter manual : Manual, Open

Occasionally Low Sensitivity (LS).

**Photoluminescence study of BAM doped with Eu,Ce,Nd,Pr and Mn
as well as double dopants**

Excitation 254nm using Shimadzu RF5301R PC

Table No. 4.4

Serial Number	Sample Number	Sample Name	Peak Wavelengths	Peak Intensities in real units
1	A-1 (a)	BaMgAl ₁₀ O ₁₇ -Eu (0.5%)	366, 469, 616	67,27, 14
2	A-1 (b)	BaMgAl ₁₀ O ₁₇ -Eu (1%)	527, 587, 616 366, 469, 616 (LS)	1015,635, 1015 178,61,21(LS)
3	A-1 (c)	BaMgAl ₁₀ O ₁₇ -Eu (1.5%)	527,587, 616 366,469, 587,616(LS)	1015,1015, 1015 176,61,21,44(LS)
4	A-2 (a)	BaMgAl ₁₀ O ₁₇ -Ce (0.5%)	366,397,469	1000,467,484
5	A-2 (b)	BaMgAl ₁₀ O ₁₇ -Ce (1%)	366, 469,	22,27
6	A-2 (c)	BaMgAl ₁₀ O ₁₇ -Ce (1.5%)	366, 469,	22,26
7	A-3 (a)	BaMgAl ₁₀ O ₁₇ -Nd (0.5%)	366, 469	27,28
8	A-3 (b)	BaMgAl ₁₀ O ₁₇ -Nd (1%)	366, 469	27,29
9	A-3 (c)	BaMgAl ₁₀ O ₁₇ -Nd (1.5%)	366, 469	27,29
10	A-4 (a)	BaMgAl ₁₀ O ₁₇ -Pr (0.5%)	366, 469	27,29
11	A-4 (b)	BaMgAl ₁₀ O ₁₇ -Pr (1%)	366, 469	30,31
12	A-4 (c)	BaMgAl ₁₀ O ₁₇ -Pr (1.5%)	366, 469	31,31
13	A-5 (a)	BaMgAl ₁₀ O ₁₇ -Mn (0.5%)	366, 469	31,31
14	A-5 (b)	BaMg ₂ Al ₁₀ O ₁₇ -Mn (1%)	366, 469	31,31
15	A-5 (c)	BaMgAl ₁₀ O ₁₇ -Mn (1.5%)	366, 469	31,31
16	A-6 (a)	BaMgAl ₁₀ O ₁₇ -Ce,Mn (0.5%, 0.5%)	366, 469, 628	31,31, 10
17	A-6 (b)	BaMgAl ₁₀ O ₁₇ -Ce,Mn (1%,1%)	366, 469, 628	31,31, 10
18	A-6 (c)	BaMgAl ₁₀ O ₁₇ -Ce,Mn (1.5%,1.5%)	366, 469, 628	31,31, 10
19	A-7 (a)	BaMgAl ₁₀ O ₁₇ -Ce,Eu (0.5%,0.5%)	366, 469	31,31
20	A-7 (b)	BaMgAl ₁₀ O ₁₇ -Ce,Eu (1%,1%)	366, 469	31,31
21	A-7 (c)	BaMgAl ₁₀ O ₁₇ -Ce,Eu (1.5%,1.5%)	366, 469	31,31
22	A-8 (a)	BaMgAl ₁₀ O ₁₇ -Ce,Nd (0.5%,0.5%)	366, 469	15,22
23	A-8 (b)	BaMgAl ₁₀ O ₁₇ - Ce,Nd(1%,1%)	366, 469	18,23
24	A-8 (c)	BaMg ₂ Al ₁₀ O ₁₇ -Ce,Nd (1.5%,1.5%)	366, 469	26,26
25	A-9 (a)	BaMgAl ₁₀ O ₁₇ -Eu,Mn (0.5%,0.5%)	366, 469, 616	27,27, 8
26	A-9 (b)	BaMgAl ₁₀ O ₁₇ -Eu,Mn (1%,1%)	366, 469, 616	27,27, 4
27	A-9 (c)	BaMgAl ₁₀ O ₁₇ -Eu,Mn (1.5%,1.5%)	366, 469, 616	27,27, 4

LS-Low Sensitivity

However red emission is more when compared to 587nm. It is interesting to note in the low sensitivity range the generation of 366 and 467nm peaks are observed simultaneously the peak at 527nm is missing

The main emission spectra of BaMgAl₁₀O₁₇:Eu 1.5% phosphor is as follows. It indicates that the excitation of the material with 254 nm wavelengths generates a strong emission at 527, 584 and a very strong emission at 616nm in the red region. The intensity of the all the peaks are very high and could not be recorded. Therefore the PL intensity in the above sample is recorded with low sensitivity range. In low sensitivity range the following emission are recorded i.e 366, 467, 587 and 616 the PL emission around 366 to 467 is very high when compared to 587 and 616nm. However red emission is more when compared to 587nm. It is interesting to note in the low sensitivity range the generation of 366 and 467nm peaks are observed simultaneously the peak at 527nm is missing.

From the above discussion it is normally concluded the specimens BaMgAl₁₀O₁₇:Eu 1.0 and 1.5% can be used as lamp phosphors.

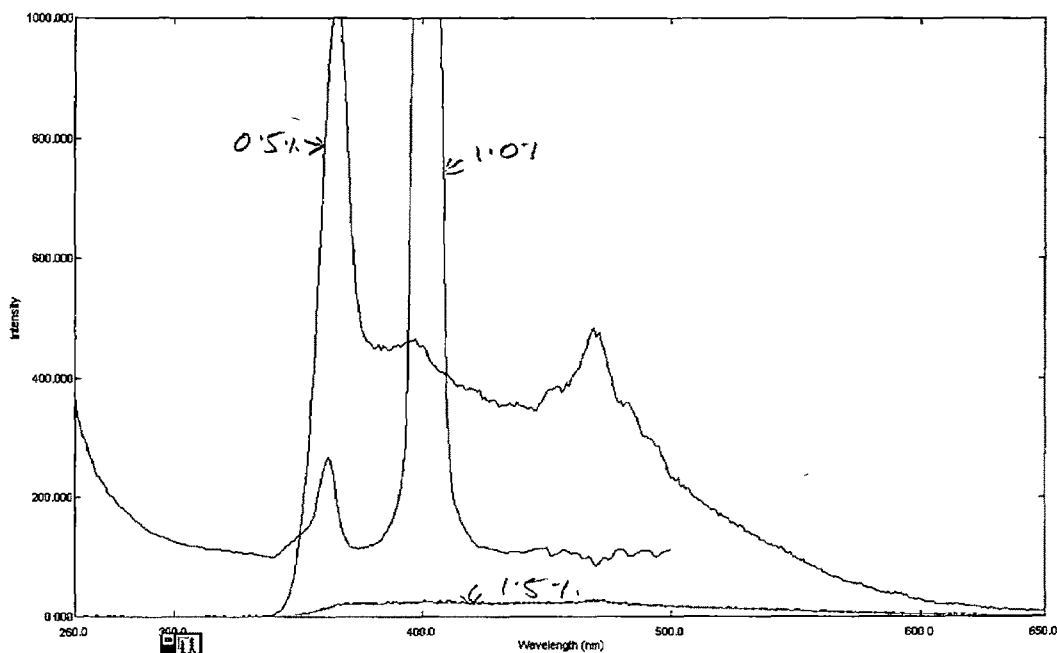


Fig. 4.6.2 Photoluminescence of BaMgAl₁₀O₁₇-Ce (0.5%), BaMgAl₁₀O₁₇-Ce (1.0%), BaMgAl₁₀O₁₇-Ce (1.5%)

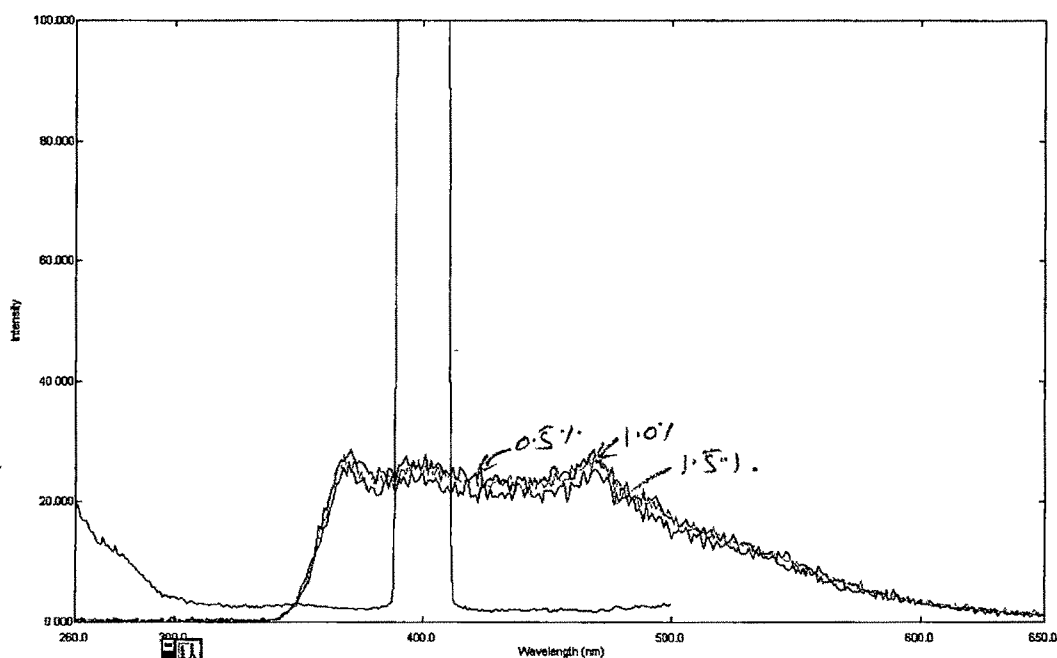


Fig. 4.6.3 Photoluminescence of BaMgAl₁₀O₁₇:Nd (0.5%), BaMgAl₁₀O₁₇:Nd (1.0%), BaMgAl₁₀O₁₇:Nd (1.5%)

Figure. 4.6.3

Figures. 4.6.3 is the photoluminescence spectra of BaMgAl₁₀O₁₇:Nd(0.5, 1.0, 1.5%). The main emission spectra of BaMgAl₁₀O₁₇:Nd doped phosphor is as follows. It indicates that the excitation of the material with 254 nm wavelengths generates a strong emission at 366 and 469nm peaks. The doping effect is not seen in the PL peak shapes nor intensity more or less the PL pattern is same for the entire three samples. . The intensity of these peaks is relatively less around 27-29 counts. The PL emission is even in the 366-469nm region.

Figure. 4.6.4

Figures. 4.6.4 is the photoluminescence spectra of BaMgAl₁₀O₁₇:Pr(0.5, 1.0, 1.5%). The main emission spectra of BaMgAl₁₀O₁₇:Pr doped phosphor is as follows. It indicates that the excitation of the material with 254 nm wavelengths generates a strong emission at 366 and 469nm peaks. The doping effect is not seen in the PL peak shapes nor intensity more or less the PL pattern is same for all the three sample. . The intensity of these peaks is relatively less around 30-31 counts. The PL emission is even in the 366-469nm regions.

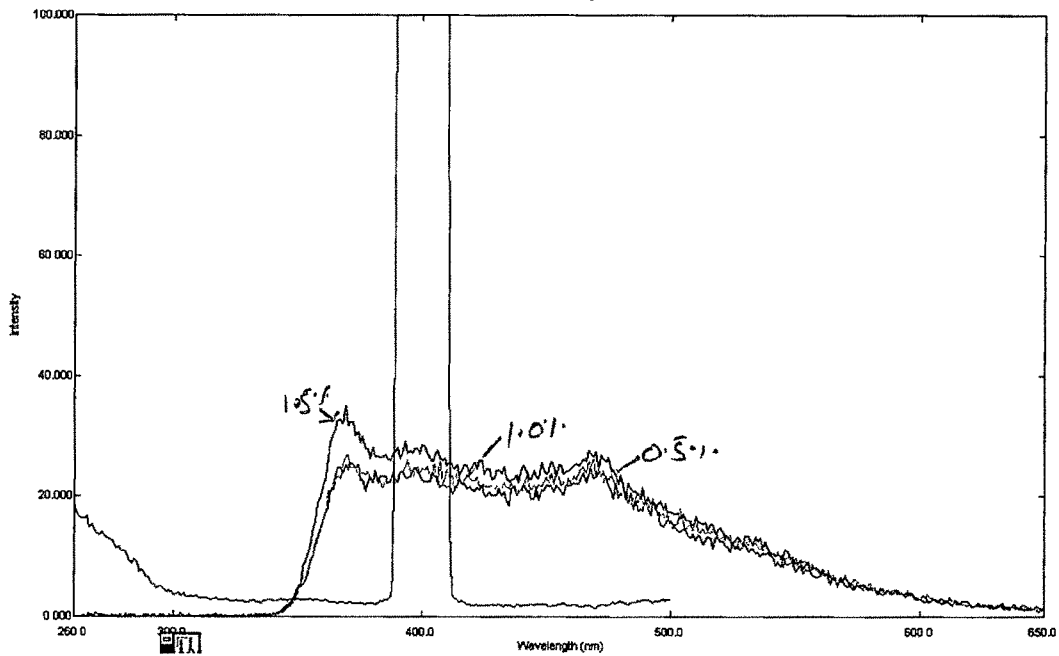


Fig. 4.6.4 Photoluminescence of BaMgAl₁₀O₁₇:Pr (0.5%), BaMgAl₁₀O₁₇:Pr (1.0%), BaMgAl₁₀O₁₇:Pr (1.5%)

Figure. 4.6.5

Figures. 4.6.5 is the photoluminescence spectra of BaMgAl₁₀O₁₇:Mn(0.5, 1.0, 1.5%). The main emission spectra of BaMgAl₁₀O₁₇:Mn doped phosphor is as follows. It indicates that the excitation of the material with 254 nm wavelengths generates a strong emission at 366 and 469nm peaks. The doping effect is not seen in the PL peak shapes nor intensity more or less the PL pattern is same for the entire three sample. . The intensity of these peaks is relatively less around 30-31 counts. The PL emission is mostly constant in the 366-469nm regions.

Figure. 4.6.6

Figures. 4.6.6 is the photoluminescence spectra of BaMgAl₁₀O₁₇:Ce,Mn(0.5, 1.0, 1.5%). The main emission spectra of BaMgAl₁₀O₁₇:Ce,Mn doped phosphor is as follows. It indicates that the excitation of the material with 254 nm wavelengths generates a strong emission at 366, 469 and 628nm peaks. The doping effect is not seen in the PL peak shapes nor intensity more or less the PL pattern is same for the entire three samples. . The intensity of these peaks is relatively less around 30-31 counts but the PL intensity of 628nm peak is still less around 10 counts.. The PL emission is mostly constant in the 366-469nm regions.

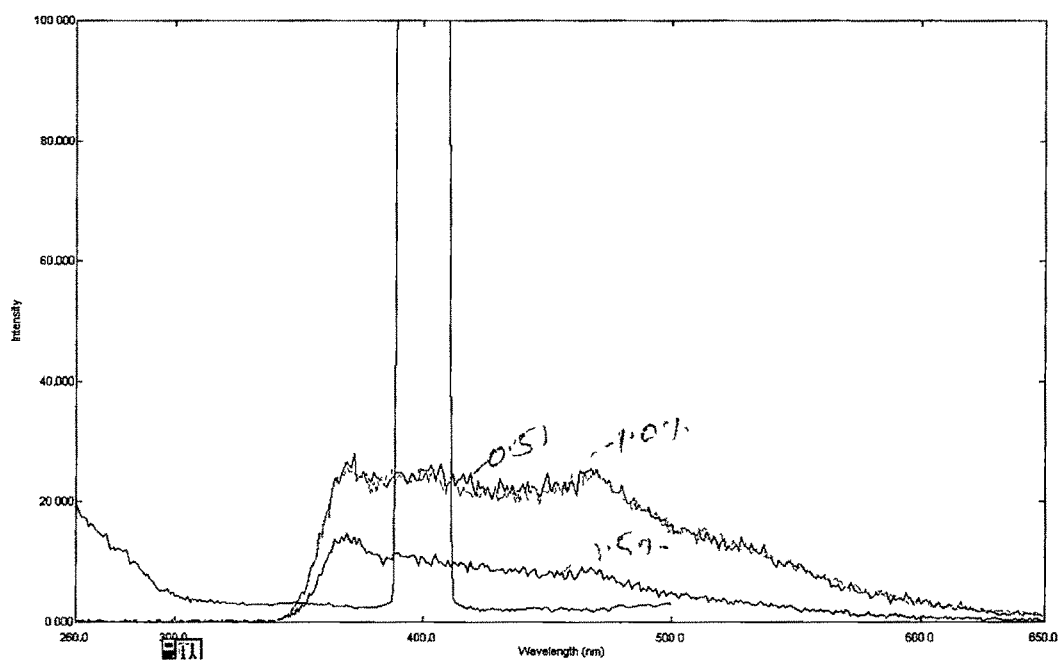


Fig. 4.6.5 Photoluminescence of BaMgAl₁₀O₁₇-Mn (0.5%), BaMgAl₁₀O₁₇-Mn (1.0%), BaMgAl₁₀O₁₇-Mn (1.5%)

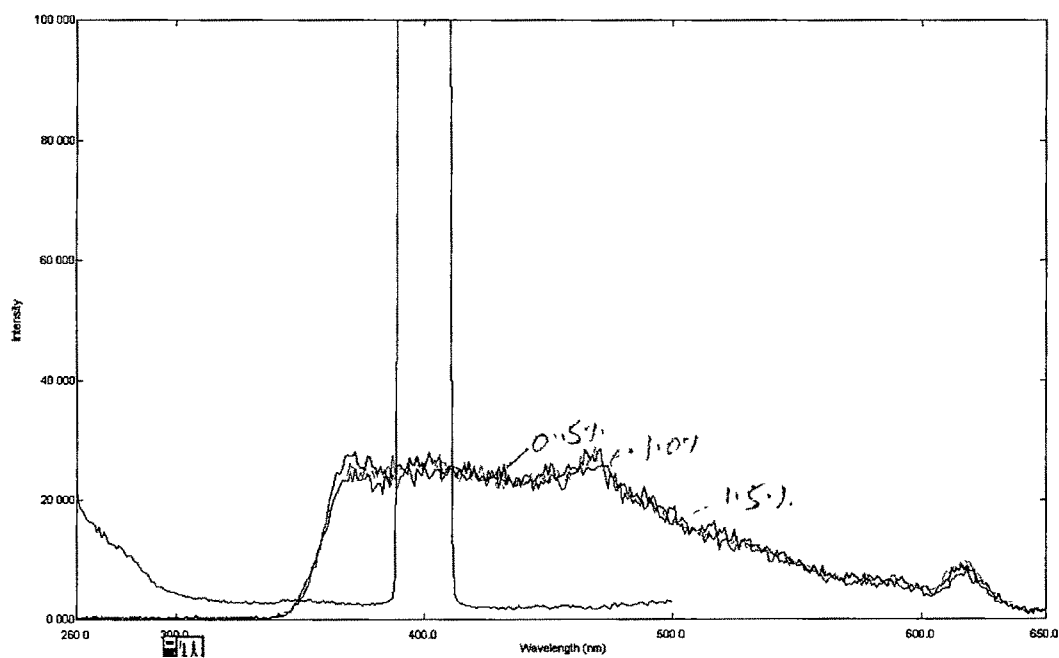


Fig. 4.6.6 Photoluminescence of BaMgAl₁₀O₁₇-Ce,Mn (0.5%), BaMgAl₁₀O₁₇-Ce, Mn (1.0%), BaMgAl₁₀O₁₇-Ce, Mn (1.5%)

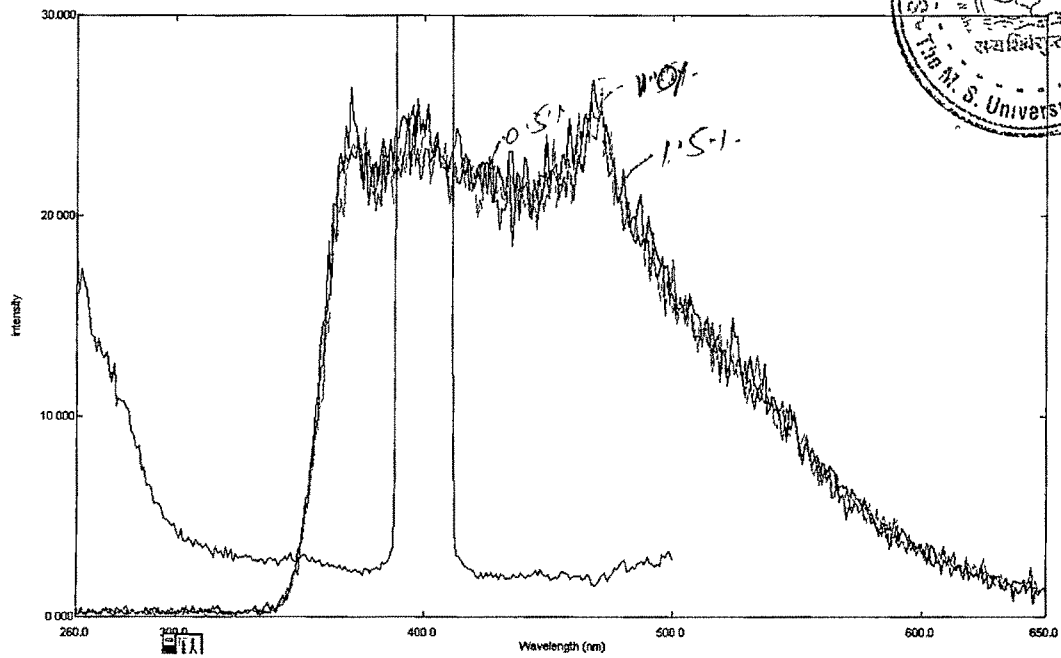


Fig. 4.6.7 Photoluminescence of $\text{BaMgAl}_{10}\text{O}_{17}\text{-Ce, Eu}$ (0.5%), $\text{BaMgAl}_{10}\text{O}_{17}\text{-Ce, Eu}$ (1.0%), $\text{BaMgAl}_{10}\text{O}_{17}\text{-Ce, Eu}$ (1.5%)

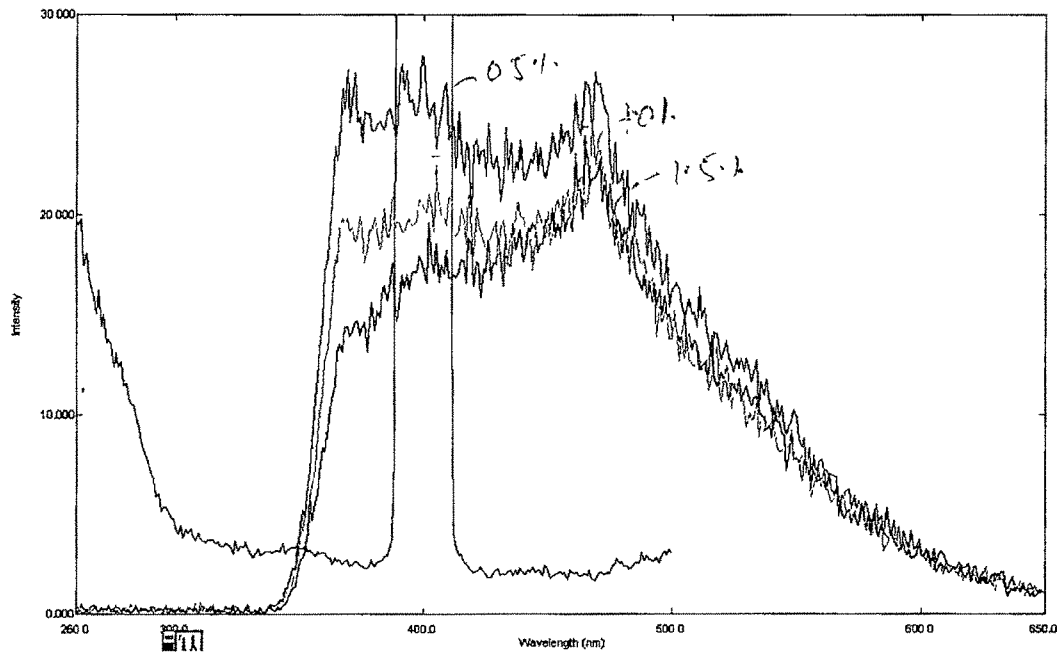


Fig. 4.6.8 Photoluminescence of $\text{BaMgAl}_{10}\text{O}_{17}\text{-Ce, Nd}$ (0.5%), $\text{BaMgAl}_{10}\text{O}_{17}\text{-Ce, Nd}$ (1.0%), $\text{BaMgAl}_{10}\text{O}_{17}\text{-Ce, Nd}$ (1.5%)

Figure. 4.6.7

Figures. 4.6.7 is the photoluminescence spectra of $\text{BaMgAl}_{10}\text{O}_{17}:\text{Ce},\text{Eu}$ (0.5, 1.0, 1.5%). The main emission spectra of $\text{BaMgAl}_{10}\text{O}_{17}:\text{Ce},\text{Eu}$ doped phosphor is as follows. It indicates that the excitation of the material with 254 nm wavelengths generates a strong emission at 366 and 469nm peaks. The doping effect is not much seen in the PL peak shapes nor intensity more or less the PL pattern is same for the entire three sample. . The intensity of these peaks is relatively less around 30-31 counts. The PL emission is mostly constant in the 366-469nm regions.

Figure. 4.6.8

Figures. 4.6.8 is the photoluminescence spectra of $\text{BaMgAl}_{10}\text{O}_{17}:\text{Ce}, \text{Nd}$ (0.5, 1.0, 1.5%). The main emission spectra of $\text{BaMgAl}_{10}\text{O}_{17}:\text{Ce}, \text{Nd}$ doped phosphor is as follows. It indicates that the excitation of the material with 254 nm wavelengths generates a strong emission at 366 and 469nm peaks. The doping concentration effect is seen in the PL peak shape and intensity. However more or less the PL pattern is same for the entire three sample. . The intensity of these peaks is relatively less around 15-26 counts. The PL emission is mostly concentrated in the 366-469nm regions. The increase in dopant concentration leads the growth of 366nm peak increase finally at 1.5% concentration the 366 and 469nm peaks emerged with same intensity.

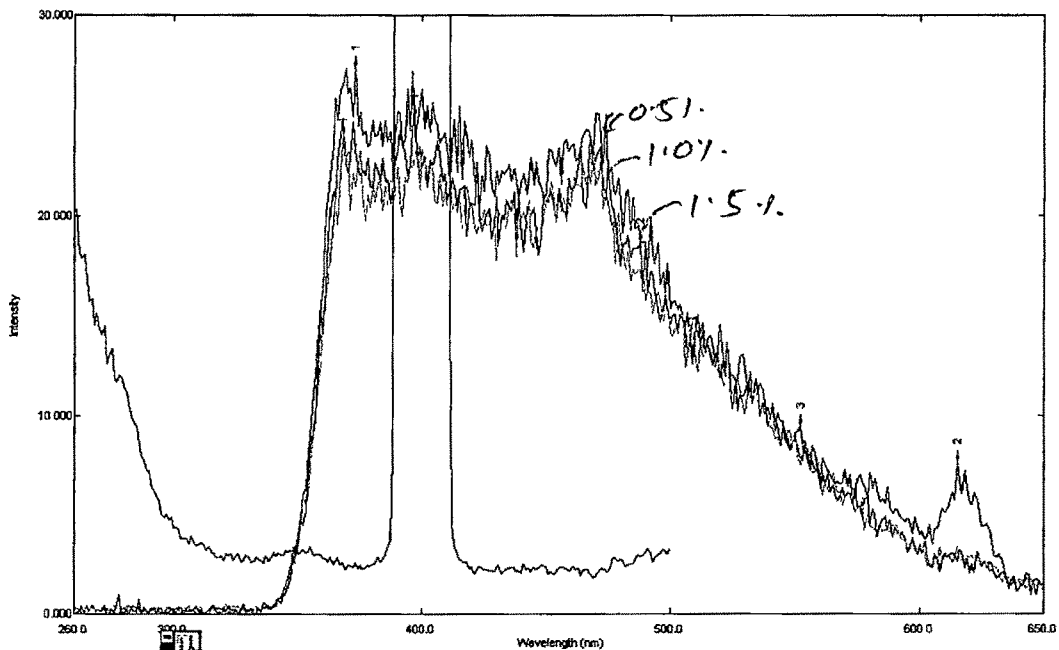


Fig. 4.6.9 Photoluminescence of $\text{BaMgAl}_{10}\text{O}_{17}:\text{Eu},\text{Mn}$ (0.5%), $\text{BaMgAl}_{10}\text{O}_{17}:\text{Eu},\text{Mn}$ (1.0%), $\text{BaMgAl}_{10}\text{O}_{17}:\text{Eu},\text{Mn}$ (1.5%)

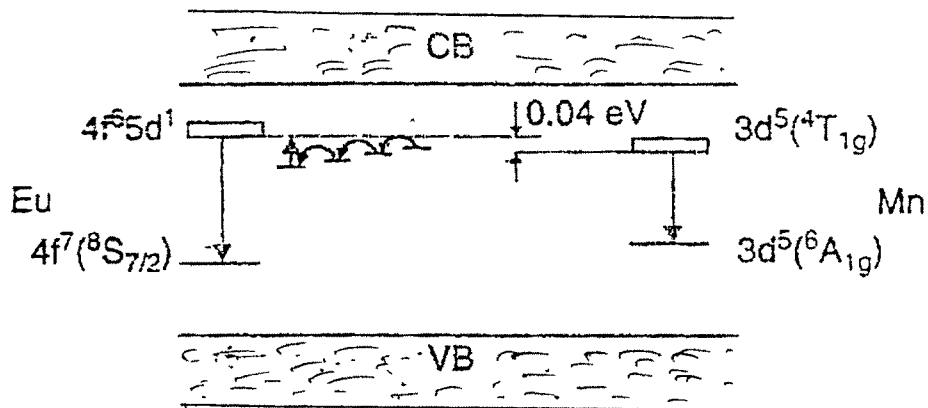
Figure. 4.6.9

Figure 4.6.9 shows the photoluminescence spectra of BaMgAl₁₀O₁₇:Eu, Mn (0.5, 1.0, 1.5%). The main emission spectra of BaMgAl₁₀O₁₇:Eu, Mn doped phosphor is as follows. It indicates that the excitation of the material with 254 nm wavelengths generates a strong emission at 366 and 469 nm peaks apart from a low intensity 616 nm peak. The doping concentration effect is not seen in the PL peak shape and intensity. However, more or less the PL pattern is the same for the entire three samples. The intensity of these peaks is relatively low, around 27-26 counts. The PL emission is mostly concentrated in the 366-469 nm regions. The increase in dopant concentration leads to the 616 nm peak intensity decreasing. However, the concentration effect is not seen for the 366 and 469 nm peaks which emerged with the same intensity.

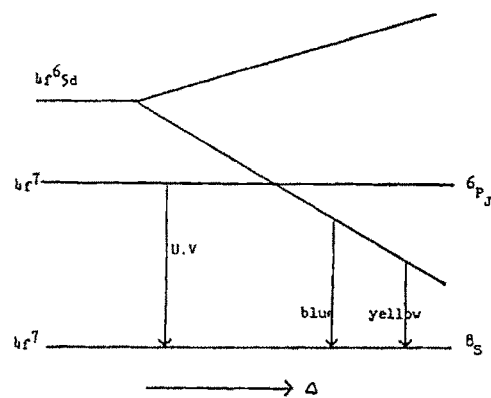
From the literature, the following are the luminescence of specific ions in different host matrices. However, the luminescence in the BAM with Eu, Ce, Nd, Pr, Mn, Ce, Mn, Ce:Eu, Ce:Nd, Eu:Mn are not reported except Eu, Mn in Barium Magnesium Aluminates.

Hoshina T reports a number of luminescence lines due to $^5D_1 \rightarrow ^7F_J$ of Eu³⁺ in Y₂O₂S. As it is reported, the emissions from 5D_2 and 5D_1 are quenched, with an increase in the Eu³⁺ concentration due to a cross-relaxation process, ($^5D_1 \rightarrow ^5D_0$) ($^7F_6 \rightarrow ^7F_J$). The photoluminescence emission in the vicinity of 600 nm is due to the magnetic dipole transition $^5D_0 \rightarrow ^7F_1$ which is insensitive to the site symmetry. The emission around 610-630 nm is due to the electric dipole transition of $^5D_0 \rightarrow ^7F_2$, induced by the lack of inversion symmetry at the Eu³⁺ site, and is much stronger than that of the transition to the 7F_1 state. The luminescent Eu³⁺ ions in commercial red phosphors such as YVO₄, Y₂O₃ and Y₂O₂S, occupy the sites that have no inversion symmetry. The strong emission due to the electric dipole transition is utilized for practical applications. As per Blasse G and Brill A, if the Eu³⁺ site has inversion symmetry, then the electric dipole emission is weak, and the magnetic dipole transition becomes relatively stronger and dominates.

The spectral luminous efficacy as sensed by the eye has its maximum at 555 nm. In the red region, this sensitivity drops rapidly as one moves toward longer wavelengths. Therefore, red luminescence composed of narrow spectra appears brighter to the human eye than various broad red luminescence having the same red chromaticity and emission energy.



The above figure is the Localized transition scheme for recombination incorporating spatially localized excitation states and different trap levels. In BAM:Eu the recombination centers are the activator Eu^{2+} , which relaxes due to a $4f^6 5d^1 \rightarrow 4f^7(^8S_{7/2})$ transition located at 453nm. The recombination centers in BAM:Mn are the Mn^{2+} ions atoms which relaxes due to a $3d^5(^4T_{1g}) \rightarrow 3d^5(^6A_{1g})$ transition located at 515nm.



Schematic diagram of the energies of $4f_7$ and $4f_6 5d_1$ levels in Eu^{2+} influenced by crystal field Δ (From Blasé.G Material science of the luminescence of inorganic solids, in Luminescence of Inorganic Solids, DiBartolo.B, Plenum Press, 1978, 457.)

For the red emission of color TV to be used in the NTSC system, the red chromaticity standard has been fixed at the coordinates $x = 0.67$, $Y = 0.33$, the ideal emission spectra were proposed as a narrow band around 610 nm, before the development of Eu^{3+} .

The sequence of excitation, relaxation, and emission processes in $\text{Y}_2\text{O}_2\text{S}; \text{Eu}^{3+}$ is explained by configuration coordinate model. The excitation of Eu^{3+} takes from the bottom of the ${}^7\text{F}_0$ curve, rising along the straight vertical line, until it crosses the charge transfer state (CTS). Relaxation occurs along the CTS curve. Near the bottom of curve, the excitation is transferred to ${}^5\text{D}_j$ states. Relaxation to the bottom of the ${}^5\text{D}_j$ states is followed by light emission downward to ${}^7\text{F}_j$ states. This model can explain the following experimental findings.

- A. No luminescence is found from ${}^5\text{D}_3$ in $\text{Y}_2\text{O}_2\text{S}:\text{Eu}^{3+}$. Luminescence efficiency is higher for phosphors with higher CTS energy
- B. The quenching temperature of the luminescence from ${}^5\text{D}_j$ is higher as J (0,1,2,3) decreases. The excited 4f states may dissociate into an electron-hole pair. This model is supported by the observation that the excitation through the ${}^7\text{F}_0 \rightarrow {}^5\text{D}_2$ transition of $\text{La}_2\text{O}_2\text{S}:\text{Eu}^{3+}$ causes energy storage that can be converted to luminescence by heating. The luminescence is the result of the recombination of a thermally released hole with an Eu^{2+} ion.

By taking a model where CTS is a combination of $4f^7$ electrons plus a hole, one finds that the resulting spin multiplicities should be 7 and 9. It is the former state that affects optical properties related to the ${}^7\text{F}_j$ state by spin-restricted covalency. The intensity ratio luminescence from ${}^5\text{D}_0 \rightarrow {}^7\text{F}_2$ and from ${}^5\text{D}_0 \rightarrow {}^7\text{F}_1$ decreases with increasing CTS energy sequentially as ScVO_4 , YVO_4 , ScPO_4 , and YPO_4 , all of which have the same type zircon structure. The above intensity ratio is small in $\text{YF}_3:\text{Eu}^{3+}$, even though Eu^{3+} , a site without inversion symmetry. These results suggest that higher CTS energies reduce the strength of the electric dipole transition ${}^5\text{D}_0 \rightarrow {}^7\text{F}_2$ in Eu^{3+} .

The electronic configuration of Eu^{2+} is 4f and is identical to that of Gd^{3+} . The lowest excited state of 4f levels is located at about $28 \times 10^3 \text{ cm}^{-1}$ and is higher than the 4F^6 and 5d^1 level in most crystals, so that Eu^{2+} usually gives broad-band emission due to f-d transitions. The wavelength positions of the emission bands depend very much on hosts, changing from the near UV to the

red This dependence is interpreted as due to the crystal field splitting of the 5d level With increasing crystal field strength, the emission bands shift to longer wavelength The luminescence peak energy of the 5d-4f transitions of Eu^{2+} and Ce^{3+} are affected most by crystal parameters denoting electron - electron repulsion - on this basis, a good fit of the energies can be obtained.

The near-UV luminescence of Eu^{2+} in $(\text{Sr},\text{Mg})_2\text{P}_2\text{O}_7$ is used for lamps in copying machines using photosensitive diazo dyes. The blue luminescence in $\text{BaMgAl}_{10}\text{O}_{17}$ is used for three-band fluorescent lamps. Red luminescence is observed in Eu^{2+} -activated CaS ; the crystal field is stronger in sulfides than in fluorides and oxides. The lifetime of the Eu^{2+} luminescence is 10^{-5} to 10^{-6} s, which is relatively long for an allowed transition. This can be explained as follows. The ground state of $4f^7$ is ^8S , and the multiplicity of the excited state $4f^6 5d^1$ is 6 or 8; the sextet portion of the excited state contributes to the spin-forbidden character of the transition. Sharp-line luminescence at 360 nm due to an f-f transition and having a lifetime of milliseconds is observed when the crystal field is weak so that the lowest excited state of $4f^7 (6P_1)$ is lower than the $4f^6 5d^1$ state. The host crystals reported to produce UV luminescence are BaAlF_5 , SrAlF_5 , $\text{BaMg}(\text{SO}_4)_2$, $\text{Sr Be}_2 \text{Si}_2\text{O}_7$.

From the above discussions of the electronic transitions in the Europium and the PL studies of the present work (Fig.4.6.1, 4.6.7 and 4.6.9) on the PL emission is comparable with the literature Sharp-line luminescence at 366 nm due to an f-f transition and having a lifetime of milliseconds is observed when the crystal field is weak so that the lowest excited state of $4f^7 (6P_1)$ is lower than the $4f^6 5d^1$ state

Among the lanthanide ions, the 4f- 5d transition energy is the lowest in Ce^{3+} , but the energy gap from the $5d^1$ states to the nearest level ($^2\text{F}_{7/2}$) below is so large that the 5d level serves as an efficient light-emitting state. The luminescence photon energy depends strongly on the structure of the host crystal through the crystal-field splitting of the 5d and varies from near -ultraviolet to the green region. The two emission peaks are due to the two terminating levels, $^2\text{F}_{5/2}$, and $^2\text{F}_{7/2}$, of the 4f configuration of Ce^{3+} .

The decay time of the Ce^{3+} emission is 10^{-7} to 10^{-8} s, the shortest in observed lanthanide ions. This is due to two reasons: the $d \rightarrow f$ transition is both parity-allowed and spin allowed since $5d^1$ and $4f^1$ states are spin doublets

From fig.4.6.2, 4.6.6, 4.6.7 and 4.6.8 and the above literature the PL observed in the present investigated samples the main PL emission is around 366 and 469 with less intensity which is allowed transitions of Ce^{3+}

The four lower-lying levels of Nd^{3+} provide a condition favorable to the formation of population inversion. For this reason, Nd^{3+} is used as the active ion in many high-power, solid-state lasers (at $1.06 \mu m$ wavelength), the most common hosts are single crystals of Yttrium aluminum garnet, YAG or glass. However Nd^{4+} gives luminescence in the regions 415, 515, 550 and 705 nm has been reported.

From fig.4.6.3 and fig.4.6.8 also from the above literature the PL observed in the present investigated samples the main PL emission is around 366 and 469 with less intensity which is allowed transitions of Nd^{3+} and Nd^{4+}

Luminescence of Pr^{3+} consists of many multiplets, as follows $\sim 515 nm$ ($^3P_0 - ^3H_4$), $\sim 670 nm$ ($^3P_0 - ^3F_2$), $\sim 770 nm$ ($^3P_0 - ^3F_4$), $\sim 630 nm$ ($^1D_2 - ^3H_6$), $\sim 410 nm$ ($^3S_0 - ^1I_6$), and ultraviolet ($5d - 4f$) transitions. The relative intensities of the peaks depend on the host crystals. The radiative decay time of the $^3P_0 \rightarrow ^3H_1$ or 3F_1 emission is $\sim 10^{-5}$ s, which is the shortest lifetime observed in $4f-4f$ transitions. The short decay time of Pr^{3+} is ascribed to the spin-allowed character of the transition. Since the short decay time of Pr^{3+} is for fast information processing.

The quantum efficiency of the more than 1 was reported for Pr^{3+} luminescence when excited by 185 nm light. The excitation-relaxation process takes the following paths. $^3H_4 - ^1S_0$ (excitation by 185 nm), $^1S_0 - ^1I_6$ (405 nm emission), $^1I_6 - ^3P_0$ (phonon emission), $^3P_0 - ^3H_4$ (484.3 nm emission), $^3P_0 - ^3H_5$ (531.9 nm emission), $^3P_0 - ^3H_6$, 3F_2 610.3 nm emission) and $^3P_0 - ^3F_3$, 3F_4 (704 nm emission).

From fig.4.6.4 and the above literature the PL observed in the present investigated samples the main PL emission is around 366 and 469 which is allowed transitions of Pr^{3+} .

However the sharp-line luminescence at 366 nm due to an f-f transition and having a lifetime of milliseconds is observed when the crystal field is weak so that the lowest excited state of $4f^7$ ($6P_1$) is lower than the $4f^6 5d^1$ state.

Transitions in Mn^{2+} Phosphors are 3d_5 Luminescence due to Mn^{2+} is known to occur in more than 500 inorganic compounds. Of these, several are being used widely for fluorescent lamps and CRTs. The luminescence spectrum consists of a structureless band with a half width of 1000 to 2500 cm^{-1} at peak wavelengths of 490 to 750nm. When a metal ion occupies a certain position in a crystal, the crystal field strength that affects the ion increases as the space containing the ion becomes smaller. For increases in the field, the transition energy between the 4T_1 and 6A_1 levels is predicted to decrease (shift to longer wavelengths). In fact, the peak wavelength of the Mn^{2+} luminescence band is known to vary linearly to longer wavelength (547 to 602 nm) with a decrease in Mn-F distance (2.26 to 1.99 Å) in a group of fluorides already studied. A similar relationship also holds for each group of oxo-acid salt phosphors having an analogous crystal structure, the wavelength is longer when Mn^{2+} replaces a smaller cation in each group. On the other hand, a larger anion complex makes the cation space shrink, leading to longer-wavelength luminescence. In materials containing a spinel structure, Mn^{2+} can occupy either octahedral or tetrahedral sites. From the fact that the luminescence occurs in the shorter-wavelength (green) region, the tetrahedral site is expected to be occupied preferentially by Mn^{2+} . Many scientists observed different Mn^{2+} sites in crystal. Since the luminescence wavelength due to Mn^{2+} is sensitive to the magnitude of the crystal field, several emission bands are observed when different types of Mn^{2+} sites exist in a host crystal. In $SrAl_{12}O_{19}$, bands at 515, 560 and 590 nm are considered to originate from Mn^{2+} ions replacing tetrahedrally coordinated Al^{3+} , fivefold coordinated Al^{3+} , and 12-fold coordinated Sr^{2+} , respectively. In lanthanum aluminate, which has a layer structure of spinel blocks, a 680-nm band is observed due to Mn^{2+} in octahedral coordination, in addition to a green-emitting band due to tetrahedral coordination. Two emission bands separated by about 50 nm were recognized long ago in Mn^{2+} doped alkaline earth silicates. The polarization of the luminescence light observed in a single crystal is also related to the site symmetry of Mn^{2+} . Broad bands in the longer wavelength side accompany the zero-phonon lines. These originate from lattice-electron interactions and are known as vibronic sidebands.

From fig.4.6.5, 4.6.6, 4.6.9 and also from the table 4.4 it is commonly observed the transitions of Mn^{2+} as well as Eu^{2+} .

Discussion and Summary of TL studies of β - irradiated BAM with various dopants:

The TL of $\text{BaMgAl}_{10}\text{O}_{17}:\text{Eu}$ when compared to all the Eu concentrations studied one main point to be noted is that the peak at 280°C appears to be a strong and interesting in nature. It is believed that 280°C peak may be associated with the Eu impurity. One another point to be noted is concentration of Eu in the host matrix changes the TL pattern of beta irradiated $\text{BaMgAl}_{10}\text{O}_{17}:\text{Eu}$.

TL of $\text{BaMgAl}_{10}\text{O}_{17}:\text{Ce}$ the important point to be noted here is that the TL intensity of 225°C peak reduced when the Ce concentration increased from 0.5 to 1.0%. The TL intensity of 370°C peak remains same in both the samples.

TL of $\text{BaMgAl}_{10}\text{O}_{17}:\text{Nd}$ it is to be noted here is the peak around 200°C is the same one as in the case of Nd 0.5% concentration only point is the well-resolved peak at 320°C reduced as an hump in Nd 1.0% concentration.

TL of $\text{BaMgAl}_{10}\text{O}_{17}:\text{Pr}$ the main point to be discussed here is the peak around 210°C is the same one as in the case of Pr 0.5% concentration only point is the well-resolved peak at 360°C reduced as an less intensity peak in Pr 1.0% concentration. An other point to be noted is the TL intensity of both the peaks reduced by $1/3$ incase of 210°C and $1/6^{\text{th}}$ in case of 360°C peak when compared to 0.5% Pr.

The peak around 200°C is the same one as in the case of Mn 0.5% concentration of TL of $\text{BaMgAl}_{10}\text{O}_{17}:\text{Mn}$ only point is the well-resolved peak at 360°C emerged as a high intensity peak in Mn 1.0% concentration. An other point to be noted is the TL intensity of the 200°C peak reduced by $1/3$ when compared to 275°C peak in 0.5% Mn concentration.

TL of beta irradiated BAM: double dopants like, CeMn, CeEu, CeNd, EuMn, did not show any noticeable TL pattern when compared with single dopant BAM. However it is interesting to note that the TL intensity of BAM with Ce,Nd gives an excellent TL emission with very high intensity.

The TL grain size results are required to find out the effect of grain size on the TL properties of the phosphor. As the grain size of the phosphor material reduces from 180-45 microns the TL glow peaks show reduction in the number of the humps and increase in the intensity of the main peaks.

Discussion and Summary of TL studies of γ -irradiated BAM with various dopants:

The TL of $\text{BaMgAl}_{10}\text{O}_{17}:\text{Eu}$ When compared to all the Eu concentrations studied one main point to be noted is that the 121°C peak appears to be a strong. However it is not well resolved but the 209°C is a very well resolved one. It is very interesting to note that the doublet disappears and well-defined dominant peak at 209°C appears. Besides this, the peak at 340°C appears, but with a higher intensity, however not resolved properly in all the above cases. It seems that the isolated strong peak at 209°C develops at the cost of doublet and 340°C high temperature peak. It is believed that 209°C peak may be associated with the Eu impurity. One another point to be noted is irrespective of Eu concentration in the host matrix the 209°C peak remains as a well resolved one with high intensity in 4 cases of the phosphors under TL study.

The TL of gamma irradiated $\text{BaMgAl}_{10}\text{O}_{17}:\text{Ce}$ when compared to all the Ce concentrations studied one main point to be noted is that the 121°C peak appears to be a strong and a very well resolved one. It is very interesting to note that the doublet peak at 340°C not resolved, but with a higher intensity in all above cases. It seems that the isolated strong peak at 121°C believed that may be associated with the basic $\text{BaMgAl}_{10}\text{O}_{17}$ (BAM). The impurity Ce effect is not much seen in the present set of samples. One another point to be noted is irrespective of Ce concentration variation in the host matrix the 121°C peak remains as a well resolved one with good intensity in all 6 cases of the above TL study. Only the intensity of 121°C peak decreases by 15% with increase in Ce concentration.

The TL of $\text{BaMgAl}_{10}\text{O}_{17}:\text{Nd}$ when compared to all the Nd concentrations studied one main point to be noted is that the 121°C peak appears to be a strong and a very well resolved one. It is very interesting to note that the doublet peak at 340°C not resolved, but with a higher

intensity in all above cases. It seems that the isolated strong peak at 121°C believed that may be associated with the basic BaMgAl₁₀O₁₇ (BAM). The impurity Nd effect is seen only the increase and decrease in intensities in the present set of samples. One another point to be noted is irrespective of Nd concentration variation in the host matrix the 121°C peak remains as a well resolved one with good intensity in all 6 cases of the above TL study.

The TL (all curves) of gamma irradiated BaMgAl₁₀O₁₇: Pr when compared to all the Pr concentrations studied one main point to be noted is that the 121°C peak appears to be a strong and a very well resolved one. It is very interesting to note that the doublet peak at 340°C not resolved, but with a higher intensity in all above cases. It seems that the isolated strong peak at 121°C believed that might be associated with the basic BaMgAl₁₀O₁₇ (BAM). The impurity Pr effect is not seen only the increase and decrease in intensities in the present set of samples.

The mixed peaks in the gamma irradiated BaMgAl₁₀O₁₇ (BAM):Mn believed that might be associated with the basic impurity Mn effect. The above TL pattern is not seen in the other set of samples studied.

The gamma irradiated TL (all curves) of BaMgAl₁₀O₁₇: Ce,Mn when compared to all the Ce,Mn concentrations studied one main point to be noted is that the 121°C peak appears to be a strong and a very well resolved one in the single dopants but in the present case it appears as a hump in Ce,Mn 1.5% concentrations and a main peak at 209°. It seems that the isolated strong peak at 209°C believed that might be associated with the BaMgAl₁₀O₁₇ Ce,Mn (1.5%). It is clearly observed that, the TL pattern displays two humps around 121°C and 340°C. The main peak at 209°C develops and appears as strong peak. It is interesting to note that, peak at 209°C may be the combined effect of Ce,Mn

It appears that the mixed peaks in the gamma irradiated BaMgAl₁₀O₁₇ (BAM):Ce,Eu believed that might be associated with the basic impurity Ce, Eu effect. The above TL pattern is not seen in the other set of samples studied.

It seems that the mixed peaks in the gamma irradiated $\text{BaMgAl}_{10}\text{O}_{17}$ (BAM):Ce,Nd believed that might be associated with the basic impurity Ce, Nd effect. The above TL pattern is seen in the other set of samples studied i.e BAM Ce,Eu.

One interesting point to be noted that the gamma irradiated BAM doped with Eu, Mn 0.5% the peak at 209°C appears well resolved followed. It seems that the mixed peaks in the $\text{BaMgAl}_{10}\text{O}_{17}$ (BAM): Eu, Mn believed that might be associated with the basic impurity Eu, Mn effect. The above TL pattern is seen in the other set of samples studied except BAM Ce,Eu. .

The TL behavior of the prominent peaks exhibited by RE, NRE, RE:RE and RE:NRE impurities doped BaMg aluminates is mixed behavior. The main peaks at 121 and 340°C are not well resolved in double dopants.

From the TL emission studies (figure 4.3.A) it is evident that the $\text{BaMgAl}_{10}\text{O}_{17}$ activated with Eu^{2+} gives emission in the entire visible range the same is observed. From the TL emission studies (4.3.B Curve A5b) it is evident that the $\text{BaMgAl}_{10}\text{O}_{17}$ activated with Mn^{2+} gives emission in the blue green region the same is observed. From the TL emission studies it is evident that the $\text{BaMgAl}_{10}\text{O}_{17}$ activated with Eu^{2+} , Mn^{2+} gives emission at 516nm (4.3.B Curve A9c) with higher intensity followed by 610 and 640nm emissions. It is evident from the figures of TL emission that the 516nm emission is more for Eu,Mn specimen followed by few red lines. Since the effect of Temperature on Eu emission is studied by Iwama and Takawa. The same result is observed in case of Eu, Mn doped BAM.

For a detailed investigation of the multi trap level system the thermoluminescence experiments have been repeated with beta and gamma irradiations. The shape of the TL glow curves is almost independent of the excitation energy. The TL pattern of the glow peaks appears in all glow curves with hardly any correlation with the peak temperatures as well as dopant concentrations. The TL observation implies on the one hand that the trapping levels can also be populated after a Eu^{2+} centered $4f^7-4f^6 5d^1$ excitation.

Glow curves of BAM:Eu as function of the dopant Eu, Ce, Nd, Pr and Mn Concentrations. To evaluate the energetic structure of the multilevel trap system BAM samples have been prepared with Eu, Ce, Nd, Pr, Mn, CeMn, Ce Eu' CeNd and Eu,Mn concentrations between 0.5,1% and 1.5%. The TL glow curves of these materials were recorded with a heating rate of 6 6 °C/Sec.

The glow curves obtained reveal that the patterns of the TL peaks are independent of the dopant concentration. In some cases the TL glow curves demonstrate that the TL intensity decreases with increasing dopant concentration.

This behavior can be explained either by many traps presence or by the fact that for a given trap density the trapping probability is reduced if the density of the activator ion is increased due to the statistical reduced spatial distance between the activator ions and the excitons formed after band absorption.

BAM:Mn is considered as a green phosphor for PDPs as well as tri color lamps due to its high VUV efficiency and excellent green color point. In contrast to BAM: Eu, the activator Mn^{2+} substitutes Mg^{2+} and is thus incorporated into the spinel blocks instead into the conduction layers. The excitation spectrum of BAM:Mn is very similar to that of BAM, since Mn^{2+} has only forbidden transitions resulting in low absorption coefficients. The only difference to the un doped BAM is that the band edge is somewhat shifted towards lower energy, which is caused by the replacement of Mg^{2+} by Mn^{2+} . The low temperature part of the glow curves of BAM:Mn are very similar to those of BAM:Eu, indicating that the defect structure responsible for the complex glow curves are an intrinsic feature of the BAM host lattice. Independent on the type of dopant, however, the integral TL intensity of BAM:Mn is about twice as high as that of BAM:Eu. The glow curves of BAM.Mn exhibit in the high temperature section an additional glow curves of BAM:Eu. This deep trap is thus ascribed to the incorporation of Mn^{2+} in the BAM lattice.

Since the present samples are prepared in air (oxygen) a major concern related to the application of BAM:Eu is the distinct reduction of its efficiency if it is annealed in an

oxidizing atmosphere, i.e. in air or in oxygen. This is a necessary step during the PDP manufacturing process to remove organic matter, e.g. binder residues, from the screen-printing steps. Oshio and Justel T found that the reduction of the efficiency of BAM:Eu due to a thermal treatment above 600°C is related to the oxidation of the activator Eu^{2+} to its trivalent state.

From the literature the excitation results in the formation of excitons that can be trapped either by the activator or by defect sites. While trapping of the excitons at the activator directly yields luminescence, trapping at defect sites does not result in the desired Eu^{2+} emission. It is thus expected that type and density of defects have an impact on the efficiency of BAM:Eu.

For higher photon energies the efficiency decreases steadily with increasing thermal treatment. The observed reduction of the light output for photo excitation above the band gap becomes more pronounced with interpreted in terms of the low penetration depth of gamma and beta photons into the BAM grains.

Since VUV radiation is absorbed in the band gap with a very high absorption coefficient, the penetration depth of the incident photons is low. As a result the oxidation of Eu^{2+} to Eu^{3+} at the surface of the BAM Eu particles can be monitored. Since Eu^{3+} is not blue luminescent, its thermal treatment in air yields a reduction of the light output by the reduction of the concentration of luminescent Eu^{2+} centers in the surface layer. Alternatively, it can be ascribed to the energy transfer from Eu^{2+} to Eu^{3+} or to the trapping of excitons due to Eu^{3+} . Under beta and gamma excitation the photons are absorbed due to the $4f^7-4f^65d^1$ transition of Eu^{2+} that have a lower absorption coefficient than host lattice absorption. Therefore, the oxidation of Eu^{2+} to Eu^{3+} in a thin surface layer hardly affects the excitation spectrum above 350nm. All observations concerning the glow curves of BAM: X and X,Y can be briefly summarized as follows:

- (i) The glow curves fine structure, i.e. the superposition of several glow peaks, is still observed for thermally treated samples.
- (ii) A detailed analysis of the individual TL pattern reveals more or less similar results. Many small peaks or humps, which indicate different trap depths and the frequency factors.
- (iii) The high temperature TL peak around 350°C is observed in many cases of TL of beta and gamma irradiated phosphors.

Takekawa et al. suggested two different models for energetic positions of the trap levels in inorganic solids. The first model is based on shallow traps located below the conduction band, whereby thermal activation of trapped electrons results in the release and diffusion of electrons to the activator via the conduction band. The second model is based on trap states located in the band gap, energetically below the excited state of the recombination center. Because the recombination center and the traps are spatially localized and the recombination takes place without a transition of the electron into the conduction band, these processes are referred to as localized transitions. In literature it is already mentioned, TL is also observed after excitation with radiation energies lower than the band gap of BAM, which is only in line with an electronic trap structure corresponding to the second model with localized transitions. A localized transition scheme is depicted which is in line with all results gained from the TL experiments. The trap states are spatially localized and are energetically below the lowest crystal field component of the excited $4f^6 5d^1$ state (visualized in the scheme by the dotted line) Eu^{2+} .

The allowed transitions of BAM:Eu and the schematic diagram of the energies of Eu^{2+} are discussed in the above figures. From this model the traps in the band gap can also be occupied by applying radiation with energy well below the band gap energy as in the experiments. The resonant TL behavior occurring at excitation energies matching the energy gap between the valence and the conduction band can be explained by a reduced mobility of the electron-hole pairs energetically positioned at the lower band edge of the conduction band. These electron-hole pairs are more effectively trapped by lattice defects than those

being energetically high above the band edge. This also explains the 360 nm peak in the excitation spectrum of BAM, indicating an efficient exciton trapping by the lattice defects.

The observation, that the excitation of BAM with an energy distinctly higher than the band gap, results in less thermoluminescence, can be explained by an increase in the density of higher Eu^{2+} states, resulting in an enhanced transfer efficiency to the recombination center Eu^{2+} , by circumventing the trapping states.

If BAM is doped by Mn^{2+} similar glow curves have been obtained proving that the traps are host lattice related and not specific to the applied activator. As shown before, the analysis of the trap depth energies of Mn^{2+} doped material reveals values ~ 0.04 eV below the trap depth energies determined for the Eu^{2+} doped material. This suggests that in this lattice the lowest excited $3d^5(^4T_{1g})$ state of Mn is shifted by 0.04 eV with respect to the lowest crystal field component of the excited $4f^65d^1$ state of Eu^{2+} . The defect density of BAM crystals is relatively high, since the integral intensity of the glow peaks are rather high, viz, about ten times higher than for other PDP phosphors, e.g. Willemite $\text{Zn}_2\text{SiO}_4:\text{Mn}$. It is also confirmed by the relatively intense defect luminescence of undoped BAM crystals. The presence of a high concentration of defects in BAM crystal is in line with the observation that even a tiny deviation from the ideal composition during BAM synthesis, results in the formation of impurities, e.g. the β -alumina phase $\text{Ba}_{0.75}\text{Al}_{11}\text{O}_{17.25}$, which is an oxygen deficient composition. Therefore, the shallow traps are assigned to oxygen vacancies, located in the conduction layers of BAM, which is well established as the source of the high ion conductivity of β -alumina. In other words, the concentration of oxygen vacancies is reduced by the post-annealing step in air due to the Eu^{2+} oxidation accompanied by oxygen diffusion into the conduction layer or by diffusion from oxygen ions from the spinel blocks into the conduction layer. The reduction of the light output caused by the oxidation of Eu^{2+} to Eu^{3+} (Eu_{Ba}^x to Eu_{Ba}^*) occurs mainly at the surface of the BAM:Eu particles. The formation of Eu^{3+} at the surface probably causes the high temperature glow peak energetically located below the recombination center. The oxygen vacancies in the conduction layer of BAM are probably caused by the application of a reducing atmosphere during BAM synthesis, that is required to reduce Eu^{3+} (starting material is Eu_2O_3) to Eu^{2+} . The application of a reducing

atmosphere during the synthesis of BAM or during a post –annealing step, results besides the reduction of Eu^{3+} also in the removal of some oxygen atoms from the lattice (reduction), leading again to oxygen vacancies in the lattice.

The defect structure of Eu^{2+} and Mn^{2+} doped BAM was determined by means of thermoluminescence and TL spectroscopy. The glow curves revealed that BAM comprises several shallow traps below the recombination center. It was demonstrated that the type of activator does not affect the energetic position of the traps in the band gap of BAM. By the investigation of BAM:Eu samples, thermally treated in air or nitrogen, it was elucidated that the concentration of the shallow traps decreases with increasing annealing time. By annealing of “defect free” BAM in nitrogen/hydrogen the shallow traps can be recovered, Which is caused by the removal of oxygen from the conduction layers in BAM, leaving oxygen vacancies behind. The shallow traps have hardly any impact on the VUV efficiency.

Zambare et al reported the activation energy of the low temperature regions main peak (170° 230°C) of the Ce^{3+} doped BaMg- aluminates is seen to be reduced with the double doping of them with other Eu^{3+} , Nd^{3+} and Pr^{3+} impurities. . The peak position of the peak around 340°C does remain more or less same in all these specimens. This encourages the author to suggest that the origin of the peak must be closely associated with BaMg-aluminate host lattice. The position and shape of the peak do not change significantly in RE and RE:NRE BaMg aluminates. This also supports the above-mentioned suggestion of association of 340°C peak with BAM host lattice. It is found that Ce^{3+} activated BaMg aluminate exhibits the main peak around 340°C, which observes first order kinetics. The double doping of this specimen with another RE [Eu^{3+} , Nd^{3+} , Pr^{3+} and Mn^{2+}] shifts the peak to 121°C. It is interesting to note that the peak around 210°C peak is found to follow second order kinetics. This indicates that double doping of $\text{BaMgAl}_{10}\text{O}_{17}$ phosphor with RE impurities changes the order of kinetics of the main peak. It is very important to note that no change is observed in probability per second of electron from trap of dominant peak in RE (single) and RE:RE doped BaMg aluminates

References

1. T. Justel, H. Bechtel, H. Nikol, C.R. Ronda, D.U. Wiechert, Proceedings of the Seventh International Symposium on Physics and Chemistry of Luminescent Materials, 1998, p. 103.
2. Justel et al J of Luminescence, 101 (2003)195 –210.
3. S. Oshio, T.Matsuoka, S. Tanaka, H. Kobayashi, J. Electrochem. Soc. 145(1998) 3903
4. M. Ilmer, S. Kotter, H. Schweizer, M. Seibold, Proceedings of IDW'99, p.65.
5. A.L. Diaz, C.F. Chenot, B.G. deBoer, Proceedings of Eurodisplay, 1999, p. 65.
6. M. Zachau, D. Schmidt, U. Mueller, C.F. Chenot, 1999, WO 99/34389.
7. R. Chen, S.W.S. McKeever, Theory of Thermoluminescence and Related Phenomena, World Scientific Publishers, Singapore, London, Hong Kong, 1997.
8. R.H. Bube, Photoconductivity of Solids, Wiley, New York, 1960.
9. D.R. Vij, Luminescence of Solids, Plenum Press, New York, 1978.
10. P. Kivits, H.J.L. Hagebeuk, J Lumin. 15(1977).
11. P. Ceve, M. Schara. C. Raonik, Dadiation research, 51, 581-589 (1972).
12. D. Lapraz, A. Banmer and P. Iacconi, Phys. Status Solidi, A 54, 605 (1979).
13. D. Lapraz and A. Banmer, Phys. Status Solidi, A 68, 309 (1981).
14. K.V.R. Murthy et al., J of Radiation Measurements, Vol36 (1-6), June 2003, 483-485
15. K.C. Patil et. al Bull. Material sci. vol-18 No.7 Nov. 1995, PP 922-930.
16. T. Justel, J.C. Krupa, D.U. Wiechert, J. Lumin. 93(2001)179.
17. N. Iyi, S. Takekawa, S. Kimura, J. Solid State Chem. 83(1989) 8.
18. S. Shionoya, W.M. Yen, Phosphor Handbook, CRC Press, Boca Raton, 1999.
19. M. Gobbels, S. Kimura, E. Woermann, J. Solid State Chem. 136 (1998) 253.
20. A.R. West, solid State Chemistry, VCH, Weinheim, 1992.
21. K.V.R. Murthy et al., J of Radiation Measurements, Vol36 (1-6), June 2003, 483-485.
22. Proc. of NPTLR-2001, Pub. Luminescence society of India, Sept. 2001.
23. D. Lapraz and A. Baumer, Phys. Stat. Sol (a) 68 (309) (1981).
24. Proc. Int. Conf. On Luminescence and its applications Vol. 1&2 Edited by K.V.R. Murthy et. al Dec. 2000, Publ. By M.S. University of Baroda.

25. 13th Int. Conf. On Solid-state dosimetry 9-13 July 2001, Athens, Greece, Abstracts.
- 26 K.C.Patil et.al Bull. Material sci. vol-18 No.7 Nov.1995, PP 922-930
27. J.M.P.J.Verstegen, J. Electrochemical. Soc.; Solid-state Science And Technology, Vol. 121, No. 12, pp.1623-1631, (Dec. 1974).
28. D.Ravichandran, R. Roy, W.B.White and S.Erdei, J. Mater Res., Vol. 12, No.3, pp 819-824, (Mar 1997).
29. B Smets, J. Rutten, G. hoeks and J. Verlijsdonk, J. Electrochemical. Soc., Vol.136, No.7, pp.2119-2123, (July 1989).
30. A.L.N. stevels and A.D.M. Schrama-De Pauw, Journal of Luminescence, 14, pp.147-152, (1976).
31. A.L.N.Stevels, Journal of Luminescence, 17, pp.121-133, (1978).
32. P.Dorenbos, Journal of Luminescence, 91, pp.155-176, (2000).
33. Zambare et al, Proceedings of NSLA-2002 (Jabalpur) Edited by K.V.R.Murthy et.al
34. Zambare et al, Proceedings of NSLA-2001 (Hyderabad) Edited by A.G. Page et.al
35. Zambare A.P Ph.D., thesis, M S.University of Baroda, July 2002.
36. Zambare Proceedings of NSLA-2003 (NPL, Delhi) Edited by K.V.R.Murthy et.al
37. Zambare Proceedings of ICLA-2004 (BARC, Mumbai) Edited by AS Pradhan et.al
38. Raukas M, Basin S.A, Schaik W.V, Yen WN. and Happek U., Luminescence efficiency of cerium doped insulators: The role of electron processes; Applied Physics Letters 69 3300 (1996)
39. Mo L.Y, Guillen F, Fouassier C and Hagenmuller P, Comparative study of sensitization of the luminescence of trivalent rare-earth ions by Ce³⁺ in LaOBr, Journal of the Electrochemical Society 132, 717 (1985)
- 40 Hoshina T, 5d to 4f radiative transition probabilities of Ce³⁺ and Eu³⁺ in crystal, Journal of the Physical Society of Japan, 48, 1261 (1980)
41. Smets B, Advances in the sensitization of phosphors;Optical properties excited states in solids Ed. Di Bartolo Plenum Publ. 349 (1992)
42. Zhang Jin Chao, Parent C, Le Flem G and Hagenmuller P, White light emitting glasses, Journal of solid state chemistry, 93 17 (1991)
43. Band A.M, Photoluminescence study of Ce-Tb doped hexagonal ABR(PO₄)₂, Ph.D. Thesis, Nagpur University 103 (2000)

44. Ankur chatterjee, G. Alexander, P. Ramkrishnan, M. Anitha and H. Singh, Proceedings of NSPTLR-2001 (Jalgaon)
45. G. Blasse and B.C.Grabmaier, "Luminescent Material—", Berlin, Springer- Proceedings of NSPTLR-2001 (Jalgaon) Edited by R.T Chuadhary et.al
46. R.V.Subrahmanyam, S. Sivaraman ,Shishir Jain and Ashish Verma, Proceedings of NSLA-2001 (Hyderabad) PL-4, pp-207 Edited by A.G.Page et.al
- 47 S.Ekambaram and K C.Patil, Bull. Mater., Sci., Vol.18, No 7, pp. 921-930, (Nov. 1995).
48. B.M.J.Smets, Mater. Chem. Phys., 16, 283, (1987)
49. G.Oversluigen, Electroche Soc., Fall Mtg. Extended Abstracts No.711, Sandiego, 1986
50. N.El Jouhari, C. Parent, J.C.Zhang, A.Daoudi and G. le Flem, J de Physiq-IV, 2, C2-257, (1992)
51. N.Yamashita, J. Electrochem., 140, 840, (1993).
52. N.B.Ingale, D.S.Thakre, S.K.Omanwar and S.V.Mohril, Proceedings of NSLA-2002 (Jabalpur) pp-78, Edited by K.V.R.Murthy et.al
53. A.R.Dhobale, S.V.Godbole, N.Natarajan, T.K Sheshgiri, A.G.Page and M.D.Shatry, Proceedings of NSLA-2002 (Jabalpur) pp-90 Edited by K.V.R.Murthy et.al
54. J.K.Kapoor, Proceeding of the National Symposium on Thermoluminescence and It's Application, pp-18-20 (1992). Edited by K.V.R.Murthy et al
55. J.L.Sommerdijk, J.A.W. Van Der Does De Bye and P.H.J.M. Verberne, Journal of Luminescence, 14, pp.91-99, (1976).
56. J.M. P.J. Verstegen and A.L.N. Stevels, Journal of Luminescence, 9, pp.406-414, (1974).
57. Proceeding of the National Seminar on Luminescence and It's Application, Bilaspur (M.P), India, Ed. J.S.Nagpal. et.al (1994)
58. J.H.Schulman, E.H.Attix, E.J.West and J.Ginther, Presented at Symposium on Personal Dosimetry Techniques for External Radiation, Madrid, 1st-5th April pp-319-339.

59. J.H.Schulman, R.D.Kirk and E.J.West, Proceeding of the International Congress of Radiology, Rome, pp-1797-1801 (1965). J.R.Cameron, N.Suntharalingan and G.N.Kenny, Thermoluminescence Dosimetry, The University of Wisconsin Press.
60. A.R.Lakshmanan et.al, Journal Appl. Radi. Inst. 34, 107 (1979)
61. A.R.Lakshmanan and J.W.N.Tuyn, Radi. Prot. Dosi., 18, 229, (1987).
62. Y.S.Horowitz, Radi. Prot. Dosi. 33, 255, (1990).
63. Y.Z.Horowitz, M.Moscovitch and M.Wilt, Nucl. Instrum. Methods, A 244, 566, (1986).
64. T.Nakajima, Y.Murayama, T.Matsuzawa and A.Koyano, Nucl. Instrum. Methods, 157, 155, (1978).
65. W.Soushan, C.Guolong, W.Fang, L.Yuanfang, Z.Ziying and Z.Jianhuan, Radi. Prot. Dosi., 14(3), 223, (1986).
66. S.S.Wang, G.G.Cai and R.X.Zhou, Radi. Prot. Dosi., 33(1-4), 247, (1990)
67. K.G.Vohra, R.C.Bhatt, Chandru Bhuwan, A.S.Pradhan, A.R.Lakshmanan and S.S.Shastry, Health Physics. 38, 193.(1980).
68. V.Natarajan, S.V.Godbole, T.K.Sheshgiri, P.Ramkrishnan, G.Alexander, A.G.Page and M.D.Sastry, Proceedings of NSLA-2002 (Jabalpur) pp-94, Edited by K.V.R.Murthy et.al.
69. Narita,K. and Taya,A. Tech Digest,Phosphor Res.Soc.147 th Meeting, 1979.
70. Butler,K.H.,Fluorescent Lamp Phosphors,Technology and Theory, The Pennsylvania State Univeristy Press, 1980, 261
71. Hoshina, T., Luminescence of Rare Earth Ions, Sony research center Rep.,1983
72. Piper, W.W.,Deluca, J.A.,and Ham, F S ,J.Luminesc.,8,344,1974
73. Blasse,G. and Bril,A.Philips Tech .Rev., 31,304,1970
74. Struck,C.W. and Fonger,W.H.,J.Luminesc.,1/2,456,1970
75. Blasse,G.,Material science of the luminescence of inorganic solids, in Luminescence of Inorganic Solids, DiBartolo,B.,Plenum Press, 1978,457
76. Smets,b.M.J. and Verlijdsdonk, J.G.,Mater.Res.Bull.,21,1305,1986
77. Hews,R.A. and Hoffman,M.V.,J.Luminesc.,3,261,1970
78. Blasé,G.,Wanmaker,W.L.,Tervrugt,J.W.,and Bril,A.,PhilipsRes.Rept.,23,189,1968
79. Sommerdijk,J.L.and Verstegen,J M.P.J.,J.Luminesc.9,415,1974

80. Yamada,H.,Suzki,A.,Uchida,Y.,Yoshida,M ,Yamaoto,H , and Tsukuda,Y.,*J.electro.chem.soc.*,136,2713,1989
81. Sommerdijk,J.L.,Bril.A.,and de Jager,A.W.,*J.Luminesc.*,8,341,1974
82. Kushida,T.,Macros,H.M.,and Geusic,J.E.,*Phys.Rev.*,167,289,1968
83. Vaga,L.P.,*J.Chem.Phys.*,49,4674,1968
84. Avella,F.J.,Sovers,O.J.,and Wiggins,C.S.*J.electrochem.Soc.*,114,613,1967
85. Bril,A.,and Klassens,H.A.,*PhilipsRes.Rept.*,10,305,1955
86. Levine,A.K.and Pallila,F.C.,*Appl.Phys.Lett.* ,5,118,1964
- 87 Kano.T.,Kinamer,K.,and Seki,S.,*J.electrochem.Soc.*129,2296,1982
88. Struck,C.W.and Fonger,W.H *J.Luminescence.*,1&2,456,1970
89. Blasse,G.,*J.Chem.Phys.*,45,2356,1966
90. Forest,H.,Cocco,A.,and Hersh,H.,*J.Luminesc.*,3,25,1970
91. Struck,C.W.,and Fonger,W.H.*Phys.Rev.*,B4,22,1971.
92. Hoshima,T.,Imanaga,S.,and Yokono,S ,*J.Luminesc* ,15,455,1977
93. V.Natarajan, T.K.Sheshgiri, and M.D.Sastry, *Proceeding of NSLA-2001 (Hyderabad)* pp-138, Edited by A G.Page et.al.
94. A.G.Page, *Proceedings of ISLA-2000, vol.I* pp.46-49, (M.S.U) Baroda Edited by K.V.R. Murthy et.al.
95. B.C.Bhatt, T.K.Gumdu Rao and S.S.Shinde, *Proceedings of ISLA-2000, vol.I,* pp.118-123, (M.S.U) Baroda Edited by K.V.R. Murthy et.al.
96. A.S.Pradhan, *Proceedings of ISLA-2000, vol.I,* pp.131-144, (M.S.U) Baroda Edited by K.V.R. Murthy et al.
97. R.K.Gratia, *Proceedings of ISLA-2000, vol.I,* pp. 145-152, (M.S.U) Baroda Edited by K.V.R. Murthy et.al.
98. T.R.Joshi, *Proceedings of ISLA-2000, vol.I,* pp.199-206, (M.S.U) Baroda Edited by K.V.R. Murthy et.al.
99. S.R.Padwal-Desai and A.G.Behere, *Proceedings of ISLA-2000, vol I,* pp.213-214, (M.S.U) Baroda Edited by K.V.R.